5-2015

Local Modulation and Measurement of Macrophage-Derived Bioactive Proteins from Implanted Biomaterials in Rat

Geetika Bajpai
University of Arkansas, Fayetteville

Local Modulation and Measurement of Macrophage-Derived Bioactive Proteins from Implanted Biomaterials in Rat

Local Modulation and Measurement of Macrophage-Derived Bioactive Proteins from Implanted Biomaterials in Rat

A dissertation submitted in partial fulfillment
of the requirements for the degree of
Doctor of Philosophy in Cell and Molecular Biology

by

Geetika Bajpai
Bundelkhand University,
Institute of Engineering and Technology,
Bachelors of Technology, 2006

May 2015
University of Arkansas

This dissertation is approved for recommendation to the Graduate Council

Dr. Julie A. Stenken
Dissertation Director

Dr. Jeannine M. Durdik
Committee Member

Dr. Yuchun Du
Committee Member

Dr. Charles L. Wilkins
Committee Member

Dr. David A. Zaharoff
Committee Member

Abstract

Fibrosis around the implanted medical devices is a severe problem that can plague long-term device reliability. Activation of macrophage phenotype (macrophage polarization) has emerged as a new and possible means for reducing fibrosis in the fields of biomaterials and regenerative medicine. Macrophages are phagocytic cells that respond to microenvironmental cues that direct their phenotype. Macrophage activation has been widely studied in mouse and human in the context of tumor biology, yet little information is available regarding how macrophage activation could be used in a biomaterials context. Further, rats rather than mice are the common subjects in biomaterials experiments. A significant need is to determine if directed macrophage activation can be achieved in a biomaterials context.

Cultured rat-derived macrophages (NR8383, peritoneal and spleen) were tested with modulators (dexamethasone, LPS, IL-4 and IL10) to ensure activation towards the expected phenotype. Phenotypic characterization involved gene expression assays (ARG2, CD163, CD206, NOS2, IL-12), protein analysis (IL-6, IL-10, TNF-α), and flow cytometry (for receptors CD86, CD163, CD206, MHC II). The successful in vitro immunomodulation suggested the feasibility of modulation *in vivo*.

Microdialysis has been used for cytokine sampling (from various tissues including rat mammary tissue for Leptin, CCL2 and IL-6; procedures developed in this work), but can also be employed for modulator delivery. To achieve *in vivo* immunomodulation, microdialysis experiments were performed to locally deliver either IL-4 or IL-10. No significant differences in dialysate cytokine levels (CCL2, IL-1β, and IL-6) or histological sections (H&E and Masson's trichrome) of tissue surrounding the probe were observed between control and treatment groups.

However, gene expression analysis of tissue to which IL-4 was delivered suggests down-regulation in CCL2 and IL-6. To enhance modulator amount and surface area, a polyvinyl alcohol (PVA) sponge model was employed. The IL-4 impregnated sponges had reduced IL-1β concentrations compared to controls. However, no significant differences in gene expression were observed. For IL-10, down regulation of CCL2 (also at protein level), IL-1β, IL-12 and NOS2 genes was observed. This initial work in macrophage activation for biomaterials in rats provides a fundamental framework for future work in this field.

Acknowledgments

I would like to graciously thank people who played a role directly or indirectly in the completion of this journey. First and foremost, I would like to thank my advisor Dr. Julie A. Stenken who provided immense support throughout my graduate studies. Her training helped me sharpen my critical and analytical thinking/writing skills. She gave me tremendous support and freedom to pursue my own research hypothesis weather or not the outcomes were thoroughly fruitful. She arranged several practice talk sessions and provided constructive feedback for development of public presentation skills. I am highly appreciative of her time she spent in revising and proof reading my manuscripts and this dissertation. I am deeply thankful to Dr. Stenken for providing mentorship that helped in my overall professional development as an independent scientist.

I would like to thank my committee member Dr. Jeannine M. Durdik. Her valuable advice helped a great deal in the project. Without her guidance, I wouldn't have learned flow cytometry and be an independent user of this technique. I thank her for letting me use her laboratory for all the cell culture experiments I performed. I am grateful to her for involving me in her own experiments which helped me broaden my horizons. She was always available for consultation with patient listening ears, I am indebted to her for her always welcoming demeanor and constant encouragement to keep going.

I would like to thank my other committee members Dr. David Zaharoff, Dr. Yuchun Du and Dr. Charles Wilkins who provided constructive feedback during each committee meeting to successfully move forward in research.

I am thankful to Dr. Geisla Erf for my initial training in flow cytometry at the Cell Isolation and Characterization facility at the Dept. of Poultry Science at the University of Arkansas. I am also thankful to her for allowing me to learn various immunology experiments in her laboratory. As a first year student, I also took an advanced immunology course work with her and her teaching sparked even more interest in immunology.

I would like to acknowledge Mr. David Cross at the Dept. of Poultry Science at the University of Arkansas for preparing the histology slides.

I am thankful to Dr. Kumar at the Chemistry and Biochemistry Dept. at the University of Arkansas with whom I initially worked on a collaborative project and also took biochemistry classes he taught. Through his classes, I could learn biochemistry at a much deeper level. I am thankful to him for his consultations on research problems and his constant moral support.

I would like to acknowledge previous post-doctoral fellow Dr. Erika VonGrote in the lab who helped me in learning animal handling and surgical procedures. She also helped in learning qRT-PCR assays. I am thankful to Alda, Thad, Sarah, Randy, Matthias, Valerie and Geoff for being great colleagues who are supportive and helpful.

The journey has not been straightforward and enduring hardships of graduate school wouldn't be possible without the support of family and friends. I am especially thankful to Alda for being my awesome buddy, for providing a helping hand whenever I needed it the most and cheering me up when times were rough. I am thankful to Kolawale at Mcintosh lab in organic

chemistry department for being a great friend who helped in chemistry problems apart from supporting in usual ups and downs of grad school life. I would like to thank Sachit, Debasish, Anees and Shilpa for being great friends and for their love and support.

Last but not the least, I am thankful to my family. I am thankful to my uncles, Dr. K. S. Bajpai and Dr. H. S. Bajpai for providing an inspirational environment at an early childhood that motivated me to develop science faculties. I am thankful to my brother, Dr. Geet Bajpai, for long scientific discussions on skype as well as for moral and emotional support. I am indebted to my mom and my dad for their unconditional love and support. Without their support, I wouldn't be able to pursue my dreams and goals. It's through their faith in me, I could come this far.

This Dissertation is dedicated to my grandparents, uncles, mom, dad and my brother, and all the teachers, mentors and advisors who have helped me in my learning process

Contents

List of Figures

List of Tables

List of Abbreviations

ACK- Ammonium-Chloride-Potassium

AF647- Alexafluor 674

ANOVA- Analysis of variance

APC- Allophycocyanin

Arg – Arginase

ATCC – American type culture collection

BMDM – Bone marrow derived macrophages

CCL2- chemokine CC motif ligand 2

CCR 7- CC motif chemokine receptor 7

CD 206 – Cluster of differentiation 206, M2 marker

CD 80- Cluster of differentiation 80, M1 Marker

CD 86 – Cluster of differentiation 86, M1 Marker

CD163- Cluster of differentiation 163, M2 Marker

CHX – Chitohexose-6-HCl

COS 6 – Hexa-N-Acetyl Chitohexose

DC - Dendritic cells

ECM- Extracellular matrix

FBR - Foreign body response

FGF- Fibroblast growth factors

FITC- Fluorescein Isothiocyanate

GM-CSF - Granulocyte macrophage colony stimulating factor

Hrs- Hours

IFN- Interferon

IL- Interleukin

iNOS – inducible Nitric oxide synthase

LPS – Lipopolysaccharide

M1 – Classically activated M1 defined macrophage

M2 – Alternatively activated M2defined macrophages

M-CSF – Macrophage colony stimulating factor

MHCII – Major histocompatibility complex class II

MPS - Mononuclear phagocytic system

NF-κB - Nuclear Factor kappa B

PBS – Phosphate buffered saline

PCR- Polymerase chain reaction

PDGF- platelet derived growth factor

PD-L1 – Programmed cell death ligand 1

PE- Phycoerythrin

PVA- Polyvinyl alcohol

RPM – Revolutions per minute

rr – Recombinant rat

SD- Standard Deviation

SE – Standard error

TGF – Tumor growth factor

Th1- T helper cell type 1

Th2- T helper cell type 2

TLR- Toll like Receptor

TNF- Tumor necrosis factor

VEGF- Vascular endothelial growth factor

Publications from this Dissertation

1. Bajpai, G., Simmen, R. C., and Stenken, J. A. (2014). In vivo microdialysis sampling of adipokines CCL2, IL-6, and leptin in the mammary fat pad of adult female rats. *Mol BioSyst, 10*(4), 806-812.

Chapter 1: General Introduction

1.1 Foreign Body Response and Wound Healing

Surgical implantation of biomaterial medical devices leads to a series of cellular and molecular cascades that are broadly termed the foreign body response (FBR). The FBR [1, 2] is a mechanism to protect the host against foreign materials. For medical devices, the FBR leading to encapsulation of the device is not desirable as it results in chronic inflammation and prevents complete healing. The ultimate result of the FBR is the encapsulation of the implant in a collagenous bag owing to its big size (> 5μm) which the body is unable to destroy.

Encapsulated devices have questionable "reliability". For example, glucose sensors after being encapsulated might still be functional, but signals will be relevant only to the microenvironment of the collagenous bag and will not reflect glucose levels of the normal body homeostasis. Implantable glucose sensors are approved to be used only for up to seven days by the FDA [3]. This is an issue as the patient has to use a new device every 7 days and go through the implantation procedure associated with it. Thus, it would be desirable to enhance the implant life by modulating the FBR. Figure 1 depicts the microenvironment of the sensor as a result of FBR.

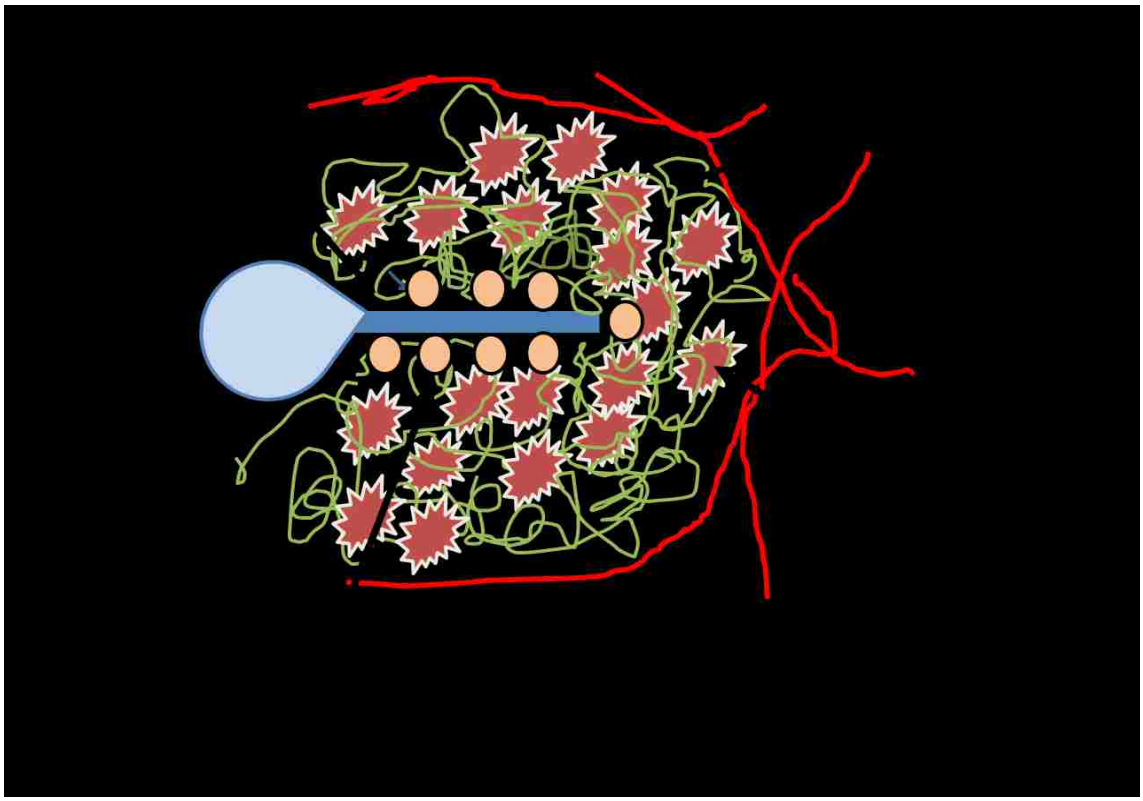

Figure 1. Microenvironment of sensor due to FBR

The picture depicts the various events that take place around the implanted biomaterial: the adsorption of proteins onto the surface, cellular infiltration, followed by capillary formation and collagen deposition that ultimately lead to fibrosis. (Adapted from Sensors (Basel). 2009; 9(11): 9275–9299)

Implantation of any device requires surgery resulting in wounding, trauma and perturbation of the local tissue homeostasis. Thus, the wound healing process is initiated after any device is implanted including sensors. Sometimes investigators consider FBR as a distinct phenomenon not related to the events that take place in the normal wound healing process, but FBR and wound healing are similar processes, except that the chronic presence of the artificial biomaterial leads to encapsulation and thus deviation from the normal wound healing process. The FBR begins with the wound healing. A brief review of the process is required and where the contrasts lie in the two processes will be dissected as the discussion of the stages of FBR and wound healing progresses. Generally, wound healing can be divided into "inflammatory stage", "reparative stage" and "remodeling stage". It is crucial to point out that wound healing is a continuous dynamic process; however, for the sake of understanding and convenience, it is divided into stages.

The inflammatory stage begins with the initial injury. Figure 2 shows the various stages of wound healing. The inflammatory stage facilitates healing and aims at destroying or neutralizing the injurious agent. Platelets play a role in fibrin matrix formation, which causes blood clot formation. thereby stopping the bleeding. Platelets adhere to the fibrin matrix, aggregate and release platelet derived growth factor (PDGF) and other chemokines (small proteins between 8-12 kDa that mediate kinesis or movement of cells toward a specific site) that later aids in neutrophil recruitment [4, 5]. After cessation of blood loss, blood vessels dilate to allow other chemical mediators, proteins and cells (first neutrophils and then macrophages) to arrive at the injured site. This results in swelling at the site of the injury caused by the influx of fluid. The fluid is called the exudate. At this stage, signs of inflammation are called erythema (redness), edema (swelling), heat and pain. Neutrophils are short lived cells (24 to 48 hrs) and are the first ones to arrive at the site within the first few hours of injury. These phagocytic cells help in debriment (removal of debris

and dead cells) of the wound [6]. Neutrophils subside within 48 hours and monocyte/ macrophages start to migrate to the site. Macrophages remain at the site throughout the wound healing phase and carry out wide variety of functions which will be discussed in later sections.

The reparative or proliferative stage begins to close the wound area or, in other words, to rebuild the wound area with new tissue. The new tissue is called granulation tissue and it is comprised of collagen, extracellular matrix, macrophages and fibroblasts. Formation of new blood vessels takes place via angiogenesis. Fibroblasts and myofibroblasts cells multiply to fill up the wound area. Fibroblasts secrete collagen and deposit matrix to close the wound area. Finally, a process known as “epithelialization” results into resurfacing of the wound by epithelial cells. Resolution of the wound takes place in the final remodeling phase. During this phase, matrix components mature. Collagen is converted from type III to type I collagen [7, 8]. Healing is achieved and scar tissue is formed.

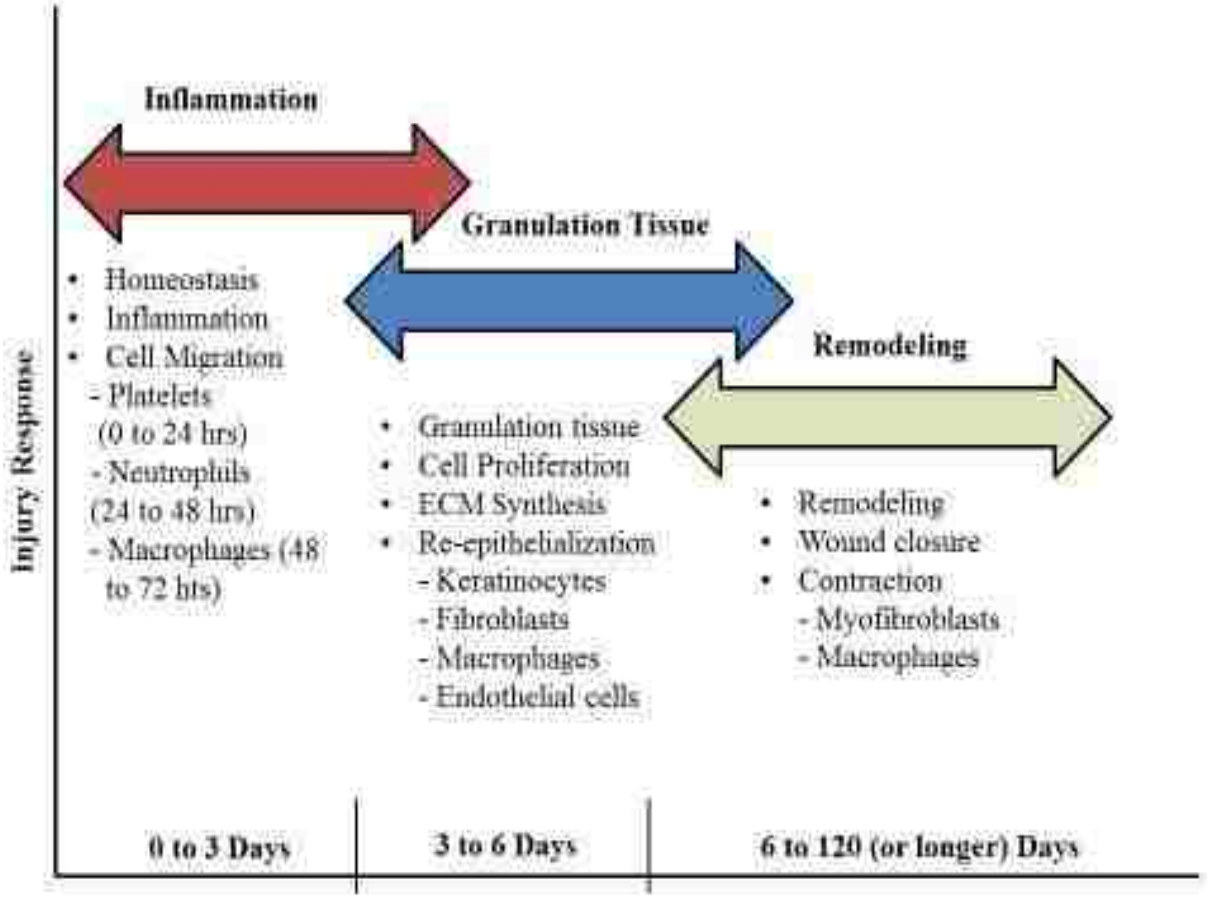

Figure 2. Stages of wound healing

The Figure shows the progression of wound healing through various stages with the various mediators at each stage. (Adapted from www.worldwidewounds.com)

As mentioned before, FBR stages are similar to the wound healing stages. FBR involves similar steps of blood material interactions, blood clotting, adsorption of proteins at the material surface, cellular infiltration and granulation tissue formation. Complete healing is inhibited because of the persistent presence of the implant which results in chronic inflammation, foreign body giant cell formation (FBGC, multinucleated macrophages formed by fusion of 10 or more macrophages) and encapsulation of the implant in an avascular collagenous bag [1]. Why healing does not occur as normal healing around the implant is an active area of research. Understanding of underlying mechanisms would help in modulating the biological outcome of the implants so that their performance and longevity can be enhanced *in vivo*.

Among the key cellular players in FBR are macrophages [2]. Since devices/biomaterials are too big to be phagocytosed, macrophages fuse to form foreign body giant cells that remain at the implant site secreting mediators to destruct the surface. Macrophages carry out wide variety of roles and secrete a wide array of chemical mediators which will be discussed in following sections. These cells exist in different phenotypic states promoting inflammation or healing [9]. One of the possible ways to modulate the outcome of FBR is through the modulation of macrophage phenotypes using stimulants (cytokines or glucocorticoid drugs such as dexamethasone) towards a phenotype that promotes healing. The aim of this dissertation is to understand the macrophage phenotypic changes in response to modulators using a microdialysis probe implant model and PVA sponge implant models *in vivo*.

1.2 Macrophages

1.2.1 Macrophage and Mononuclear Phagocytic System

The mononuclear phagocytic system (MPS) includes dendritic cells (DC), monocytes, and macrophages [10]. Dendritic cells specialize in antigen presentation. Macrophages are phagocytic cells of the innate immune system originally discovered by Illya Mechnikov in 1884. Macrophages originate from monocytes, which are white blood cells. Monocytes originate from common myeloid progenitors in the bone marrow. The macrophage colony stimulating factor (MCSF-1) and the granulocyte colony stimulating factor (GM-CSF) direct the production of mononuclear phagocytes from the progenitor cells [11]. At the macrophage and DC progenitor (MDP) stage, commitment to mononuclear phagocyte lineage is determined. From MDPs, monocytes and common DC progenitors (CDP) are derived. Monocytes differentiate into macrophages or DC, but CDPs are committed to DC lineage only. Monocytes circulate in the blood stream and migrate to tissues. Almost every tissue type has a resident tissue macrophage population. Based on the in-tissue distribution macrophages have a given special names.

1.2.2 Macrophage Heterogeneity

Mature macrophages are heterogeneous cells varying in cell surface receptor expression, morphology and functions [12, 13]. Peripheral blood monocytes that give rise to various tissue macrophages are also heterogeneous [14]. Human peripheral blood monocytes have been classified into classical, intermediate and non-classical subsets depending on the relative expression of cell surface receptors CD14 (LPS Co-receptor), CD16 (Fcγ RIII) and CD64 (Fcγ

RIV), and also chemokine receptor expression CCR2 and CX3CR1 [15]. These subsets have relative expression of TNFR (tumor necrosis factor receptor) as well. Non-classical subsets have highest expression of TNFR2 receptor. The intermediate subsets have low expression of TNFR2 while classical subsets have the lowest of all three. The TNFR1 expression is highest in intermediate subsets, then classical subsets, and lowest in non-classical subsets.

Mouse and rat macrophage marker subsets also share similar heterogeneity. Mouse monocytes have three subsets based on the cell surface receptor expression of Ly6C (differentiation marker on monocyte/dendritic cell precursors in mid stage development), CD43 (transmembrane sialoglycoprotein on monocytes, T cells and B cells) and CD11b (integrin alpha M/Macrophage-1 antigen), and chemokine receptor CCR2 (receptor for chemokine CCL2) and CX_3CR1 (receptor for chemokine fractalkine involved in cell adhesion) [16-18]. The classical subset is defined as $Ly6C^{high}CD43^{low}CD11b^{+}CCR2^{high}CX_3CR1^{low.}$ The intermediate subset is defined as $Ly6C^{high}CD43^{high}CD11b^{+}$. The non-classical subset is defined as $Ly6C^{low}CD43^{high}CD11b^{+}$ with low expression of CCR2 but high expression of CX_3CR1 chemokine receptor. In rats, monocyte subsets exist as $CD43^{high}$ and $CD43^{low}$. The $CD43^{low}$ monocytes have higher expression of CCR2, CCR7 and CD32 whereas $CD43^{high}$ monocytes have higher expression of CD4, CX3CR1 and CD11c [12].

The spleen can be used as an example to show macrophage heterogeneity. The rodent spleen is rich in sub-populations of macrophages. Macrophages in the red pulp part of the spleen have express high levels of F4/80 antigen and mannose receptor (MR) [19]. Their key role is in the clearance of senescent erythrocytes. Marginal zone (MZ) macrophages in the spleen lack expression of antigen F4/80 [20]. Macrophages found in the white pulp of the spleen express pan macrophage marker CD68 but lack F4/80 antigen marker.

The peritoneal cavity contains distinct populations of macrophages which vary in receptor expression and size [21]. The subset one has relatively larger cell size and expresses markers CD11b and F4/80. They are the predominant subset in unstimulated animals (not treated with LPS or thioglycolate). Upon stimulation of the peritoneal cavity with thioglycolate or lipopolysaccharide (LPS) they significantly decrease in number and another subset becomes the dominant population. The other subset has lower levels of CD11b and F4/80 expression but they have high expression of MHCII marker. Both the subsets have phagocytic and nitric oxide (NO) production capabilities.

1.2.3 Macrophage Functions

It has now been well established that macrophages perform a wide variety of functions and are not limited to simply phagocytosis in host defense. Macrophages have been shown to regulate developmental processes. Not only do they clear debris of dead cells but also play a role in apoptosis [22]. Thus, they initiate and protect cells from apoptosis. Macrophages play a role in tissue patterning. Studies in PU.1$^{-/-}$ strain of mice (which lack the transcription factor required for differentiation of immune cells and macrophages) showed altered hindbrain vasculature [23]. Studies in mice that lack *csf1* gene (C*sf1*$^{op/op}$ mice) (colony stimulating factor-1), which have severe deficiency of MPS, show abnormal vascular patterning in the hindbrain [24].

Macrophages participate in lipid metabolism. Macrophages have been correlated with fat mass in studies involving whole body lipid metabolism [25]. Studies have shown that macrophages are involved in maintenance of blood pressure [26]. Another critical function of macrophages in homeostasis is in maintenance of hematopoietic cell levels. Macrophages clear

millions of neutrophils and erythrocytes from circulation every day. They also clear dead cells from the spleen, thymus and other tissues. This process does not cause them to release pro-inflammatory molecules.

Macrophages not only play role in innate immune response by phagocytosis of pathogens they are also involved in activating adaptive immune responses. Along with DCs, they are the major cells in antigen presentation to T-lymphocytes and are thus included in the category of professional antigen presenting cells. Presentation of antigens is a crucial step for activation of adaptive immunity. They express MHCII receptors on their surface that are engaged in antigen presentation to CD4 T helper cells.

As mentioned previously, macrophages play critical roles in inflammation, tissue repair and healing. Upon injury, macrophages migrate from blood to the site in response to chemokines specifically CCL2. Infiltrated macrophages secrete various inflammatory mediators to clear pathogens from the site. They remove neutrophils at the wound site, a process known as efferocytosis. Studies have shown that neutrophil clearance is a critical part of wound healing. Macrophages are capable of secreting various cytokines, chemical mediators (NO and prostaglandins) and growth factors such as PDGF (platelet derived growth factor), TGF (transforming growth factor) and FGF (fibroblast growth factor). These factors promote proliferation and migration of cells such as fibroblasts at the wound site, which indirectly influences the extracellular matrix (ECM) formation. They also secrete pro-angiogenic factors such as VEGF (vascular endothelial growth factor), which promote vascularization at the wound site to promote wound healing [27]. Macrophages are also a source of chemokines, inflammatory and anti-inflammatory cytokines such as IL-1β, IL-4, IL-6, IL-10 and TNF-α. These cytokines are secreted during various stages of FBR/wound healing progression as discussed before.

1.3 Macrophage Polarization/Activation

It is clear that macrophages are highly versatile and pleiotropic in nature, carrying out a wide variety of functions. This certainly begs the question: how macrophages are able to carry out such diverse functions? The answer lies in their phenotypic plasticity. Macrophages get activated by engagement of specific cell surface receptors with a variety of stimulants such as bacterial products, lipid products [28] and cytokines present in local milieu and are able to adapt to the microenvironment accordingly. Macrophages have been classified according to the activation patterns which follows the previously established Th1/Th2 (T helper type 1 / T helper type II) paradigm. According to new recommendations and nomenclature guidelines by Suttles et al. [29], macrophage polarization should be referred as macrophage activation, and macrophage phenotypes should be stated according to the stimulus and not just broad M1/M2. For instance, macrophage activated in response to IL-4 should be stated as M(IL-4) and so on. Since this is a very recent recommendation, this dissertation will use the new nomenclature, but will also provide background on what nomenclature has been for three decades in the field.

1.3.1 Classically Activated Macrophages

Inflammatory macrophages or **"M1"** macrophages are elicited in response to bacterial endotoxin lipopolysaccharide (LPS) or inflammatory cytokines including but not limited to Interferon-Y (IFN-γ) and Interleukin-1 (IL-1). The M1 profile activation is also termed as *"classical activation"* of the macrophages. The classically activated macrophages are generally recognized as IL-12^{high}, IL-23^{high} and IL-10^{low} profiles [30]. They are inflammatory in nature secreting pro-inflammatory cytokines including, but not limited to, interleukin-1β (IL-1β),

interleukin-6 (IL-6) and tumor necrosis factor-α (TNF-α), and mediators, inducible nitric oxide synthase (iNOS), which results in nitric oxide (NO) production enhancing microbicidal activities. Classical activation also causes enhancement of certain surface receptors, CD86, CD80 and MHCII. Macrophages generated in response to LPS will be referred as M(LPS).

1.3.2 Alternatively Activated Macrophages

The "*alternative activation*" of macrophages was first described by Stein et al., [31]. The alternatively activated macrophages or "**M2**" macrophages are generated in response to cytokines IL-4 and IL-13. The alternatively activated profile is recognized as IL-10^{high}, IL-12^{low} and IL-23^{low} profile. They are considered to be anti-inflammatory in nature. The M2 profile has been sub-classified as "M2a", "M2b" and "M2c". M2a profile is generated in response to IL-4 which according to new nomenclature should be referred as M(IL-4)[29]. The M2b profile is generated via IL-1R ligands, immune complexes with LPS which now will be referred to as M(Ic). The M2c profile activation occurs in response to IL-10, TGF-β and glucocorticoids such as dexamethasone. Again, this is based on previous norms, but according to new nomenclature (to avoid confusion), M (IL-10) or M(dex) will be used. Overall, the M2 profile shows shifts in arginine metabolism viz high arginase activity. The M2 profile show enhancement of cell surface receptors CD206, CD163 and CD209 [32]. The M2 macrophages help in the development of Th2 responses such as parasite encapsulation, allergies and tissue remodeling.

1.3.3 Biomarkers and Identification of Differentially Polarized Macrophages

Combinations of assays have been used for the identification of various macrophage phenotypes. There is no agreed upon standard as to which assay should be used. Measurement of secreted cytokines using ELISA, identification of cell surface receptor expression using flow cytometry assays or immunohistochemistry, and/or measurements of RNA transcript using qRT-PCR analysis have been the most commonly used methods. Some researchers have used transcriptomics analyses as well to elucidate the detailed changes in the gene expression profile of differentially polarized states of macrophages and for the identification of novel markers [33]. Table 1 shows the list of cell surface receptor expression profiles of differentially polarized states of macrophages. The M2 subsets are harder to identify due to the relative expression profile of various markers. To summarize,

M1 phenotype will be expected to have: $MHCII^{high}$ $CD86^{high}CD80^{high,}CCR7^{high}CD163^{-}CD204^{-}$

M2a profile will be expected to have: $CD209^{high}CD206^{high}CD163^{low}CD16^{low}$

M2c profile will be expected to have: $CD163^{high}CD16^{high}CD206^{low}CD209^{low}$

To date, most of the *in vitro* studies have been performed in mouse macrophages. Thus most of the biomarker information has come from these studies. In alternatively activated mouse macrophages, Ym1, Fizz1 and arginase 1 serve as important biomarkers [34]. However, expression of Ym1 and Fizz1 in human macrophages is not present. Ym1 and Fizz1 markers have not been studied in rats in detail [35]. This clearly indicates interspecies differences and therefore the need to evaluate macrophage phenotypes on a case-by-case basis. The identification of novel markers is still open ground.

Table 1. List of markers and their degrees of expression between differentially-activated macrophages

Markers	M(LPS/IFN-Y)	M(IL-4)	M(IC)	M(IL-10)	References
CD 80	++	-	+	-	[9], [36]
CD86	++	-	+	_	[9], [36]
MHC II	+++	+	+	_	[37], [38], [39]
CD 40	++	-		_	[40]
CD 36	_	+		+++	[33]
CD 163	-	+		+++	[41], [42]
CD 206	-	+++		+	[29], [41], [36]
CD209	-	+++		+	[30], [43]
Stabilin 1	-	+++		+	[43]
CD 204	-	+		+++	[43]
Dectin 1	-	+++		+	[43], [44]
CD16/32	-	+		+++	[45]
CD14	-	+		+++	[45], [46]
CCR7	+++	-	-	-	[9], [47]
CD68	++	+		+	[9], [42]

- indicates no expression

+ indicates expression present

++ indicates moderate expression

+++ indicates abundant expression

1.3.4 Clinical Implications

Different phenotypic states of macrophages have been implicated in various pathological conditions including, but not limited to, atherosclerosis, tumor biology and metabolic disorder. Elucidation of pathways governing macrophage polarization/activation will be of significant interest for the development of novel clinical strategies in a given pathological condition. There is an enormous interest in the various macrophage phenotypic states in the field of regenerative medicine. The idea is to "re-educate" the macrophages to phenotypically adapt a desired phenotypic profile in a given pathological condition. For example, research in tumor biology has shown presence of alternatively activated M2-like macrophages that promote tumor progression. It would be desired to modulate the phenotype to an "M1"-like pro-inflammatory state to have tumoricidal properties.

A long term aim in the biomaterials community is to enhance the implant life and reduce fibrotic encapsulation around the implant. In this case it would be desirable to shift the macrophages towards pro-wound healing and tissue remodeling "M2c or M(IL-10)" phenotype. This is a novel strategy and not enough literature is available with respect to modulating macrophages to reduce fibrosis. The idea is to be able to achieve M2c/M(IL-10) phenotype *in vivo* based on several published *in vitro* results. However, it is important to mention that classification has been applied for the sake of simplicity and understanding. *In vivo*, macrophages exist as a continuum of various polarization/activation states. *In vivo* it is extremely challenging to isolate and identify differently activated phenotypic states due to relative expression of various markers. Phenotypes present *in vivo* are mixed that do not really fit the M1/M2 paradigm [48]. Thus, as mentioned before, an in-depth understanding of full spectrum of macrophage phenotypic states needs to be carefully dissected on a case-by-case basis.

1.4 Cytokines

Cytokines are proteins that are involved in cell signaling and communication. The chemokines, interferons and interleukins are all classified as cytokines in broad terms. They are produced by macrophages as discussed above and also by variety of other cell types, including T- cells, B-cells, fibroblasts and endothelial cells. So far more than 100 cytokines have been identified [49]. The mechanism of action involves binding of cytokines to their receptor which results into the further signaling cascade downstream of receptors. Cytokines play roles in a variety of mechanisms such as apoptosis, cell proliferation, cell migration, survival and growth. The cytokines that have been measured experimentally for this dissertation will be discussed in more detail in the sections below.

1.4.1 Interleukin-1

The IL-1 family is one of the major pro-inflammatory cytokine families. IL-1 is involved in the initiation and regulation of inflammatory phases of wound healing and FBR [50, 51]. This family is represented by two ligands: IL-1α and IL-1β; one receptor, antagonist IL-1Ra (receptor antagonist); and two receptors, IL-1R tI (type I receptor) and IL-1R tII (type II receptor). Ligands IL-1α and IL-1β are biochemically distinct, but are structurally related [52]. A short stretch of amino acid homology (about 20%) exists between them. Both forms are encoded by separate genes located on chromosome 2. The IL-1 gene is comprised of six introns and seven exons. Both the forms are produced as precursor proteins of size 31 kilo Dalton (kDa), and biological activity is acquired upon cleavage by specific enzymes resulting in mature active forms that are of 17 kDa

each [53]. Both the forms are non-glycosylated. IL-1 Ra is the natural receptor inhibitor of IL-1α and β forms.

IL-1 is produced in response to antigenic challenge or injury. Macrophages are the primary source of IL-1 production but other cell types such as epithelial, epidermal, other lymphoid and vascular tissues also secrete IL-1 [54]. IL-1 is the key player in immediate events of host defense reaction to the pathogen. It works in a paracrine mode by stimulating neighboring cells to synthesize and release chemokines for the recruitment of various cell types such as polymorphonuclear cells, monocytes and T lymphocytes. It also signals other cells to secrete other cytokines such as IL-2, IL-4 and IL-6.

Binding of IL-1 to its receptor IL-1R leads to signal transduction pathway that ultimately activate transcription factor NF-κB. The NF-κB is an important transcription factor involved in many processes of cell survival, apoptosis and proliferation. The IL-1R has two receptor associated kinases IRAK (interleukin receptor associated kinases) 1 and 2 that take part in the activation of NF-κB. Binding IL-1Ra to IL-1R blocks the signaling.

1.4.2 Interleukin-4

The IL-4 is a pleotropic cytokine with a molecular weight of ~15 kDa. It is known for its role in differentiation of naïve T helper cells to a Th2 phenotype. It is regarded as an anti - inflammatory cytokine. Sources of its secretion are T cells, macrophages, basophils, eosinophils and mast cells. IFN-γ producing CD4+ T cells are suppressed by IL-4. It also controls the immunoglobulin class-switching in B cells from IgE to IgG.

IL-4 regulates the macrophage alternative activation as mentioned in previous section. IL-4 has been implicated in fibrosis; thus, it is crucial in wound healing and FBR studies [55]. IL-4 induces giant cell formation in cultured macrophages [56]. Giant cells also surround the implanted biomaterials and thus formation of foreign body giant cells has been linked to IL-4 [57].

IL-4 binds to IL-4Rα receptor (K_d 20 to 300 pM), a second common gamma chain then recognizes the IL-4-IL-4Rα complex. This arrangement is described as type-1 receptors. A type 2 receptor is comprised of IL-4Rα bound to either IL-13Rα1 or another IL-4Rα. This receptor arrangement can recognizes both IL-4 and IL-13. Engagement of IL-4 with a type 1 receptor (IL-4Rα and γc chain) results in to phosphorylation of Janus kinases (JAK) 1 and JAK3. Phosphorylated JAK1 and JAK3 then phosphorylate the "signal transducer and activator of transcription" (STAT) 6 protein, which then dimerizes and translocate to the nucleus. STAT6 is a key transcription factor for processes IgE production, Th2 differentiation and allergic reactions. Interaction of IL-4 with a type 2 receptor (IL-4Rα and IL13-Rα1) leads to phosphorylation of JAK2 and tyrosine kinases (TYK) 2 which in turn leads to an insulin substrate receptor 1/2 (IRS) signaling pathway leading to cell growth and survival.

1.4.3 Interleukin-6

IL-6 is a 38 kDa pleiotropic cytokine whose primary function *in vivo* is the initiation of the acute phase response during inflammation and infection. It is mainly regarded as a pro-inflammatory cytokine, but it has anti-inflammatory properties as well [58]. It is a multi-functional cytokine playing important roles in cell survival, proliferation and apoptosis [59, 60]. IL-6 expression is induced by LPS along with TNF-α and IL-1 from activated macrophages [61, 62]. It

regulates the expression of other cytokines and chemokines, and the differentiation of macrophages and dendritic cells during acquired immune responses [59, 60, 62-64]. In wound healing it appears during the early inflammatory phase, and expression is also present during the later phases of granulation tissue formation. Studies have shown lack of IL-6 results in impaired wound healing and epithelialization.

IL-6 receptor is comprised of a ligand binding subunit gp80 and a signal transducing subunit gp130. Ligand binding results in phosphorylation of JAK, which then phosphorylates STAT3. Phosphorylated STAT3 translocates to the nucleus where it controls the expression of genes involved in survival and apoptosis. Other signaling pathways induced by IL-6 other than the JAK/STAT pathway include the MAPK and PI3K pathways. Because of the many important roles of this cytokine, its expression is tightly regulated in a cell. Transcription factors NF-κB, NF-IL-6, CREB and AP-1 have been shown to modulate IL-6 gene expression [65-68]. Among all transcription factors recognized, NF-κB is the key nuclear factor controlling the expression of IL-6.

1.4.4 Interleukin-10

The IL-10 is 18 kDa type II cytokine and is also known as "**human cytokine synthesis inhibitory factor"** with important immunoregulatory fucntions. IL-10 was first identified by Mosmann and colleagues [69]. IL-10 is secreted by monocytes, macrophages and T helper type II cells and T regulatory cells. IL-10 is a pleiotropic cytokine. It inhibits the cell mediated branch of the immune system by inhibiting pro-inflammatory type 1 cytokines IL-1, TNF-α and INF-γ, down-regulating MHCII antigens and co-stimulatory molecules in macrophages. It enhances the

humoral branch of immune system by enhancing B cell survival, proliferation and antibody production [70]. It can block NF-κB activity.

IL-10 is involved in tissue remodeling during the later stages of wound healing [71]. Scarless healing was observed in fetal wounds as opposed to postnatal wounds that usually heal with scars [72]. Scarless and regenerative healing in fetal wounds was linked with IL-10. This led to the hypothesis that makes IL-10 a very attractive potential candidate for wound healing and biomaterial studies as anti-fibrotic agent. Few studies have shown positive effects IL-10 on wound healing and FBR [73-75]. However, there are other studies which show IL-10 induces fibrosis [76]. One study shows that mice deficient in IL-10 have expedited healing of wounds [77]. It is clear that there is dire need of thorough detailed studies on IL-10 as a potential anti-fibrotic agent in biomaterials and wound healing field. Also, the doses and timing of IL-10 delivery need to be thoroughly investigated.

IL-10 has two cell surface receptors IL-10R1 and IL-10R2. IL-10R1 binds IL-10 with high affinity (~1 nM), and IL-10R2 binds IL-10 with comparatively less affinity (~0.5 nM) [78]. Both the receptors belong to type I membrane proteins containing extra cellular and cytoplasmic domains that are connected by a membrane-spanning helix. IL-10 first binds to IL-10R1 and then IL-10R2 binds to IL-10-IL-10R1 complex resulting in functional tetramer complex. Functional receptor complex then results in phosphorylation of receptor associated Janus Kinases1 (JAK1) and Tyrosine Kinases 2 (TYK2). This results in the phosphorylation of specific tyrosine sites on the receptor which in turn act as the docking site for the STAT3 transcription factor. STAT3 then gets phosphorylated by receptor associated JAK1 and TYK2 [79]. Upon phosphorylation, STAT3 migrates to the nucleus and regulates the transcription of pro-apoptotic genes and genes for in cell cycle progression. STAT3 also results in activation of transcription factor "suppressor of cytokine

synthesis 3" (SOC3), which results in negative feedback regulation of IL-10/JAK1/STAT3, signaling and suppression of inflammatory cytokines IL-1β, IL-6 and TNF-α [80].

1.4.5 Tumor necrosis factor TNF-α

Tumor necrosis factor is the principal mediator of inflammatory responses in response to bacteria and other microbes causing infection [81]. The source of TNF is activated monocytes/ macrophages but other cell types like antigen stimulated T cells, mast cells, neutrophils and NK cells can also produce TNF. Circulating TNF-α protein is 51 kDa homotrimer. Two receptors for TNF have been recognized: Type 1 TNF receptor (TNF-RI) and Type II TNF receptor (TNF-RII) [82]. Most of the cell types have both of the receptors. Binding of TNF to these receptors lead to the activation of TNF receptor associated factors (TRAFs) in the cytoplasmic domain of the receptors which in turn activate transcription factors such as NF-kB and activation protein 1 (AP-1) leading to apoptosis.

1.5 Cell Surface Receptors

1.5.1 CD206

CD206 or mannose receptor C type 1 (MRC1) is present on macrophages and is involved in endocytosis and phagocytosis. It is involved in the recognition of mannose, fucose and N-acetylglucosamine residues in a Ca^{2+} dependent manner. It is a 162-175 kDa, C type lectin 1 transmembrane protein. It is present on other cell types as well such as epithelial cells, smooth

muscle cells, kidney mesangial cells and hepatic epithelium. CD206 is also involved in the presentation of antigens to T lymphocytes. In M2 macrophages, CD206 expression is enhanced by IL-4.

1.5.2 CD163

CD163 is 130 kDa type 1 transmembrane protein and is heavily glycosylated [83]. Its expression is restricted to monocytes and macrophages. Predominant expression of CD163 is found on the macrophages present in the red pulp of the spleen, alveolar macrophages and Kupffer cells of the liver. Tissue resident macrophages have higher expression of CD163 when compared to blood monocytes suggesting CD163 to be a differentiation marker from monocyte to macrophage lineage. Macrophages present during the acute phase and chronic phase of healing are also positive for CD163.

The CD163 receptor expression is controlled by glucocorticoids and cytokine IL-10. *In vitro* treatment of monocytes/macrophages with dexamethasone and IL-10 lead to enhanced expression of CD163 [84]. The M2c subset of M2 macrophages are identified by higher expression of this receptor. Inflammatory agents like LPS also control the expression of CD163 receptor. LPS treatment results into shedding of ectodomain of the receptor as early within 1 hour [85, 86]. The major biological function of CD163 is in the clearance of hemoglobin. The clearance of deformed red blood cells or senescent cells releases hemoglobin into plasma. Haptoglobin binds to free hemoglobin in the plasma, and this complex is recognized by the CD163 receptor leading to internalization.

1.5.3 MHCII and CD86

MHCII receptors are heterodimers of α (~35 kDa) and β (~25 kDa) transmembrane glycoprotein sub-units [87]. MHCII expression is present on macrophages, dendritic cells and B-cells. MHCII receptors play important role in antigen presentation to $CD4^+$ T lymphocytes. MHCII molecules recognize short peptide residues (12-13 amino acids long). MHCII expression is enhanced in inflammatory M1 macrophages upon activation via LPS or TNF. CD86 is also known as B7-2 protein. Its expression is present on cells of myeloid lineage (dendritic cells and macrophages). CD86 provides the co-stimulatory signal for the activation of T cells. Its expression is also enhanced in M1 macrophages.

1.6 Crucial Enzymes of Polarization States

1.6.1 Nitric Oxide Synthase (NOS)

The nitric oxide synthase enzyme catalyzes the production of nitric oxide (NO) via L-arginine in the body. In the M1 macrophages, arginine metabolism is shifted towards the production of NO which is an inflammatory mediator resulting from enhanced expression of iNOS. The NOS enzyme exists in various isoforms. NOS1 is present on neuronal tissue or smooth muscle cells. NOS2 or iNOS is present on monocytes and macrophages and plays a role in immune responses via its inducible action. NOS3 or eNOS is present on endothelial cells. Regulation of iNOS in macrophages occurs via receptor CD14 which is involved in LPS recognition. This leads

to NF-kB activation, which in turn enhances iNOS activity. Increase in iNOS activity upon IFN-γ exposure is linked to the activation of the JAK-STAT pathway.

1.6.2 Arginase

The enzyme arginase is involved in the metabolism of L-arginine to L-ornithine and urea. There are two isoforms of the enzyme, arginase 1 (Arg1) and arginase 2 (Arg2). Both enzymes catalyze the same reaction. However, their tissue distribution and regulations are different. The main location for arg1 is liver, and thus is it also called as hepatic arginase. Its subcellular location is cytosolic, but arg2 is mitochondrial. Both the isoforms are encoded by different genes, present on different chromosomes, independently. Arg2 is involved in the production of L-ornithine, which is further utilized for the production of polyamines. The polyamine production is linked to cellular proliferation and survival. Arginase expression is enhanced by IL-4, IL-13 and TGF-β, and thus regarded as the marker of M2 macrophages.

1.7 Adipokines

Adipocytes within the white adipose tissue secrete signaling proteins which are collectively called adipokines [88, 89]. Adipokines are involved in appetite and energy balance, homeostasis, immunity, lipid metabolism, insulin sensitivity, angiogenesis and inflammation and acute phase response. Some of the examples of adipokines include classical cytokines such as IL-6, IL-8 and TNF-α, hormones such as leptin, adiponectin and resistin, growth factors such as vascular

endothelial growth factor (VEGF) and acute phase factors such as haptoglobulin and metallotheionein.

1.7.1 Leptin

Leptin, a product of obese genes, is a 16 kDa non-glycosylated protein hormone secreted mainly by adipose tissues in proportion to body mass index [90, 91]. Leptin is involved in normal mammary gland development, appetite regulation and thermogenesis. There are six receptor isoforms differing in cytoplasmic domain length including four short isoforms (OB-Ra, OB-Rc, OB-Rd and OB-Rf), one soluble form (OB-Re) and one ubiquitous long isoform (Ob-Rb), and they belong to the class I cytokine family of receptors [90]. Binding of leptin to OB-Rb receptor causes activation of JAK2/STAT3 (Janus Kinases-2/Signal transducer and activator of transcription-3) signal transduction pathway [92]. JAK-2 activation results in phosphorylation of conserved residues in the cytoplasmic domain of Ob-Rb. Phosphorylated residues then act as binding sites for transcription factors such as STAT-3 and STAT-5. Leptin can also trigger the MAPK (mitogen activated protein kinase) pathway either through JAK-2 associated receptor phosphorylation or without receptor phosphorylation. PI-3K /AKT /GSK3 (Phosphatidylinositol 3-kinases/Protein kinase B/Glycogen synthase kinase 3) and AMPK (5' AMP-activated protein kinase) pathways are also activated by leptin. Ultimately these pathways activate several genes, such as *c-fos, c-jun, junB, egr-1 and SOCS3,* involved in cell proliferation and angiogenesis. Ob-Rb also activates, through unknown mechanisms, PLC-γ (Phospholipase C), P38 and PKC kinases, NO and NF-κB [93].

1.8 Microdialysis Sampling

Microdialysis is a well-established, minimally-invasive, diffusion-based sampling technique. It has been employed for the sampling of analytes from the extracellular space for over a decade, especially in the field of pharmacokinetics and neuroscience. A microdialysis probe is made up of a semi-permeable membrane, an inlet tubing and an outlet tubing. A syringe pump is used to pump the perfusion fluid (which matches in ionic strength with the extracellular fluid) from the inlet tubing and comes out of the outlet tubing and referred to as dialysate. Analytes can diffuse into the semi-permeable membrane due to concentration gradient and can be collected from the outlet tubing as the perfusion fluid is continuously moving. Figure 3 shows a typical microdialysis probe. Microdialysis sampling has been successfully employed for the collection of proteins such as cytokines. As proteins diffuse very slowly owing to their bigger size, a larger MWCO membranes (around 100 kDa) are needed. Ultrafiltration is a problem with larger MWCO membranes. To overcome this loss of fluid, Dextran or albumin are added. Dextran is complex branched polysaccharide comprising of glucose molecules. Dextran is synthesized by *Leuconostoc mesenteroides* and *Streptococcus mutans* from sucrose. Dextran size ranges from 3 to up-to 2000 kDa. Dextran, in microdialysis application, is used as an osmotic agent to prevent the loss of fluid across the semipermeable membrane (ultrafiltration). The addition of dextran to the perfusion fluid balances the osmotic pressure owing to its larger size and increase in solute concentration inside the membrane which overcomes the transmembrane hydrostatic pressure that drives the ultrafiltration. However, not any dextran can be added for this application. The size of the dextran should be large so that it does not diffuse out of the probe. Typically, Dextran 70 or higher ranges have been used.

Cytokines are typically present in low picomolar to femtomolar concentrations in the biological matrix and have low diffusivity which results in poor recovery of cytokines. Merits of the technique include continuous real time sampling over time in awake-and-freely moving animals and acquisition of analytically-clean samples that can be subjected to immunoassays without further processing. More details on the microdialysis technique are presented in chapter 6.

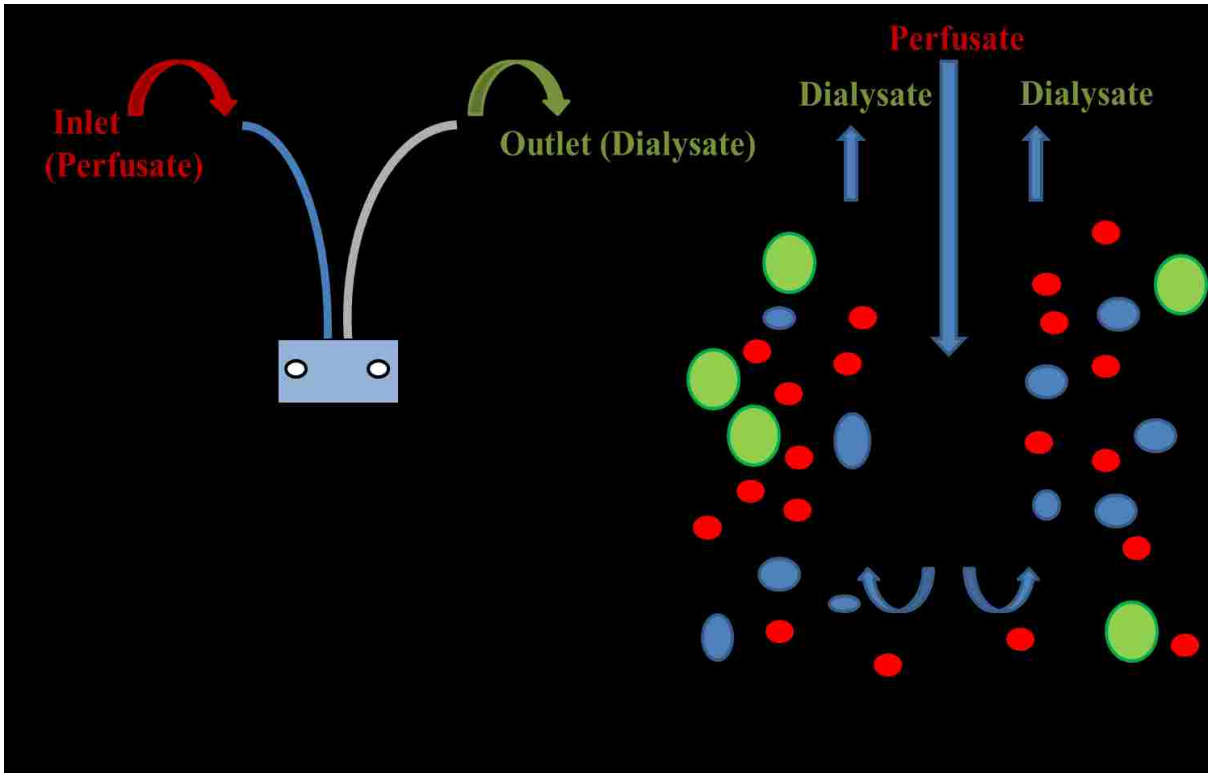

Figure 3. Schematic of microdialysis probe and functioning

A typical cannula style microdialysis probe has been shown in the Figure. The probe has an inlet and outlet tubing. Semi-permeable membrane is at the bottom. The zoomed out part of membrane region depicts the diffusion of analytes.

A microdialysis probe system can also be employed as a model system to study wound healing and FBR [94]. Insertion of a microdialysis probe requires surgical incisions leading to disruption of local tissue trauma and homeostasis disruption. Long term implantation of probe elicits the FBR finally leading to the fibrotic encapsulation of the probe. Implementation of microdialysis probe as a wound healing/ FBR model system allows for the sampling of cytokines over time as the stages of FBR progress. Since it's a diffusion-based technique, drugs of interest can also be delivered with the microdialysis probe at the site simultaneously with the sampling, and the effects brought about by the drug on the target analyte(s) can be monitored over time.

1.9 PVA Sponge Model of Wound healing and FBR

The polyvinyl alcohol (PVA) sponge model has been employed extensively for understanding wound healing. Usage of PVA-sponges dates back to 1950 in reconstructive surgery, but they were later discontinued in reconstructive surgery due to poor performance in long term applications [95]. However, it has been employed for research purposes [96]. It has been used for studying granulation/reparative tissue ingrowth. It also elicits FBR, resulting in giant cell formation and fibrosis after ~ 2 weeks. The use of PVA sponges allows for the sampling of wound fluid and variety of cytokines, and chemokines present can be quantified representative of the time point targeted. Thus, a temporal profile of cytokines and chemokines can be obtained. One of the other major advantages of employing the PVA sponge model is isolation of wound cells, which can further be characterized by either flow cytometry or gene expression assays. The collection of wound fluid and wound cells allows for both qualitative and quantitative assessment of the

FBR/wound microenvironment. Another advantage of the PVA sponge is the delivery of drugs into the sponge space to understand the drug effects on FBR/wound microenvironment. The PVA-sponge can be loaded with the drug of interest or drugs can directly be injected into the implanted PVA-sponge, and its effect on cells and cytokines or in other words manipulation of the process can be assessed from the samples collected. One major drawback of the PVA-sponge model is the usage of relatively higher number of animals, as the animal needs to be euthanized to collect data on a chosen time point of study. Thus to collect data on various times points and to have enough biological replicates many animals are needed.

1.10 Dissertation Aims

A long term aim in the biomaterials community is to enhance the implant life and reduce fibrotic encapsulation around the implant. Macrophages are the key cellular players that are involved in the cascade of events that lead to fibrosis around the implanted device. The recent discovery that macrophages can be immunomodulated to a desired phenotype offers a potential opportunity to minimize the FBR. In this case it would be desirable to shift the macrophages towards the pro-wound healing and tissue remodeling "M2c or M(IL-10)" phenotype. This is a novel strategy and not enough literature is available with respect to modulating macrophages to reduce fibrosis *in vivo*. The hypothesis that M(IL-10) phenotype is desired *in vivo* is based on in vitro cell culture stimulation studies. Thus, this is a new field and lacks translational studies.

A few points to consider are:

1. Most of the data on in vitro polarization/activation of macrophages has come from murine macrophages. Rats serve as important model organisms, and studies describing macrophage polarization biology in rats are lacking.

2. Also, *in vivo,* it is extremely challenging to isolate and identify differently activated phenotypic states due to relative expression of various markers. What phenotype is present at a given stage of the FBR progression is crucial to delineate in order to immunomodulate them to a desired profile. Thus, as mentioned before, an in-depth understanding of full spectrum of macrophage phenotypic state needs to be carefully dissected on a case-by-case basis.

Thus, the research objectives were to:

1. Establish immunomodulation of rat derived macrophages in response to various modulators. Successful immunomodulation of rat splenic macrophages was achieved in vitro in response to the modulators.

2. Perform *in vivo* microdialysis delivery experiments to establish the effects of IL-4/IL-10 around the implant site by comparing and measuring recovered cytokines (CCL2, IL-1β, IL-6, IL-10) and histology differences between the control and treatment probe. However, no differences between control and treatment probe could be established.

3. The challenges with microdialysis FBR model led to the use of sponge model. The objective were to measure and compare the cytokines in the wound fluid and to isolate and characterize the wound macrophages from control and treatment sponges *in vivo* in rats. Mild immunomodulation of macrophages was observed at protein and gene expression level in response to IL-10 treatment. Histological studies would need to be performed in separate experiments to determine how the extent of FBR was modulated.

Thus, in the context of persistent biological problem of FBR and how the new field of immunomodulation of macrophages can be a potential opportunity to solve the problem, this study is a fundamental step taken in the direction of understanding immunomodulation of macrophages in vitro and *in vivo* in rats as model system

The focus of the research revolves around understanding inflammatory responses to biomaterials. Especially of interest are macrophages and macrophage-derived proteins such as cytokines and chemokines and how they collectively modulate the outcome of FBR/wound healing. As mentioned previously, macrophages are the key cellular mediators in host responses to biomaterials. A thorough understanding of their secreted proteins and phenotypic adaptations in responses to microenvironmental cues at various stages of FBR/wound healing can provide great insight that may help in designing better *in vivo* sensors. The long term aim of the research is to modulate the macrophage phenotype towards the wound healing phenotype at the implant site which may lead to better outcomes of the FBR and thus leading to complete healing at the site without encapsulation.

The use of microdialysis probes allows for the real time sampling of proteins as well from the FBR- microenvironment created due to the insertion of the microdialysis probe. With the implanted microdialysis probe, a temporal profile of target proteins at various days of FBR can be generated. A microdialysis probe can also be used as a delivery device for the target drug at the site. Thus, a modulator/target drug can be delivered simultaneously along with the collection of target proteins. The advantage is that changes brought by delivery of modulator on a target protein can be monitored over time.

This dissertation explores the phenotypic changes of macrophages and secreted proteins by modulators *in vitro* and *in vivo* in FBR models of microdialysis and PVA sponges in rat subjects. As mentioned in previous sections, most of the macrophage polarization biology understanding has come from mouse primary cell lines *in vitro*. Given the complex nature of the subject and considering interspecies differences, it is important to understand the dynamics of macrophage polarization in rats, which serve as important model organisms in biomaterial studies. In chapter 2, modulation and derivation of various macrophage phenotypes in response to dexamethasone, IL-4, IL-10, LPS and chitohexose have been established in primary macrophages from rat spleen. Chitohexose is chitosan derived sugar. In a recently published study, Hexa-N-acteyl chitohexose has been shown to direct macrophages to the alternative pathway both *in vitro* and *in vivo* in mice models of septicemia [97]. Chitohexose is available in two different acetylated forms, Hexa-N-Acetyl Chitohexose (COS-6) and Chitohexose-6-HCl (CHX). In chapter 3, development of flow cytometry assay for the analysis of cell surface receptors of differentially polarized macrophage phenotypes has been presented. Chapters 2 and chapter 3 provide *in vitro* data on biomarkers in differentially polarized phenotypes of rat macrophages. Together, they provide a guide on what biomarkers to expect when trying to modulate macrophages in *in vivo* settings. This also helps to

answer very a important question on how *in vitro* studies translate *in vivo*. Chapter 4 and chapter 5 presents the analysis of macrophage phenotypes and quantification of secreted proteins in response to IL-4 and IL-10 as modulators using microdialysis and PVA sponges as FBR models, respectively. Chapter 6 presents the detection and quantification of adipokines using microdialysis technique in rat mammary gland. This is a novel technique that can be employed in mammary tumor models in rats where an altered phenotype of macrophages is present and together with adipocyte can lead to cancer progression. Thus, knowledge of local concentration of cytokine mediators of inflammation is of critical importance. Chapter 7 presents the overall summary and future directions. Overall, the results presented in this dissertation forward our understanding of macrophage phenotype modulation *in vitro* and *in vivo* in rat model systems.

References

1. Anderson, J. M., Rodriguez, A., Chang, D. T. (2008) Foreign body reaction to biomaterials. *Semin Immunol* 20, 86-100.

2. Ward, W. K. (2008) A review of the foreign-body response to subcutaneously-implanted devices: the role of macrophages and cytokines in biofouling and fibrosis. *J Diabetes Sci Technol* 2, 768-77.

3. Burge, M. R., Stephen, M., Sawyer, A., Schade, D. S. (2008) Continuous Glucose Monitoring: The Future of Diabetes Management. *Diabetes Spectrum* 21, 112-119.

4. Gillitzer, R. and Goebeler, M. (2001) Chemokines in cutaneous wound healing. *J Leukoc Biol* 69, 513-521.

5. Sonnemann, K. J. and Bement, W. M. (2011) Wound Repair: Toward Understanding and Integration of Single-Cell and Multicellular Wound Responses. *Annu Rev Cell Dev Biol* 27, 237-263.

6. Dale, D. C., Boxer, L., Liles, W. C. (2008) The phagocytes: neutrophils and monocytes. *Blood* 112, 935-945.

7. Haukipuro, K., Melkko, J., Risteli, L., Kairaluoma, M. I., Risteli, J. (1991) Synthesis of type-1 collagen in healing wounds in humans. *Ann Surg* 213, 75-80.

8. Ross, R. and Benditt, E. P. (1965) Wound healing and collagen formation. V. Quantitative electron microscope radioautographic observation of proline-H3 utilization by fibroblasts. *J Cell Biol* 27, 83-&.

9. Badylak, S. F., Valentin, J. E., Ravindra, A. K., McCabe, G. P., Stewart-Akers, A. M. (2008) Macrophage phenotype as a determinant of biologic scaffold remodeling. *Tissue Eng Part A* 14, 1835-42.

10. Chow, A., Brown, B. D., Merad, M. (2011) Studying the mononuclear phagocyte system in the molecular age. *Nat Rev Immunol* 11, 788-798.

11. Stanley, E. R. (2009) Lineage Commitment: Cytokines Instruct, At Last! *Cell Stem Cell* 5, 234-236.

12. Gordon, S. and Taylor, P. R. (2005) Monocyte and macrophage heterogeneity. *Nat Rev Immunol* 5, 953-964.

13. Geissmann, F., Gordon, S., Hume, D. A., Mowat, A. M., Randolph, G. J. (2010) Unravelling mononuclear phagocyte heterogeneity. *Nat Rev Immunol* 10, 453-U92.

14. Hume, D. A. (2008) Differentiation and heterogeneity in the mononuclear phagocyte system. *Mucosal Immunol* 1, 432-441.

15. Shi, C. and Pamer, E. G. (2011) Monocyte recruitment during infection and inflammation. *Nat Rev Immunol* 11, 762-774.

16. Burke, B., Ahmad, R., Staples, K. J., Snowden, R., Kadioglu, A., Frankenberger, M., Hume, D. A., Ziegler-Heitbrock, L. (2008) Increased TNF expression in CD43(++) murine blood monocytes. *Immunol Lett* 118, 142-147.

17. Sunderkotter, C., Nikolic, T., Dillon, M. J., van Rooijen, N., Stehling, M., Drevets, D. A., Leenen, P. J. M. (2004) Subpopulations of mouse blood monocytes differ in maturation stage and inflammatory response. *J Immunol* 172, 4410-4417.

18. Ziegler-Heitbrock, L., Ancuta, P., Crowe, S., Dalod, M., Grau, V., Hart, D. N., Leenen, P. J. M., Liu, Y.-J., MacPherson, G., Randolph, G. J., Scherberich, J., Schmitz, J., Shortman, K., Sozzani, S., Strobl, H., Zembala, M., Austyn, J. M., Lutz, M. B. (2010) Nomenclature of monocytes and dendritic cells in blood. *Blood* 116, E74-E80.

19. Liu, G., Xia, X.-P., Gong, S.-L., Zhao, Y. (2006) The macrophage heterogeneity: Difference between mouse peritoneal exudate and splenic F4/80(+) macrophages. *J Cell Physiol* 209, 341-352.

20. Kraal, G. (1992) Cells in the marginal zone of the spleen. *Int Rev Cytol* 132, 31-74.

21. Bou Ghosn, E. E., Cassado, A. A., Govoni, G. R., Fukuhara, T., Yang, Y., Monack, D. M., Bortoluci, K. R., Almeida, S. R., Herzenberg, L. A., Herzenberg, L. A. (2010) Two physically, functionally, and developmentally distinct peritoneal macrophage subsets. *Proc Natl Acad Sci U S A* 107, 2568-2573.

22. Lobov, I. B., Rao, S., Carroll, T. J., Vallance, J. E., Ito, M., Ondr, J. K., Kurup, S., Glass, D. A., Patel, M. S., Shu, W. G., Morrisey, E. E., McMahon, A. P., Karsenty, G., Lang, R. A. (2005) WNT7b mediates macrophage-induced programmed cell death in patterning of the vasculature. *Nature* 437, 417-421.

23. Fantin, A., Vieira, J. M., Gestri, G., Denti, L., Schwarz, Q., Prykhozhij, S., Peri, F., Wilson, S. W., Ruhrberg, C. (2010) Tissue macrophages act as cellular chaperones for vascular anastomosis downstream of VEGF-mediated endothelial tip cell induction. *Blood* 116, 829-840.

24. Wiktorjedrzejczak, W., Bartocci, A., Ferrante, A. W., Ahmedansari, A., Sell, K. W., Pollard, J. W., Stanley, E. R. (1990) Total absence of colony stimulating factor 1 in the macrophage-deficient osteopetrotic (op/op) mouse. *Proc Natl Acad Sci U S A* 87, 4828-4832.

25. Weisberg, S. P., McCann, D., Desai, M., Rosenbaum, M., Leibel, R. L., Ferrante, A. W. (2003) Obesity is associated with macrophage accumulation in adipose tissue. *J Clin Invest* 112, 1796-1808.

26. Machnik, A., Neuhofer, W., Jantsch, J., Dahlmann, A., Tammela, T., Machura, K., Park, J.-K., Beck, F.-X., Mueller, D. N., Derer, W., Goss, J., Ziomber, A., Dietsch, P., Wagner, H., van Rooijen, N., Kurtz, A., Hilgers, K. F., Alitalo, K., Eckardt, K.-U., Luft, F. C., Kerjaschki, D., Titze, J. (2009) Macrophages regulate salt-dependent volume and blood pressure by a vascular endothelial growth factor-C-dependent buffering mechanism. *Nat Med* 15, 545-552.

27. Koh, T. J. and DiPietro, L. A. (2011) Inflammation and wound healing: the role of the macrophage. *Expert Rev Mol Med* 13.

28. Bogie, J. F. J., Timmermans, S., Van Anh, H.-T., Irrthum, A., Smeets, H. J. M., Gustafsson, J.-A., Steffensen, K. R., Mulder, M., Stinissen, P., Hellings, N., Hendriks, J. J. A. (2012) Myelin-Derived Lipids Modulate Macrophage Activity by Liver X Receptor Activation. *PloS One* 7.

29. Murray, P. J., Allen, J. E., Biswas, S. K., Fisher, E. A., Gilroy, D. W., Goerdt, S., Gordon, S., Hamilton, J. A., Ivashkiv, L. B., Lawrence, T., Locati, M., Mantovani, A., Martinez, F. O., Mege, J.-L., Mosser, D. M., Natoli, G., Saeij, J. P., Schultze, J. L., Shirey, K. A., Sica, A., Suttles, J., Udalova, I., van Ginderachter, J. A., Vogel, S. N., Wynn, T. A. (2014) Macrophage activation and polarization: nomenclature and experimental guidelines. *Immunity* 41, 14-20.

30. Martinez, F. O., Sica, A., Mantovani, A., Locati, M. (2008) Macrophage activation and polarization. *Front Biosci* 13, 453-461.

31. Stein, M., Keshav, S., Harris, N., Gordon, S. (1992) Interleukin-4 potently enhances murine macrophage mannose receptor activity- A marker of alternative immunological activation. *J Exp Med* 176, 287-292.

32. Martinez, F. O., Gordon, S., Locati, M., Mantovani, A. (2006) Transcriptional profiling of the human monocyte-to-macrophage differentiation and polarization: New molecules and patterns of gene expression. *J Immunol* 177, 7303-7311.

33. Lawrence, T. and Natoli, G. (2011) Transcriptional regulation of macrophage polarization: enabling diversity with identity. *Nat Rev Immunol* 11, 750-761.

34. Raes, G., De Baetselier, P., Noel, W., Beschin, A., Brombacher, F., Hassanzadeh Gh, G. (2002) Differential expression of FIZZ1 and Ym1 in alternatively versus classically activated macrophages. *J Leukoc Biol* 71, 597-602

35. Zhong B, Sun Q, Liu L, Lan X, Tian J, He Q, Hou W, Liu H, Jiang C, Gao N, S, L. (2014) Pdcd4 modulates markers of macrophage alternative activation and airway remodeling in antigen-induced pulmonary inflammation. *J Leukoc Biol*.

36. Varin, A., Mukhopadhyay, S., Herbein, G., Gordon, S. (2010) Alternative activation of macrophages by IL-4 impairs phagocytosis of pathogens but potentiates microbial-induced signalling and cytokine secretion. *Blood* 115, 353-362.

37. Martinez, F. O., Helming, L., Milde, R., Varin, A., Melgert, B. N., Draijer, C., Thomas, B., Fabbri, M., Crawshaw, A., Ho, L. P., Ten Hacken, N. H., Jimenez, V. C., Kootstra, N. A., Hamann, J., Greaves, D. R., Locati, M., Mantovani, A., Gordon, S. (2013) Genetic programs expressed in resting and IL-4 alternatively activated mouse and human macrophages: similarities and differences. *Blood* 121, E57-E69.

38. Varin, A. and Gordon, S. (2009) Alternative activation of macrophages: Immune function and cellular biology. *Immunobiology* 214, 630-641.

39. Cao, H., Wolff, R. G., Meltzer, M. S., Crawford, R. M. (1989) Differential regulation of class-II MHC determinants on macrophages by IFN-gamma and IL-4. *J Immunol* 143, 3524-3531.

40. Lolmede, K., Campana, L., Vezzoli, M., Bosurgi, L., Tonlorenzi, R., Clementi, E., Bianchi, M. E., Cossu, G., Manfredi, A. A., Brunelli, S., Rovere-Querini, P. (2009) Inflammatory and alternatively activated human macrophages attract vessel-associated stem cells, relying on separate HMGB1- and MMP-9-dependent pathways. *J Leukoc Biol* 85, 779-87.

41. Ambarus, C. A., Krausz, S., van Eijk, M., Hamann, J., Radstake, T., Reedquist, K. A., Tak, P. P., Baeten, D. L. P. (2012) Systematic validation of specific phenotypic markers for in vitro polarized human macrophages. *J Immunol Methods* 375, 196-206.

42. Salmon-Ehr, V., Ramont, L., Godeau, G., Birembaut, P., Guenounou, M., Bernard, P., Maquart, F. X. (2000) Implication of interleukin-4 in wound healing. *Lab Invest* 80, 1337-1343.

43. Martinez, F. O., Gordon, S., Locati, M., Mantovani, A. (2006) Transcriptional profiling of the human monocyte-to-macrophage differentiation and polarization: New molecules and patterns of gene expression. J Immunol 177, 7303-11.

44. Jakubzick, C., Choi, E. S., Joshi, B. H., Keane, M. P., Kunkel, S. L., Puri, R. K., Hogaboam, C. M. (2003) Therapeutic attenuation of pulmonary fibrosis via targeting of IL-4- and IL-13-responsive cells. *J Immunol* 171, 2684-2693.

45. Staples, K. J., Smallie, T., Williams, L. M., Foey, A., Burke, B., Foxwell, B. M. J., Ziegler-Heitbrock, L. (2007) IL-10 induces IL-10 in primary human monocyte-derived macrophages via the transcription factor Stat3. *J Immunol* 178, 4779-4785.

46. Rey-Giraud, F., Hafner, M., Ries, C. H. (2012) In Vitro Generation of Monocyte-Derived Macrophages under Serum-Free Conditions Improves Their Tumor Promoting Functions. *PLoS One* 7, e42656.

47. Badylak, S. E. and Gilbert, T. W. (2008) Immune response to biologic scaffold materials. *Semin Immunol* 20, 109-116.

48. Sica, A. and Mantovani, A. (2012) Macrophage plasticity and polarization: in vivo veritas. *J Clin Invest* 122, 787-795.

49. Dinarello, C. A. (2007) Historical Review of Cytokines. *Eur J Immunol* 37, S34-S45.

50. Cardona, M. A., Simmons, R. L., Kaplan, S. S. (1992) TNF and IL1 generation by human monocytes in response to biomaterails. *J Biomed Mater Res* 26, 851-859.

51. Kao, W. J. and Schmidt, D. R. (2007) The interrelated role of fibronectin and interleukin-1 in biomaterial-modulated macrophage function. *Biomaterials* 28, 371-82.

52. Dinarello, C. A. (1994) The interleukin-1 family: 10 years of discovery. *FASEB J* 8, 1314-25.

53. Boraschi, D., Bossu, P., Macchia, G., Ruggiero, P., Tagliabue, A. (1996) Structure-function relationship in the IL-1 family. *Front Biosci* 1, d270-308.

54. Dinarello, C. A. (2009) Immunological and Inflammatory Functions of the Interleukin-1 Family. *Annu Rev Immunol* 27, 519-550.

55. Huaux, F., Liu, T., McGarry, B., Ullenbruch, M., Phan, S. H. (2003) Dual roles of IL-4 in lung injury and fibrosis. *J Immunol* 170, 2083-2092.

56. McNally, A. K. and Anderson, J. M. (1995) Interleukin-4 induces foreign body giant cell from human monocytes macrophages-differential lymphokine regulation of macrophage fusion leads to morphological variants of multinucleated giant cells *Am J Pathol* 147, 1487-1499.

57. Kao, W. Y. J., McNally, A. K., Hiltner, A., Anderson, J. M. (1995) Role for interleukin-4 in foreign body giant cell formation on a poly etherurethane urea in vivo. *J Biomed Mater Res* 29, 1267-1275.

58. Barton, B. E., Shortall, J., Jackson, J. V. (1996) Interleukins 6 and 11 protect mice from mortality in a staphylococcal enterotoxin-induced toxic shock model. *Infect Immun* 64, 714-718.

59. Kishimoto, T. (1989) The biology of interleukin-6. *Blood* 74, 1-10.

60. Kishimoto, T., Hibi, M., Murakami, M., Narazaki, M., Saito, M., Taga, T. (1992) The molecular biology of interleukin 6 and its receptor. *Ciba Found Symp* 167, 5-16; discussion 16-23.

61. Akira, S., Hirano, T., Taga, T., Kishimoto, T. (1990) Biology of multifunctional cytokines: IL 6 and related molecules (IL 1 and TNF). *FASEB J* 4, 2860-7.

62. Kimura, A., Naka, T., Muta, T., Takeuchi, O., Akira, S., Kawase, I., Kishimoto, T. (2005) Suppressor of cytokine signaling-1 selectively inhibits LPS-induced IL-6 production by regulating JAK-STAT. *Proc Natl Acad Sci U S A* 102, 17089-17094.

63. Ishiguro, H., Kishimoto, T., Furuya, M., Nagai, Y., Watanabe, T., Ishikura, H. (2005) Tumor-derived interleukin (IL)-6 induced anti-tumor effect in immune-compromised hosts. *Cancer Immunol Immunother* 54, 1191-1199.

64. Knuepfer, H. and Preiss, R. (2007) Significance of interleukin-6 (IL-6) in breast cancer (review). *Breast Cancer Res Treat* 102, 129-135.

65. Akira, S., Nishio, Y., Tanaka, T., Inoue, M., Matsusaka, T., Wang, X. J., Wei, S., Yoshida, N., Kishimoto, T. (1995) Transcription factors NF-IL6 and APRF involved in gp130-mediated signaling pathway. *Ann N Y Acad Sci* 762, 15-28.

66. Faggioli, L., Costanzo, C., Merola, M., Bianchini, E., Furia, A., Carsana, A., Palmieri, M. (1996) Nuclear factor kappa B (NF-kappa B), nuclear factor interleukin-6 (NFIL-6 or

C/EBP beta) and nuclear factor interleukin-6 beta (NFIL6-beta or C/EBP delta) are not sufficient to activate the endogenous interleukin-6 gene in the human breast carcinoma cell line MCF-7 - Comparative analysis with MDA-MB-231 cells, an interleukin-6-expressing human breast carcinoma cell line. *Eur J Biochem* 239, 624-631.

67. Fenton, J. I., Hursting, S. D., Perkins, S. N., Hord, N. G. (2006) Interleukin-6 production induced by leptin treatment promotes cell proliferation in an Apc ((Min/+)) colon epithelial cell line. *Carcinogenesis* 27, 1507-1515.

68. Matsusaka, T., Fujikawa, K., Nishio, Y., Mukaida, N., Matsushima, K., Kishimoto, T., Akira, S. (1993) Transcription factors NF-IL6 and NF-kappa-B synergistically activate transcription of the inflammatory cytokines, interleukin-6 and interleukin-8. *Proc Natl Acad Sci U S A* 90, 10193-10197.

69. Fiorentino, D. F., Bond, M. W., Mosmann, T. R. (1989) 2 types of mouse T-helper cell.IV. TH2 clones secrete a factpr that inhibits cytokine production by Th1 clones. *J Exp Med* 170, 2081-2095.

70. Couper, K. N., Blount, D. G., Riley, E. M. (2008) IL-10: The master regulator of immunity to infection. *J Immunol* 180, 5771-5777.

71. Balaji, S., Moles, C. M., Bhattacharya, S. S., LeSaint, M., Dhamija, Y., Le, L. D., King, A., Kidd, M., Bouso, M. F., Shaaban, A., Crombleholme, T. M., Bollyky, P., Keswani, S. G. (2014) Comparison of interleukin 10 homologs on dermal wound healing using a novel human skin exvivo organ culture model. *J Surg Res* 190, 358-66.

72. Leung, A., Crombleholme, T. M., Keswani, S. G. (2012) Fetal wound healing: implications for minimal scar formation. *Curr Opin Pediatr* 24, 371-378.

73. Gordon, A., Kozin, E. D., Keswani, S. G., Vaikunth, S. S., Katz, A. B., Zoltick, P. W., Favata, M., Radu, A. P., Soslowsky, L. J., Herlyn, M., Crombleholme, T. M. (2008) Permissive environment in postnatal wounds induced by adenoviral-mediated overexpression of the anti-inflammatory cytokine interleukin-10 prevents scar formation. *Wound Repair Regen* 16, 70-79.

74. Peranteau, W. H., Zhang, L., Muvarak, N., Badillo, A. T., Radu, A., Zoltick, P. W., Liechty, K. W. (2008) IL-10 overexpression decreases inflammatory mediators and promotes regenerative healing in an adult model of scar formation. *J Invest Dermatol* 128, 1852-1860.

75. Boehler, R. M., Kuo, R., Shin, S., Goodman, A. G., Pilecki, M. A., Gower, R. M., Leonard, J. N., Shea, L. D. (2014) Lentivirus delivery of IL-10 to promote and sustain macrophage polarization towards an anti-inflammatory phenotype. *Biotechnol Bioeng* 111, 1469-1469.

76. Sun, L., Louie, M. C., Vannella, K. M., Wilke, C. A., LeVine, A. M., Moore, B. B., Shanley, T. P. (2011) New concepts of IL-10-induced lung fibrosis: fibrocyte recruitment and M-2 activation in a CCL2/CCR2 axis. *Am J Physiol Lung Cell Mol Physiol* 300, L341-L353.

77. Eming, S., Werner, S., Siewe, L., Davidson, J. M., Krieg, T., Roers, A. (2007) Accelerated wound closure in mice deficient for interleukin-10. *Exp Dermatol* 16, 278-278.

78. Walter, M. R. (2002) Structure of interleukin-10/interleukin-10R1 complex: a paradigm for class 2 cytokine activation. *Immunol Res* 26, 303-8.

79. Finbloom, D. S. and Winestock, K. D. (1995) IL-10 induces the tyrosine phosphorylation of tyk2 and jak1 and the differential assembly of stat1 alpha and stat3 complexes in human T-cells and monocytes. *J Immunol* 155, 1079-1090.

80. Berlato, C., Cassatella, M. A., Kinjyo, I., Gatto, L., Yoshimura, A., Bazzoni, F. (2002) Involvement of suppressor of cytokine signaling-3 as a mediator of the inhibitory effects of IL-10 on lipopolysaccharide-induced macrophage activation. *J Immunol* 168, 6404-6411.

81. Waters, J. P., Pober, J. S., Bradley, J. R. (2013) Tumour necrosis factor in infectious disease. *J Pathol* 230, 132-147.

82. Watts, T. H. (2005) Tnf/tnfr family members in costimulation of T cell responses. *Annu Rev Immunol* 23, 23-68.

83. Akila, P., Prashant, V., Suma, M. N., Prashant, S. N., Chaitra, T. R. (2012) CD163 and its expanding functional repertoire. *Clinica Chimica Acta* 413, 669-674.

84. Hogger, P., Dreier, J., Droste, A., Buck, F., Sorg, C. (1998) Identification of the integral membrane protein RM3/1 on human monocytes as a glucocorticoid-inducible member of the scavenger receptor cysteine-rich family (CD163). *J Immunol* 161, 1883-1890.

85. Buechler, C., Ritter, M., Orso, E., Langmann, T., Klucken, J., Schmitz, G. (2000) Regulation of scavenger receptor CD163 expression in human monocytes and macrophages by pro- and antiinflammatory stimuli. *J Leukoc Biol* 67, 97-103.

86. Hintz, K. A., Rassias, A. J., Wardwell, K., Moss, M. L., Morganelli, P. M., Pioli, P. A., Givan, A. L., Wallace, P. K., Yeager, M. P., Guyre, P. M. (2002) Endotoxin induces rapid metalloproteinase-mediated shedding followed by up-regulation of the monocyte hemoglobin scavenger receptor CD163. *J Leukoc Biol* 72, 711-717.

87. Cresswell, P. (1994) Assembly, transport, and function of MHC classII molecules. *Annu Rev Immunol* 12, 259-293.

88. Trayhurn, P. and Wood, I. S. (2004) Adipokines: inflammation and the pleiotropic role of white adipose tissue. *Br J Nutr* 92, 347-55.

89. Trayhurn, P. (2005) Endocrine and signalling role of adipose tissue: new perspectives on fat. *Acta Physiol Scand* 184, 285-93.

90. Considine, R. V., Sinha, M. K., Heiman, M. L., Kriauciunas, A., Stephens, T. W., Nyce, M. R., Ohannesian, J. P., Marco, C. C., McKee, L. J., Bauer, T. L., Caro, J. F. (1996) Serum immunoreactive leptin concentrations in normal-weight and obese humans. *N Engl J Med* 334, 292-295.

91. Klein, S., Coppack, S. W., MohamedAli, V., Landt, M. (1996) Adipose tissue leptin production and plasma leptin kinetics in humans. Diabetes 45, 984-987.

92. Fruhbeck, G. (2006) Intracellular signalling pathways activated by leptin. *Biochem J* 393, 7-20.

93. Garofalo, C. and Surmacz, E. (2006) Leptin and cancer. *J Cell Physiol* 207, 12-22.

94. Sides, C. R. and Stenken, J. A. (2014) Microdialysis sampling techniques applied to studies of the foreign body reaction. *Eur J Pharm Sci* 57, 74-86.

95. Boltonmaggs, P. H. B. and Motson, R. W. (1979) Late presentation of polyvinyl alcohol sponge (ivalon) aortic graft failure. *Thorax* 34, 561-562.

96. Efron TD, Most D, HP, S. (2001) A Novel Method of Studying Wound healing. *J Surg Res* 98, 16-20.

Chapter 2: Derivation and Characterization of Primary Macrophages in Response to LPS, IL-4, IL-10, Dexamethasone and Chitohexose

2.1 Introduction

Due to their larger size, rats serve as important biological models in various studies involving the foreign body response, oncology, regenerative medicine, and reproduction [47, 98-101]. However, there are few studies that have been performed focusing on macrophage activation biology in the rat. Much of the macrophage polarization data in the literature has come from *in vitro* studies of mouse- and human-derived mononuclear phagocytes. It is clear that interspecies differences exist and thus extrapolation of the data is difficult and needs evaluation on a case-by case-basis [34, 37].

As discussed in chapter 1, this dissertation's focus lies in the field of regenerative medicine and the foreign body response to implanted materials. In this context, a significant amount of research is performed in rat models. To more fully be able to test different mediators in an *in vivo* context, requires greater understanding of how they perform *in vitro* Therefore, the objective was to understand the macrophage activation biology *in vitro* in rat-derived macrophages both from immortalized cell lines as well as primary cells in response to IL-4, IL-10, dexamethasone and chitohexose, and use the information obtained as a guide map as to what to expect when using modulators *in vivo*. The cytokines IL-4, IL-10 and the glucocorticoid drug, dexamethasone, have been well-established in as driving macrophages toward the M2 phenotype [102]. In a recently published study [103], Hexa-N-acetyl-Chitohexose has been shown to direct macrophages to the alternative pathway both *in vitro* and *in vivo* in mice models of septicemia. Chitohexose is available

in two different acetylated forms, Hexa-N-Acetyl-Chitohexose (COS-6) and Chitohexose-6-HCl (CHX). We activated and characterized macrophages in response to IL-4, IL-10, chitohexose and LPS.

2.2 Materials and Methods

2.2.1 Reagents

LPS from *Salmonella typhimurium,* dexamethasone, paraformaldehyde and non-enzymatic cell dissociation reagent were purchased from Sigma-Aldrich (St Louis, Saint Louis, MO, USA). Recombinant IL-4 and IL-10 were purchased from R&D systems (Minneapolis, MN, USA). Chitohexose-6HCl was purchased from Carbosynth (Compton, Berkshire, UK). Hexa-N-acetyl Chitohexose was purchased from Dextra Laboratories, (Reading, Berkshire, UK).

2.2.2 Cell Cultures

Peritoneal Macrophages: Under the approval of the University of Arkansas Institutional Animal Care and Use Committee, IACUC, resident peritoneal macrophages, were harvested by peritoneal cavity lavage from CO_2 asphyxiated adult male Sprague-Dawley rats (Harlan Laboratories Inc, Madison, WI, USA) weighing between 250-300 g. Intraperitoneal injection of 40 mL of ice-cold PBS (pH 7.4, Gibco, Life Technologies, Grand Island, NY, USA) supplemented with 10 U/mL heparin was given to rinse the cavity. The peritoneum was massaged gently and fluid containing the resident cells was then collected.

Spleen-derived macrophages: Spleens were minced, processed and passed through a 40 µm cell strainer (BD Biosciences, San Jose, CA, USA) to yield a single-cell suspension. Red blood cells were lysed by ACK lysis solution (Life Technologies, Grand Island, NY, USA) by adding 1 mL of ACK to the pellet for 15 min on ice then washed twice with PBS by centrifugation at 1200 rpm. Selection of monocytes/macrophages was based on adherence on the flask surface within 2 hours of incubation time. After 2 hours, flasks were washed twice with warm (37ºC) PBS to remove non-adherent cells. Cells were maintained in Ham's 12 K medium (ATCC, Manassas, VA, USA) supplemented with 10% FBS and 1% antibiotic antimycotic solution (Sigma-Aldrich, St Louis, MO, USA).

NR8383 Cultures: NR8383 (CRL-2192) rat alveolar macrophages cell line was obtained from American Type Culture Collection (ATCC, Manassas, VA, USA). Cells were maintained in Ham's F12 K medium supplemented with 15 % (v/v%) of heat inactivated fetal bovine serum (FBS), (Hyclone, Waltham, MA, USA) and 1% antibiotic, antimycotic solution (Sigma-Aldrich, Saint Louis, MO, USA) according to ATCC recommendations. All cultures were incubated at 37ºC in 5% CO_2.

2.2.3 Studies of IL-4 and IL-10 on LPS mediated TNF-α Secretion

Splenic (1×10^6 cells/well) or peritoneal (5×10^5 cells/well) macrophages were cultured in a 12-well plate. LPS (50 or 100 ng/mL) was added to the cultures alone or in combination with IL-10 (25 ng/mL) and IL-4 (25 ng/mL or 50 ng/mL) followed by incubation up to 24 hours. After incubation times were complete, cell culture supernatants were harvested, and centrifuged at 1500

rpm to ensure the solution was cell free for subsequent TNF-α ELISA. Collected solutions were stored at -80º C until analysis (Same day or within 24 hours).

2.2.4 Dexamethasone and IL-4 Dose Response on Secretion of IL-10 by Splenic Macrophages

Splenic macrophages were cultured at a concentration of 1×10^6 cells/well in 12 well plates. Cells were stimulated with IL-4 (10 ng/mL to 100 ng /mL) and dexamethasone (10 nM to 100 nM). IL-10 in the cell culture medium was quantified at both the 24 hr and 48 hr incubation times. After completion of incubation times, cell culture supernatants were collected and centrifuged at 1500 rpm to ensure it was cell free for subsequent IL-10 ELISA and were stored at -80º C until analysis (Same day or within 24 hours).

2.2.5 Chitohexose Stimulation of NR8383 Cells and Peritoneal Macrophages

NR8383 cells or peritoneal macrophages were cultured at 1×10^6 cells/well in a 12 well plate. Hexa-*N*-acetyl-Chitohexose (COS6) or Chitohexose-6HCL (CHX) treatment were given at 10 µg/mL alone or in combination with LPS (50 ng/mL). After agent addition, cultures were incubated for 24 hours. Cell culture supernatants were harvested and levels of IL-6, TNF-α and IL-10 were quantified using ELISAs.

2.2.6 ELISA for Cytokine Determination

TNF-α, IL-6 and IL-10 levels in the cell culture supernatant were measured by sandwich ELISAs (Opt-EIA sets, BD Pharmingen, San Jose, CA, USA). Costar® polystyrene 96 well plates

were used. Recombinant rat TNF or IL-6 or IL-10 were used as the protein standards. The assay concentration ranges were 16 to 1000 pg/mL, 32 to 2000 pg/mL and 75 to 5000 pg/mL for IL-10, TNF-α and IL-6 ELISA, respectively. The assays were performed as per the manufacturer's instructions.

2.2.7 RNA Isolation

Splenic macrophages were cultured at 3×10^6 cells /well in 6 well plates for 6 hours or 24 hours. Cells were treated with 50 or 100 nM of dexamethasone, 25 or 50 ng/mL of IL-4, 25 or 50 ng/mL of IL-10 and 50 or 100 ng/mL of LPS. Total RNA was extracted by directly lysing the cells on the culture plate with 1 mL of TRIzol® reagent (Life Technologies, Grand Island, NY, USA). Lysed cells were harvested using cell scrapers (Thermo Fisher, Waltham, MA, USA). The resulting lysate was passed through a 22 g needle and at least five freeze (-20º C, 5 min) and thaw (RT, 5 min) cycles to ensure complete homogenization of cells. Chloroform (250 µL) was then added to allow phase separation. Samples were then spun at 12,000g for 30 min at 4º C. The top aqueous layer containing RNA was precipitated by 550 µL of isopropanol per sample followed by incubation at room temperature for 15 min and centrifugation at 12,000g for 20 min. The precipitated RNA pellet was washed once with 1 mL of ethanol and then followed by column clean up using an RNeasy mini kit (Qaigen, Valencia, CA, USA). RNA concentration was assessed by measuring the absorbance at 260 nm using a Nanodrop spectrophotometer (Thermo scientific, Waltham, MA, USA). RNA quality and integrity check was performed by measuring the 260 nm/280 nm ratio and by integrity of 28s and 18s rRNA bands by denaturing gel electrophoresis.

2.2.8 Quantitative Real Time PCR Assays

A total of 1 µg of RNA was converted to cDNA using the High Capacity RNA to cDNA kit (Applied Biosystems, Life Technologies, Grand Island, NY, USA). A Techne TC-3000 thermocycler was used to perform the reverse transcriptase reaction for 60 min at 37ºC, followed by 5 min at 95ºC. Quantitative real time PCR was performed in duplicates. Each reaction was performed in a total volume of 50 µL using TaqMan® Gene Expression Master Mix and pre developed TaqMan® probe/primer assay reagents (Life technologies, Grand Island, NY, USA) using ABI prism 7500 sequence detection platform (PE Applied Biosystems, Life Technologies, Grand Island, NY, USA). Relative expression was normalized to the reference condition and to the levels of glyceraldehyde-3-phosphate dehydrogenase (GAPDH). Gene expression assays were performed after 6 hour or 24 hour of stimulation time points. The following TaqMan® probe/primer assay reagents were used: TNF: Rn01525859_g1; TGF: Rn00572010_m1; Arg1:Rn00567522_m1; CD163: Rn01492519_m1; NOS2: Rn00561646_m1; IL-12a: Rn00584538_m1; CD206: Rn01487342_m1; IL-10: Rn01483987_m1

2.2.9 Statistical Analysis

All data are plotted as mean ± SD. ANOVA with Bonferroni correction was performed to determine the statistical significance using the OriginPro 9.1 statistical package (OriginLab Ltd, Northampton, MA). Gene expression data analysis was performed using the Relative Expression Software Tool (version REST-MCS©). Significance was determined by Pair Wise Fixed Reallocation and Randomization Test © using REST.

2.3 Results and Discussion

2.3.1 IL-10 and IL-4 Effects on LPS-induced TNF-α Release in Primary Cultures Splenic and Peritoneal Macrophages

The anti-inflammatory activity of IL-4 and IL-10 was determined by quantifying secreted TNF-α in response to LPS. LPS acts via TLR-4 receptors on macrophages which ultimately leads to secretion of TNF-α. This cytokine plays an important role in a wide range of immune functions such as augmentation of phagocytic capacity, cytotoxicity of tumor cells and can lead to endotoxic shock. TNF-α is produced by rat splenic and peritoneal macrophages in response to LPS treatment. Figure 4A shows the concentration of TNF-α released from splenic macrophages in response to 50 ng/mL of LPS alone or in combination with IL-4 (100 ng/mL) or IL-10 (50 ng/mL). The media from controls (no LPS) had detectable levels of TNF-α of ~ 75 pg/mL. The TNF-α concentration was ~600 pg/mL in LPS treated cells. Addition of LPS with IL-10 resulted in significant ($p<0.001$) reduction TNF-α concentrations (~ 70 pg/mL) relative to LPS-treated macrophages. No detectable levels of TNF-α were obtained from macrophages given a combination of IL-4 (100 ng/mL) with LPS.

Figure 4B and Figure 4C show the concentration of TNF-α released from splenic and peritoneal macrophages, respectively. Cells were treated with a higher dose (100 ng/mL) of LPS alone or in combination with either IL-10 or IL-4 at 25 ng/mL. Control cells had no detectable levels of TNF-α released in the cell culture supernatant. Treatment with LPS at 100 ng/mL resulted in TNF-α concentrations of 630 pg/mL and 250 pg/mL in splenic and peritoneal macrophages, respectively. LPS plus IL-4 (25 ng/mL) significantly reduced the TNF-α concentration to 440 pg/mL ($p<0.001$)

in splenic macrophages. LPS combined with IL-4 (25 ng/mL) in peritoneal macrophages resulted in TNF-α levels of 210 pg/mL but this not a statistically significant difference. Co-incubation of LPS (100 ng/mL) and IL-10 (25 ng/mL) significantly reduced the TNF-α concentrations to 440 pg/mL at $p<0.001$ and 170 pg/mL at $p<0.005$ in splenic and peritoneal macrophages, respectively. At similar concentrations (25 ng/mL) of IL-4 (19.2 fM) and IL-10 (13.2 fM), IL-10 seems to be more effective in dampening the TNF-α release in response to LPS in macrophages (at $p<0.02$).

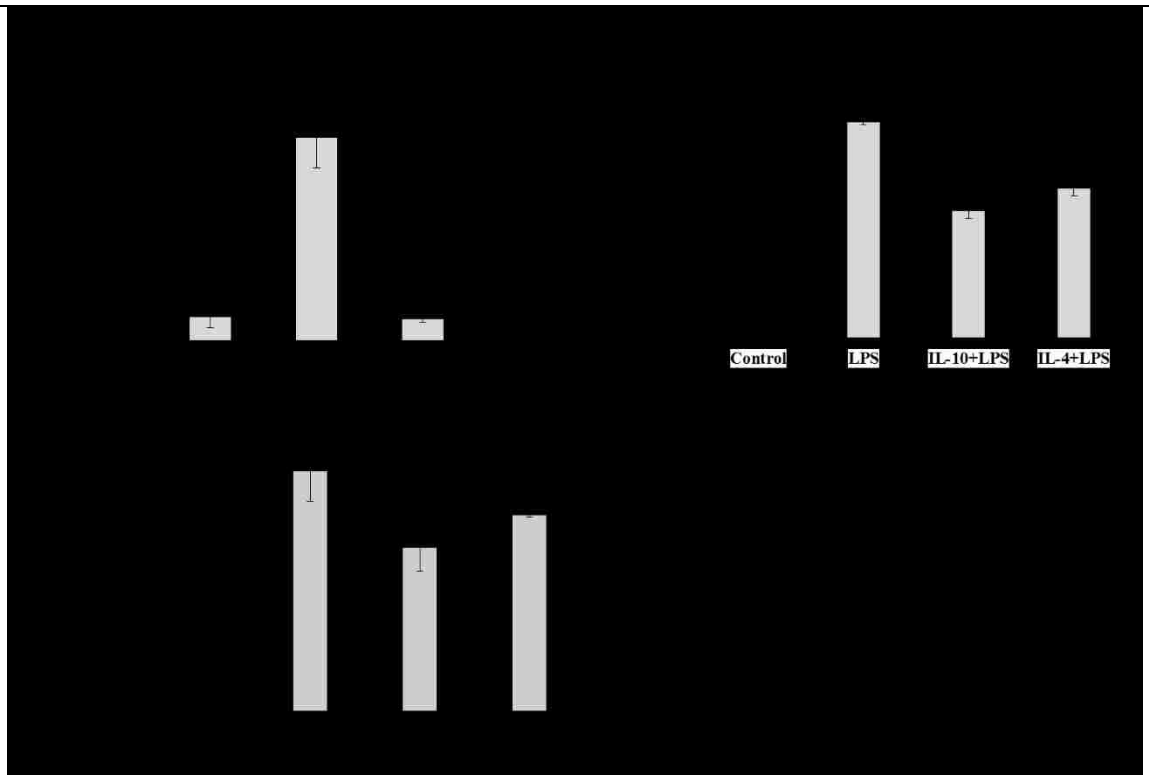

Figure 4. TNF-α secretory profile of spleen and peritoneal macrophages in IL-4/IL-10 combination with LPS

A Spleen-derived macrophage 24 hr response to LPS (50 ng/mL) in combination with various cytokines (IL-10, 50 ng/mL and IL-4, 100 ng/mL) **B** Spleen-derived and **C** peritoneal-derived macrophage 24 hr response to LPS (100 ng/mL) in combination with various cytokines (IL-10, 25 ng/mL and IL-4, 25 ng/mL), n=3. Data are plotted as mean ± SD. ANOVA with Bonferroni post hoc test demonstrated the following significance for spleen-derived macrophages: LPS vs LPS+IL4 : ***$p<0.001$; LPS vs. LPS+IL-10, ***$p<0.001$, LPS+IL4 vs LPS+IL-10: **$p<0.02$. For peritoneal macrophages: LPS vs. LPS+IL-10: *$p<0.05$. Control represents the cells grown in media alone.

The anti-inflammatory activity of IL-4 and IL-10 was determined by quantifying secreted TNF-α in response to LPS. Both IL-4 and IL-10 antagonize the LPS mediated release of TNF-α. Previous studies have confirmed the IL-4 and IL-10 mediated down regulation of TNF-α secretion in human and mice macrophages [70, 104, 105]. This study confirms these observations in rat splenic and peritoneal macrophages. Interestingly, IL-4 mediated TNF-α dampening was significant in splenic macrophages, but not in peritoneal macrophages. These results suggest that spleen-derived macrophages may be more responsive to IL-4 in antagonizing LPS mediated release of TNF-α than peritoneal macrophages [106]. IL-10 significantly affected the LPS mediated TNF-α release in both peritoneal and splenic macrophages. The data suggests, at the same concentration/dose IL-10 seems to be more effective in dampening the TNF-α release as compared to IL-4 in both peritoneal and splenic macrophages. Some studies have attempted to elucidate the mechanisms of IL-4 and IL-10 mediated TNF-α suppression, but the complete mechanisms are still unclear [45, 107, 108].

IL-4 (10 to 100 ng/mL) and dexamethasone (10 to 100 nM) were tested on splenic macrophages to quantify for the release of IL-10 after 24 hr and 48 hr incubation. None of these treatments produced quantifiable levels of IL-10. However, IL-10 and IL-6 levels increase in the culture supernatant following stimulation with LPS (Figure 5A, B and C). There are reports on alternatively activated human and mice macrophages where detectable levels of IL-10 have been quantified in response to IL-4 [46, 109, 110]. Rodriguez-Prados, et al., quantified ~ 0.2 ng/mL of IL-10 when peritoneal macrophages from C57BL/6 mice were treated with 20 ng/mL of IL-4/IL-13 [110]. Zanin et al. used peritoneal macrophages from Swiss mice and cultured them with 10 ng/mL of IL-4 [109]. They were able to detect up to 2000 pg/mL of IL-10 in response to IL-4. Rey-Giraud, et al., used monocytes from whole blood from human subjects [46]. They found

detectable levels of IL-10 (~0.1 ng/mL) in IL-4 (10 ng/mL) induced macrophages. However, in this work, we could not detect secreted IL-10 in response to various doses of IL-4 or dexamethasone. Lolmede, et al., [40] failed to detect IL-10 in response to IL-4 in human blood-derived macrophages. The variations and differences in these results may be due to difference in the species, *in vitro* culture conditions, serum factors, different ELISA manufacturer and/or other laboratory conditions.

2.3.2 Chitohexose Causes Classical Activation in NR8383 and Peritoneal Macrophages

Figure 5 (A, B and C) shows the secretory profile of NR8383 cells when stimulated with CHX and COS-6 with or without LPS. LPS treatment resulted in 2190 pg/mL of TNF-α secretion (Figure 5A) whereas combined with CHX or COS-6 resulted in significantly ($p<0.001$) increased TNF-α concentrations of 4320 and 4780 pg/mL, respectively. IL-6 (Figure 5B) and IL-10 secretory profile (Figure 5C) are in line with TNF-α secretion. CHX/COS-6 alone failed to cause any detectable amount of TNF-α release. Figure 6 (A, B and C) shows the secretory profile of peritoneal derived macrophages in response to CHX (10 µg/mL) alone or in combination with LPS (50 ng/mL). CHX in combination with LPS resulted in secreted TNF-α levels at 2160 pg/mL as opposed to 1425 pg/mL with LPS alone which is significant at $p<0.001$. Secretion of IL-6 is highest in combination with CHX at 12660 pg/mL as compared to LPS alone at 3220 pg/mL. These experiments confirm that observed synergism of CHX/COS-6 with LPS is not related to acetyl modification in CHX or COS-6 and is also not a phenomenon limited to an immortalized/continuous macrophage cell line.

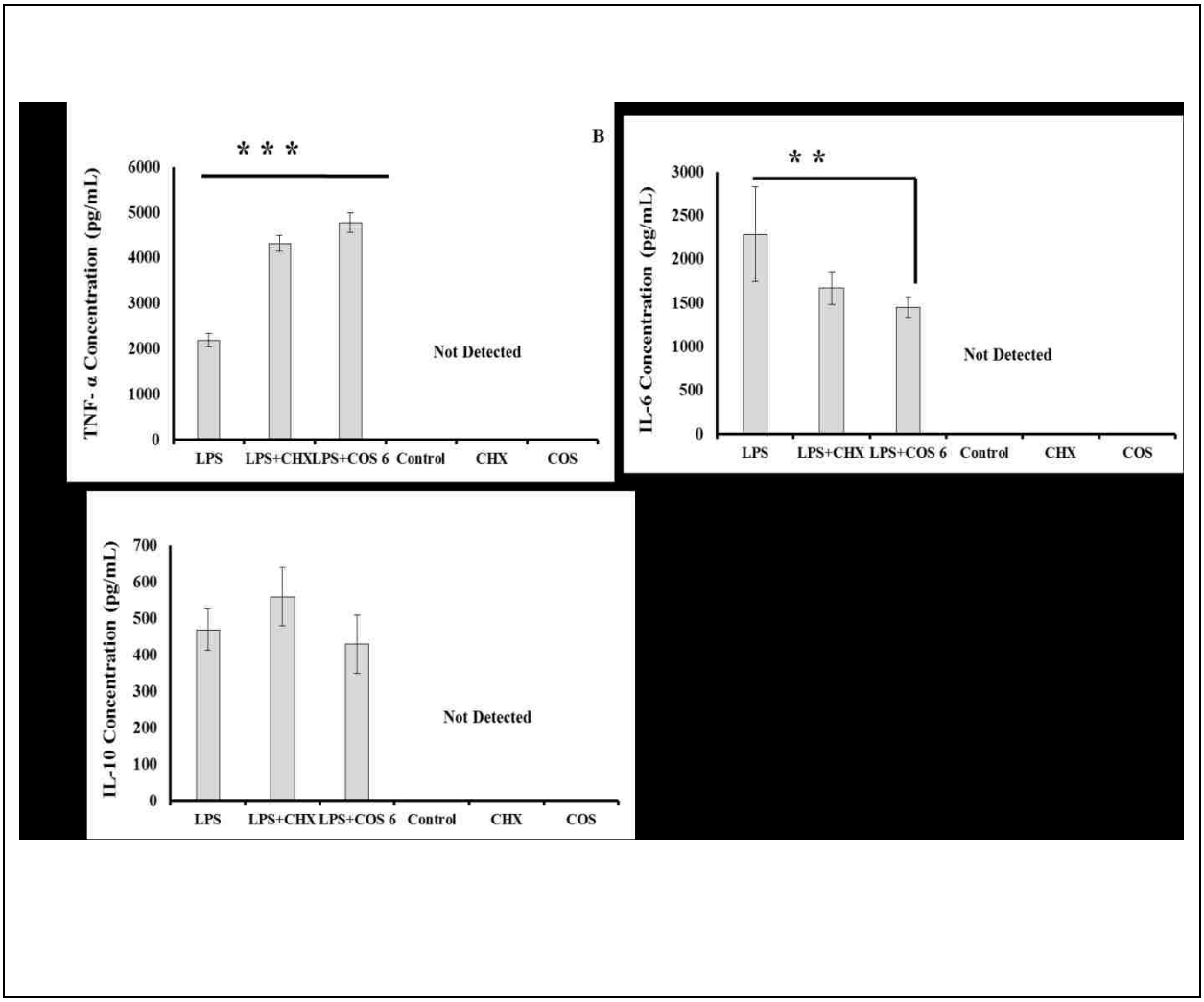

Figure 5. Secretory profile of NR8383 cells with chitohexose

A, B and C TNF-α, IL-6 and IL-10 secretory profile of NR8383 cells, respectively, Stimulated with LPS (50 ng/mL) alone or with COS6 and CHX (10 µg/mL) for 24 hours. Error bars represent the ± SD (N=3 and N=6 for LPS+CHX and LPS+COS6). Significance is denoted by *** $p<0.001$, **$p<0.004$, *$p<0.02$

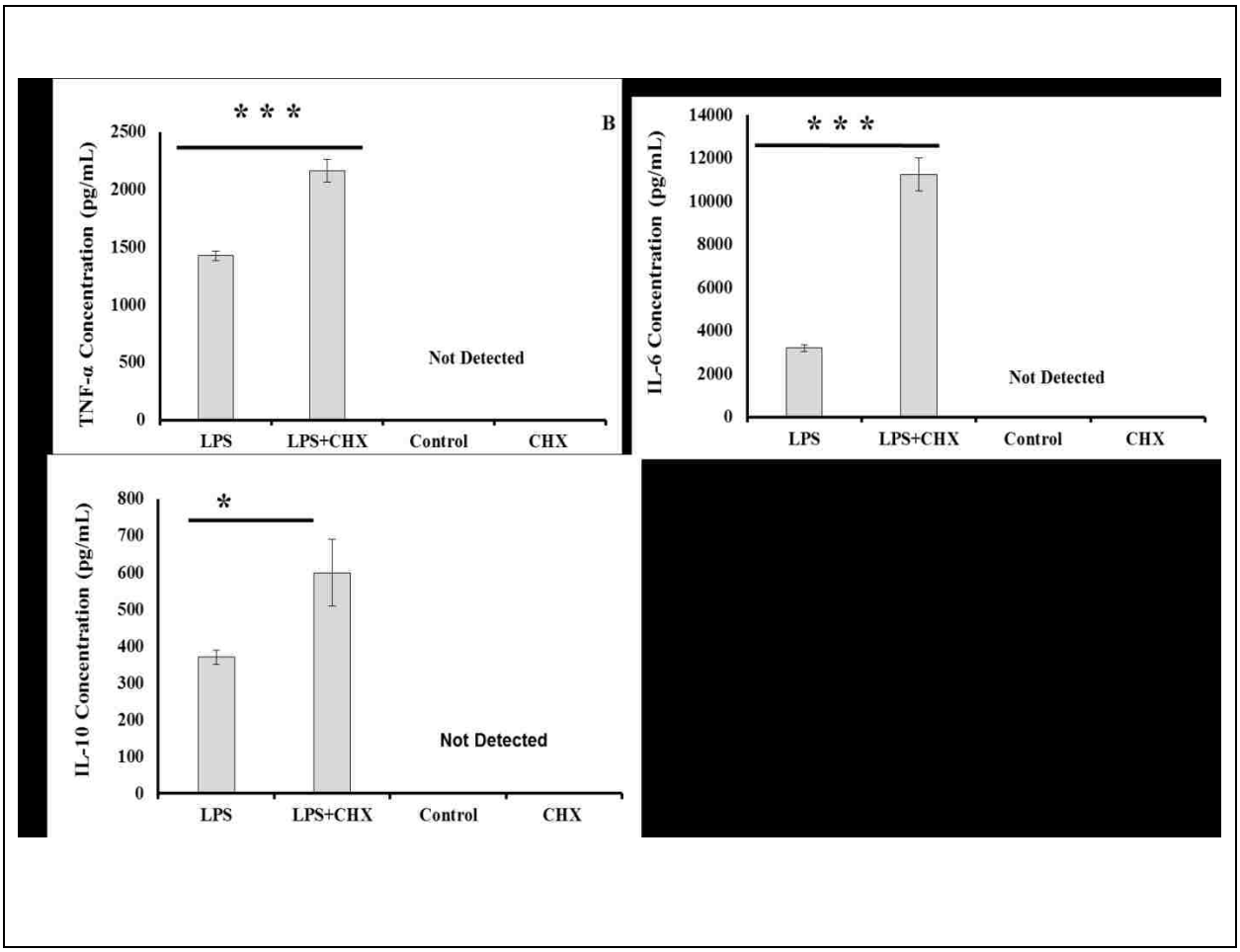

Figure 6. Secretory profile of CHX/LPS stimulated peritoneal macrophages

A, B and C. TNF-α, IL-6 and IL-10 secretory profile of peritoneal macrophages, respectively. Stimulated with LPS (50 ng/mL) alone or with CHX 10 µg/ml) for 24 hours. Error bars represent the ± SD (N=3). Significance is denoted by ***$p<0.001$, *$p<0.02$

A synergistic inflammatory response upon co-treatment of cells with LPS and small molecular weight acetylated chitosans was observed. Tokoro et al., [111] found that CHX and COS-6 had growth inhibitory effect on Meth-A solid tumors in BALB/c mice at a dose of 1 mg/kg. They also showed release of IL-1 which is an inflammatory cytokine from casein elicited macrophages upon treatment with CHX and COS-6 as stimulants *in vitro*. Anti-tumor effects have been associated with M1-like macrophages suggesting that these compounds lead to classical activation of macrophages. In this study, CHX and COS-6 have shown to have no effect on their own but immunopotentiating effect in conjunction with LPS.

Feng et al., showed oligochitosan mediated a stimulatory effect on the release of TNF-α and IL-1β in the mouse RAW 264.7 macrophage like cell line [112]. Gaun et al., evaluated the effects of chitosan hydrolysate, low molecular weight chitosan (LMWC) and oligomixture (a heterogeneous mixture of saccharides) on the nitric oxide production in RAW 264.7 cells and further effect on the NF-κB activation [113]. Their results were interesting. They found that LMWC, chitosan hydrolysate and oligomixture alone had no effect on NO production and iNOS up-regulation. However, when these cells were treated with a combination of IFN-γ and hydrolysate/oligomixture the NO production was significantly affected. On the other hand, LMWC and IFN-γ treatment resulted in inhibition of NO production. In this study, similar trend of heightened inflammatory response of CHX and COS-6 upon co-stimulation with LPS was observed. In another similar study by Jeong et al., [114], NO oxide production was shown to be enhanced upon treatment of RAW 264.7 cells with IFN-γ and high molecular weight water soluble chitosan (WSC). WSC alone had no effect on the production of NO in RAW246.7 cells. Synergistic response resulted in TNF-α secretion and required NF-κB activation. These studies

demonstrate the classical activation of macrophages under study via chito-oligosan sugars. However, the exact mechanism and receptors involved require further investigation.

The observed enhanced inflammatory response in this study can be due to a possible species difference between rat and mice. Dr. Jeannine Durdik's colleagues at National Institute of Immunology, India have confirmed that the compound used in this study is not stimulating RAW 246.7 cells [115]. Further this agrees with mice models of septicemia [97], and results obtained in this study on rat continuous alveolar macrophage cell line (NR8383) and peritoneal derived macrophage, suggest a possible species difference on how COS-6/CHX interact with macrophages in these two species.

2.3.3 Gene Expression Responses to Immunomodulation of Splenic Macrophages

Splenic macrophage phenotypes were characterized by gene expression assays at 6 hour and 24 hour time points after stimulation with different effector molecules. Figure 7 shows the gene expression profile of adherent splenic macrophages after 6 hours of stimulation with LPS (100 ng/mL), IL-4 (25 ng/mL), IL-10 (25 ng/mL) and dexamethasone (100 nM). Here, LPS significantly up-regulated the expression of four genes; IL-12a, TNF-α, iNOS (NOS2) at $p<0.05$ and IL-10 at $p<0.01$. Expression of NOS2 is ~8.5 fold higher as compared to other treatments. Expression of IL12a is ~ 6 fold higher and that of IL-10 and TNF-α is ~4.5 and ~2.5 fold higher, respectively.

IL-4 has significantly up-regulated CD206 at $p<0.05$ and IL12a at $p<0.01$. Dexamethasone has caused significant up-regulation (up to ~2.5 fold higher) of IL-10 at $p<0.001$ as compared to IL-4. Expression of IL-12a is significantly ($p< 0.01$) up -regulated in both dexamethasone and IL-4 treated cells.

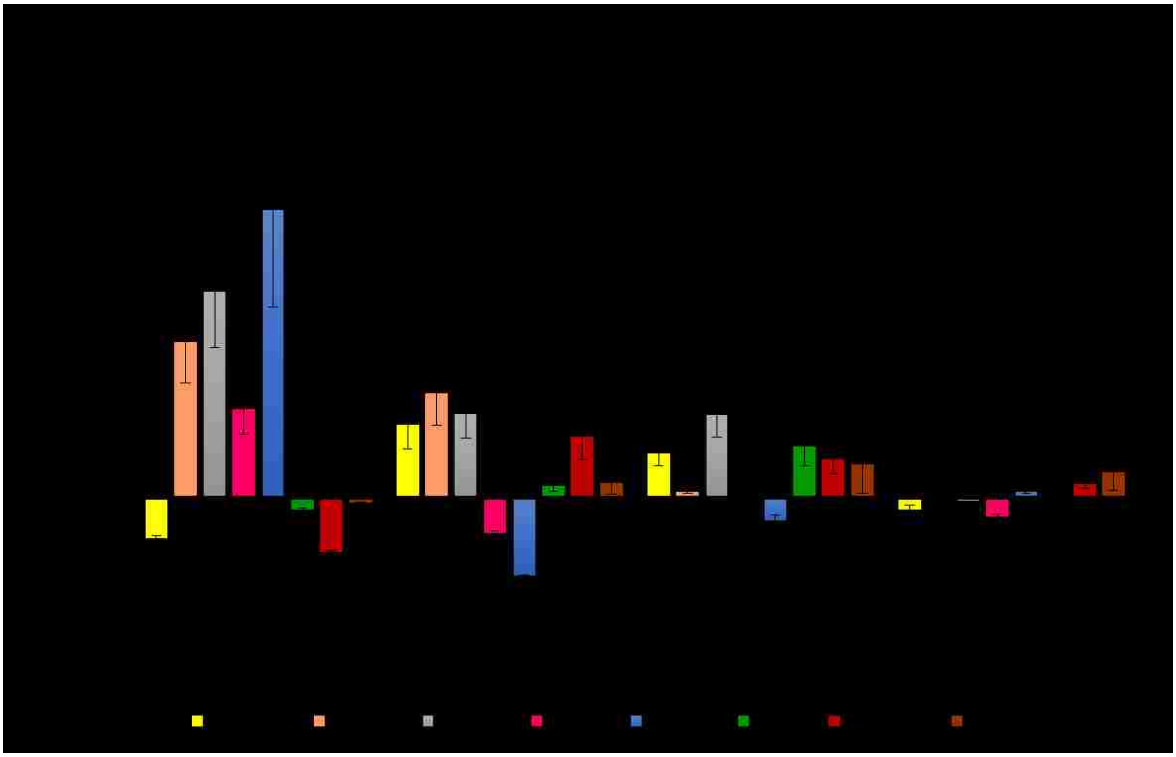

Figure 7. Gene expression of splenic macrophages at 6 hr

Gene expression profile of LPS (50 ng/mL), IL-4 (50ng/mL), IL-10 (50 ng/mL) and Dexamethasone (50 nM) treated splenic-derived macrophages at 6 hour time point. The log base 2 transformed expression ratios (fold change) represent the mean values of 3 independent experiments per treatment (±SD represented by error bars). GAPDH was used as reference gene and control cells grown in media alone have been used as reference condition. Significance is denoted as *$p < 0.05$, ** $p < 0.001$

Dexamethasone has also caused significant up-regulation of CD163 ($p< 0.01$) and CD206 ($p< 0.05$). The IL-10 treatment has resulted in up-regulation of CD163 and TGF-β. There is down-regulation of CD206 in response to IL-10 which is different than the profile generated by IL-4 and dexamethasone treatment.

Figure 8 shows the gene expression profile of LPS, dexamethasone and IL-4 treated splenic macrophages at 24 hour time point. Profiles generated by dexamethasone and IL-4 are distinguishable at 24 hr time point that appeared similar at 6 hr time point. At 24 hours, iNOS is significantly up-regulated at $p<0.01$ in LPS treated cells. Up-regulation of iNOS ~ 4 fold higher than other treatments. At 24 hours, there is significant ($p<0.05$) up-regulation of Arg2 in IL-4 treated cells compared to LPS and dexamethasone treated cells where it is down-regulated. There is significant ($p<0.05$) up-regulation of CD163 with the dexamethasone treatment.

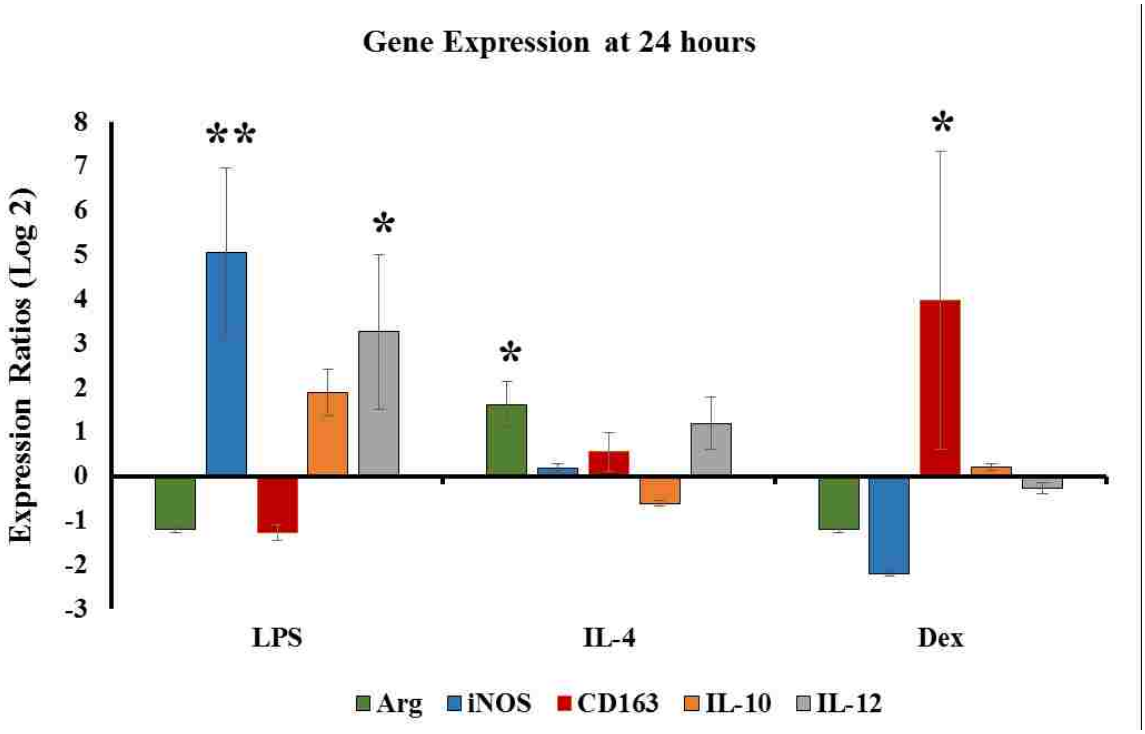

Figure 8. Gene expression of splenic macrophages at 24 hrs

Gene expression profile of LPS (50 ng/mL), IL-4 (50ng/mL), IL-10 (50ng/mL) and Dexamethasone (50 nM) treated splenic-derived macrophages at 24 hour time point. The log base 2 transformed expression ratios (fold change) represent the mean values of 3 independent experiments per treatment (±SD represented by error bars). GAPDH was used as reference gene and control cells grown in media alone have been used as reference condition. Significance is denoted as *$p < 0.05$, ** $p < 0.001$

This study provides a detailed gene expression analysis of known markers in differentially activated macrophages in our rat model system. Here, LPS significantly up-regulates expression of four genes; TNF, iNOS (NOS2), IL-10 and IL-12a. LPS is known to generate an M1 profile in macrophages through classical activation via TL4 receptors. Dexamethasone, IL-4 and IL-10 generate what is generally classified as M2 macrophage phenotypes. At 6 hours, dexamethasone (100 nM) caused significant up-regulation of IL-10, IL-12a, CD163 and CD206 while inflammatory markers (iNOS and TNF) are down regulated. Macrophages treated with IL-4 at 25 ng/mL exhibit similar gene expression profile as dexamethasone-treated macrophages. IL-4 has significantly up-regulated CD206 and IL12a. Up-regulation of CD206 is expected in response to IL-4 and dexamethasone based on published literature. However, not enough literature is available on IL-4 and dexamethasone mediated up-regulation of IL-12a. The expression ratio for IL-12a is highest for LPS treatment which is expected based on the published literature. Dexamethasone and IL-4 mediated IL-12a up-regulation is interesting at 6 hour time point and may be a phenomenon unique to rat splenic macrophages. The expression ratio for Arg2 is highest in IL-4 treated macrophages as compared to dexamethasone or IL-10 treated cells. There have been problems in using Arg1 as a marker for IL-4 activation due to its up-regulation in response to LPS as well in some studies [116, 117]. In this study, Arg2 is in fact down-regulated in response to LPS suggesting that Arg2 can be a marker for IL-4 generated profile without any ambiguity.

IL-10 causes M2c like profile activation which are considered to be regulatory in nature. Dexamethasone generated profile is different than IL-10 induced profile. It is evident from Figure 7 that IL-10 has caused down-regulation of all the genes analyzed except CD163 and TGF-β. This is expected in response to IL-10. Overall, this data indicates successful generation of various macrophage phenotypes *in vitro* in rat model system.

2.4 Conclusion and Significance

In conclusion, this chapter shows the successful characterization of differentially activated phenotypes of rat splenic macrophages cultured *in vitro* through a detailed gene expression analysis, secreted cytokines measurement using ELISA and cell surface receptor expression analysis using flow cytometry. Chitohexose in conjunction with LPS resulted in enhanced inflammatory response which is contrary to what has been observed *in vitro* and *in vivo* for murine macrophages. The data shows that Arg2 is up-regulated by IL-4 and remains unstimulated by LPS hence can be used a marker for alternative activation in rat splenic macrophages. Further data shows the overlapping expression of activation markers in IL-4 and dexamethasone generated subsets is also time dependent varying between 6 hour and 24 hour post stimulation.

Overall Significance: Knowledge of in vitro macrophage activation biology has been acquired majorly from the study of murine macrophages. Macrophage activation is a complex dynamic process. Recent studies have shown interspecies differences as mentioned in Chapter 1. Within the same species, macrophage phenotypes can vary depending on the microenvironmental conditions and the source of macrophage derivation (alveolar, peritoneal, bone marrow, peripheral blood monocytes, and spleen). Thus, the need to understand macrophage activation on a case-by-case basis is highly crucial to fully elucidate the complexity of the process. Rats are used extensively as model organisms in biomaterials studies. A detailed basic study describing activation and characterization of rodent macrophages is sparse. This study is the first to compare five different modulators (LPS, Dexamethasone, IL-4, IL-10 and Chitohexose) side-by-side and provide a

detailed characterization of differentially activated rodent splenic macrophages. This study also highlights deviation points from the data observed in murine macrophages.

Specific points of significance

1. Rats are the least sensitive species to LPS. Thus, how rat macrophages will respond to the modulators is crucial to the study.

2. *In vitro* activation and characterization of macrophages not only provides information on the biological efficacy of the modulators but also provide insights on how data falls in line with what is already known with murine or human macrophages. Secreted IL-10 levels remaining undetected in the cell culture supernatant in response to IL-4 and dexamethasone was unexpected.

3. The majority of *in vitro* studies from mice and humans have utilized peripheral blood monocytes or bone marrow macrophages. Macrophage populations from these sources are known to be more homogenous, less differentiated and naïve which makes them relatively more responsive to the modulators. This adds to the further complexity as responses will vary according to the source of macrophage derivation. Also, culturing of peripheral blood monocytes or bone marrow macrophages involves an additional 7 days for culturing and differentiation, which makes it time consuming and prone to contamination due to longer incubation times. The spleen is an important lymphoid organ that deploys macrophages to

the wound site as well. This study provides insight on the ability of rat splenic macrophages to be activated by various modulators. This adds to the novelty of this study.

4. Chitohexose, a small molecular weight oligosaccharide, was tested as a non-protein potential modulator to avoid protein bioactivity loss issues, and feasibility of diffusion across the dialysis probe owing to its smaller size. Chitohexaose in conjunction with LPS resulted in enhanced inflammatory responses which is contrary to what was observed *in vitro* and *in vivo* for murine macrophages. This combination can be tested for its potential to enhance *in vivo* classical activation of macrophages where conditions call for necessary inflammatory activation of macrophages (tumors where M2 like phenotype predominates).

5. The data shows that Arg2 is up-regulated by IL-4 and remains unstimulated by LPS, and therefore can be used as a marker for alternative activation in rat splenic macrophages. Arg1 as a marker for alternative activation is problematic as it is also expressed upon LPS treatment. Thus, Arg2 results obtained in this study are of high significance. Also, this study shows that Arg1 is also expressed upon IL-10 treatment. This shows another point of significance that Arg2 is a marker to differentiate M(IL-4) vs M(IL-10) profiles.

6. Further, data shows the variations in expression of markers at 6-hour and 24-hour time points. For example, TNF-α transcript remains undetectable at the 24-hour time point but can be measured at the 6-hour time point. At the 6-hour time point, four different markers (TNF-α, IL-12a, IL-10 and iNOS) can be used for M(LPS) characterization whereas at 24-

hour time point, only two markers (IL-12a and iNOS) can be used. Similarly, four different markers (IL-10, IL-12a, CD163 and CD206) can be used for M(dex) characterization at 6 hr time point whereas at 24 hr time point only CD206 remains specifically upregulated. Also, IL-12a marker appears at 6 hr time point in both M(LPS) and M(dex) but remains specific for M(LPS) at 24 hr time point. This has important implications with respect to choice of markers when characterizing differentially activated phenotypes as expression will vary according to the time point chosen for analysis.

7. Finally, *in vitro* data provided a guiding map with respect to expectation of markers in vivo in the model organism (rat) under investigation.

References

34. Raes, G., De Baetselier, P., Noel, W., Beschin, A., Brombacher, F., Hassanzadeh Gh, G. (2002) Differential expression of FIZZ1 and Ym1 in alternatively versus classically activated macrophages. *J Leukoc Biol* 71, 597-602.

37. Martinez, F. O., Helming, L., Milde, R., Varin, A., Melgert, B. N., Draijer, C., Thomas, B., Fabbri, M., Crawshaw, A., Ho, L. P., Ten Hacken, N. H., Jimenez, V. C., Kootstra, N. A., Hamann, J., Greaves, D. R., Locati, M., Mantovani, A., Gordon, S. (2013) Genetic programs expressed in resting and IL-4 alternatively activated mouse and human macrophages: similarities and differences. *Blood* 121, E57-E69.

40. Lolmede, K., Campana, L., Vezzoli, M., Bosurgi, L., Tonlorenzi, R., Clementi, E., Bianchi, M. E., Cossu, G., Manfredi, A. A., Brunelli, S., Rovere-Querini, P. (2009) Inflammatory and alternatively activated human macrophages attract vessel-associated stem cells, relying on separate HMGB1- and MMP-9-dependent pathways. *J Leukoc Biol* 85, 779-87.

46. Rey-Giraud, F., Hafner, M., Ries, C. H. (2012) In Vitro Generation of Monocyte-Derived Macrophages under Serum-Free Conditions Improves Their Tumor Promoting Functions. *PLoS One* 7, e42656.

97. Panda, S. K., Kumar, S., Tuperware, N., Vaidya, T., George, A., Bal, V., Rath, S., Ravindran, B. (2012) Chitohexaose activates macrophages by alternate pathway through TLR4 and blocks Endotoxemia. *PLoS Pathog.* 8, e1002717.

98. Badylak, S. F., Valentin, J. E., Ravindra, A. K., McCabe, G. P., Stewart-Akers, A. M. (2008) Macrophage phenotype as a determinant of biologic scaffold remodeling. *Tissue Eng. Part A.* 14, 1835-42.

99. Halin, S., Rudolfsson, S. H., van Rooijen, N., Bergh, A. (2009) Extratumoral Macrophages Promote Tumor and Vascular Growth in an Orthotopic Rat Prostate Tumor Model. *Neoplasia* 11, 177-186.

100. Winnall, W. R., Muir, J. A., Hedger, M. P. (2011) Rat resident testicular macrophages have an alternatively activated phenotype and constitutively produce interleukin-10 in vitro. *J Leukoc Biol* 90, 133-143.

101. Brown, B. N., Valentin, J. E., Stewart-Akers, A. M., McCabe, G. P., Badylak, S. F. (2009) Macrophage phenotype and remodeling outcomes in response to biologic scaffolds with and without a cellular component. *Biomaterials* 30, 1482-1491.

102. Mantovani, A., Sica, A., Sozzani, S., Allavena, P., Vecchi, A., Locati, M. (2004) The chemokine system in diverse forms of macrophage activation and polarization. *Trends Immunol* 25, 677-686.

103. Panda, S. K., Kumar, S., Tuperware, N., Vaidya, T., George, A., Bal, V., Rath, S., Ravindran, B. (2012) Chitohexaose activates macrophages by alternate pathway through TLR4 and blocks Endotoxemia. *PLoS Pathog* 8, e1002717.

104. McBride, W. H., Economou, J. S., Nayersina, R., Comora, S., Essner, R. (1990) Influences of interleukins 2 and 4 on tumor necrosis factor production by murine mononuclear phagocytes. *Cancer Res* 50, 2949-52.

105. Hart, P. H., Vitti, G. F., Burgess, D. R., Whitty, G. A., Piccoli, D. S., Hamilton, J. A. (1989) Potential antiinflammatory effects of Interleukin-4- Suppression of human monocyte tumor necrosis factor-alpha, Interleukin-1 and Prostaglandin-E2. *Proc Natl Acad Sci U S A* 86, 3803-3807.

106. Hart, P. H., Bonder, C. S., Balogh, J., Dickensheets, H. L., Donnelly, R. P., Finlay-Jones, J. J. (1999) Differential responses of human monocytes and macrophages to IL-4 and IL-13. *J Leukoc Biol* 66, 575-578.

107. Levings, M. K. and Schrader, J. W. (1999) IL-4 inhibits the production of TNF-alpha and IL-12 by STAT6-dependent and -independent mechanisms. *J Immunol* 162, 5224-5229.

108. Clarke, C. J. P., Hales, A., Hunt, A., Foxwell, B. M. J. (1998) IL-10-mediated suppression of TNF-alpha production is independent of its ability to inhibit NF chi B activity. *Eur J Immunol* 28, 1719-1726.

109. Zanin, R. F., Braganhol, E., Bergamin, L. S., Ingrassia Campesato, L. F., Zanotto Filho, A., Fonseca Moreira, J. C., Morrone, F. B., Sevigny, J., Chitolina Schetinger, M. R., de Souza Wyse, A. T., Oliveira Battastini, A. M. (2012) Differential Macrophage Activation Alters the Expression Profile of NTPDase and Ecto-5 '-Nucleotidase. *PLoS One* 7, e31205.

110. Rodriguez-Prados, J.-C., Traves, P. G., Cuenca, J., Rico, D., Aragones, J., Martin-Sanz, P., Cascante, M., Bosca, L. (2010) Substrate fate in activated macrophages: a comparison between innate, classic, and alternative activation. *J Immunol* 185, 605-14.

111. Tokoro, A., Tatewaki, N., Suzuki, K., Mikami, T., Suzuki, S., Suzuki, M. (1988) Growth inhibitory effect of Hexa-N-Acetylchitohexose and chitohexose against Meth-A solid tumor. *Chem Pharm Bull* 36, 784-790.

112. Feng, J., Zhao, L. H., Yu, Q. Q. (2004) Receptor-mediated stimulatory effect of oligochitosan in macrophages. *Biochem Biophys Res Commun* 317, 414-420.

113. Wu, G. J. and Tsai, G. J. (2007) Chitooligosaccharides in combination with interferon-gamma increase nitric oxide production via nuclear factor-kappa B activation in murine RAW264.7 macrophages. *Food Chem Toxicol* 45, 250-258.

114. Jeong, H. J., Koo, H. N., Oh, E. Y., Chae, H. J., Kim, H. R., Suh, S. B., Kim, C. H., Cho, K. H., Park, B. R., Park, S. T., Lee, Y. M., Kim, H. M. (2000) Nitric oxide production by high molecular weight water-soluble chitosan via nuclear factor-kappa B activation. *Int J Immunopharmacol* 22, 923-933.

115. Rath, S. (April 30th, 2014) Personal communication. (J. M. Durdik, ed), National Institute of Immunology, India.

116. El Kasmi, K. C., Qualls, J. E., Pesce, J. T., Smith, A. M., Thompson, R. W., Henao-Tamayo, M., Basaraba, R. J., Koenig, T., Schleicher, U., Koo, M.-S., Kaplan, G., Fitzgerald, K. A., Tuomanen, E. I., Orme, I. M., Kanneganti, T.-D., Bogdan, C., Wynn, T. A., Murray, P. J. (2008) Toll-like receptor-induced arginase 1 in macrophages thwarts effective immunity against intracellular pathogens. *Nat Immunol* 9, 1399-1406.

117. Pesce, J. T., Ramalingam, T. R., Mentink-Kane, M. M., Wilson, M. S., El Kasmi, K. C., Smith, A. M., Thompson, R. W., Cheever, A. W., Murray, P. J., Wynn, T. A. (2009) Arginase-1-Expressing Macrophages Suppress Th2 Cytokine-Driven Inflammation and Fibrosis. *PloS Path* 5.

Chapter 3: Flow Cytometry Assays for the Cell Surface Receptor Assessment of Polarized Macrophages

3.1 Introduction

The word flow cytometry literally means counting of cells that are moving in a stream. Flow cytometry has been used extensively for cell counting, sorting and assessment of biomarkers. It is a fluorescence-based method. Briefly, a flow cytometer has three main components 1) Fluidics 2) Optics and Detection, and 3) Signal Processing. Cells are tagged with fluorescent dyes and passed in single file in a streamlined manner (hydrodynamic focusing), with the help of fluidics. Lasers are used as a light source. Scattering of light and fluorescence emission by the target are recorded. Light scattered in forward direction is known as forward scatter (FSC) which is collected by the lens is indicative of the target size. The side scatter is measured at the 90º angle of the excitation line. The side scatter (SSC) provides information about the granularity/internal complexity of the target. Signal processing converts the analog to digital signals from FSC, SSC or fluorescent signals from light to electrical signals.

As described in chapter 1, M1 macrophage profiles differ from M2 profiles in general. Within M2 macrophages, M(IL-10)/M(Dex) subtypes can be distinguished from M(IL-4) by relative expression analysis of cell surface receptors. Again, to summarize

M1 (LPS/IFN-γ) phenotype will expected to be:

$MHCII^{high}$ $CD86^{high}$ $CD80^{high,}$ $CCR7^{high}$ $CD163^{low}$ $CD204^{low}$

M(IL-4) profile will expected to be: $CD209^{high}$ $CD206^{high}$ $CD163^{low}$ $CD16^{low}$

M(IL-10)/ M(Dex) profile will expected to be: $CD163^{high}CD16^{high}CD206^{low}CD209^{low}$

Thus, using flow cytometry cell surface receptor expression can be analyzed and compared between differently stimulated macrophages. Macrophage marker CD68 or CD11b is analyzed for gating of macrophage population or in other words to select for macrophage population in a sample that may have other cell types too. Thus, aim of these experiments were to develop flow cytometry assays for the identification of activated states of macrophages based on differential cell surface receptor expression profiles in rats and understand if these markers fall along the same pattern as has been described in mouse and humans [36, 41].

3.2 Materials and Methods

3.2.1 Reagents

LPS from *Salmonella typhimurium,* dexamethasone, paraformaldehyde and non-enzymatic cell dissociation reagent were purchased from Sigma-Aldrich (St Louis, Saint Louis, MO, USA). Recombinant IL-4 and IL-10 were purchased from Rand D systems (Minneapolis, MN, USA). FITC conjugated anti-rat mouse monoclonal CD86 antibody, PE conjugated anti-rat mouse monoclonal CD11b antibody and APC conjugated anti-rat mouse monoclonal MHCII antibody were purchased from eBioscience (San Diego, CA, USA). Alexaflour 647 conjugated rabbit polyclonal CD206 antibody was purchased from Bioss (Woburn, MA, USA). PE conjugated anti-rat mouse monoclonal CD68 antibody and FITC conjugated anti-rat mouse monoclonal CD163 antibody were purchased from AbD Serotec (Raleigh, NC, USA). Insotype control for CD11b antibody was mouse IgG2a K isotype control conjugated with PE. Isotype control for CD68 antibody was mouse IgG1 negative control-PE conjugated. Mouse IgG1 negative control

conjugated with FITC was used as isotype for CD163 antibody. Mouse IgG1 K isotype control conjugated with APC was used control for MHCII antibody and mouse IgG1 K isotype conjugated with FITC was used as control for CD86 antibody. All the matched isotypes were bought from the same vendors as their matched antibodies.

3.2.2 Isolation of Splenic Macrophages

Spleens were harvested from CO_2 asphyxiated male adult Sprague-Dawley rats weighing between 275-350g. Spleens were minced, processed and passed through 40 µm cell strainer (BD Biosciences) to yield single cell suspension. Red blood cells were lysed by ACK lysis solution (Life technologies) by adding 1 mL of ACK to the pellet for 15 min on ice. Selection of macrophages was based on adherence on the flask surface within 2 hours of incubation times. After 2 hours, flasks were washed with warm PBS to remove non-adherent cells.

3.2.2 Cell Cultures

NR8383 (CRL 2192) rat alveolar macrophage cell line was obtained from American Type Culture Collection (ATCC). Cells were maintained in Ham's F12 K medium (ATCC) supplemented with 15 % of heat inactivated fetal bovine serum (FBS, Hyclone) and 1 % antibiotic, antimycotic solution (Sigma-Aldrich) according to ATCC recommendations. Splenic macrophages were maintained in Ham's F 12K medium supplemented with 10% FBS and 1 % antibiotic and antimycotic solution (Sigma-Aldrich). All cultures were incubated at 37ºC in 5 % CO_2.

3.3.3 *In vitro* Stimulation of Macrophages

Cells were seeded in 6 well or 12 well plates at concentrations from 10^6 to 2×10^6 cells /well. Cells were treated with 50 or 100 nM of dexamethasone, 25 or 50 ng/mL of IL-4, 25 or 50 ng/mL of IL-10 and 50 or 100 ng/mL of LPS. Cells used as control were grown in the media alone. Cultures were incubated for 18 or 24 hours.

3.2.4 Flow Cytometry Assays

After incubation times were over, cells were detached from the culture plates using cell dissociation reagent, washed and re-suspended in FACS buffer (PBS with 1% BSA and 0.1% sodium azide). Cell surface receptors were tagged with fluorescently-labeled primary antibodies for 30-40 minutes in the dark at 4ºC followed by fixation with 2% paraformaldehyde for 15 minutes. Fixed cells were then washed and permeabilized with 0.3% saponin for intracellular staining of pan macrophage marker CD68. Cells were fixed again with 2% paraformaldehyde, washed and finally re-suspended in 200 µL of FACS buffer in BD polypropylene FACS tubes (BD pharmingen). Three color analysis was performed using FACSort™ platform (Becton Dickinson Immunocytometry Systems) at the Cell Isolation and Characterization multiuser facility at the University of Arkansas.

3.2.5 Data Analysis and Statistics

The generated data sets were analyzed using FlowJo software (Tree Star Inc. OR, USA). ANOVA with a post hoc test (Bonferroni correction), to compare populations, was performed for determination of statistical significance using Origin 9.1 data analysis software.

3.3 Results and Discussion

3.3.1 Optimization Experiments with NR8383 Cells and Splenic Macrophages

Initial experiments were initiated with NR8383 rat alveolar continuous macrophage cell line. The purpose was to test the antibodies and get some ideas about the instrument parameters for the rat macrophages. In Figures 9 and 10 histograms show the NR8383 staining profile with CD68 (Pan Macrophage marker), and CD86 respectively overlaid with the matched isotype control and unstained cells. It is evident from the histogram (Figure 9) that CD68 staining is weak when matched with the isotype control. Histograms for isotype-PE match and CD68-PE have considerable overlap. Figure 10 shows the histogram overlay of matched isotype-FITC and CD86-FITC. Considerable overlap suggests either non-specific binding or lack of CD86 receptor expression. A weak signal for CD68 staining and no signals for CD86 staining in NR8383 cells were observed. This could be due to the differences in the phenotypes that arise in cell lines due to handling in different laboratories with different serum conditions and number of divisions in cells. This could also be due to the fact that NR8383 cells are a continuous macrophage cell line and they do not behave as primary cells rather as monocytoid cells which could lead to differences in the expression of cell surface receptor expression. Another possibility is not enough stimulation for the enhanced expression of CD86 receptor.

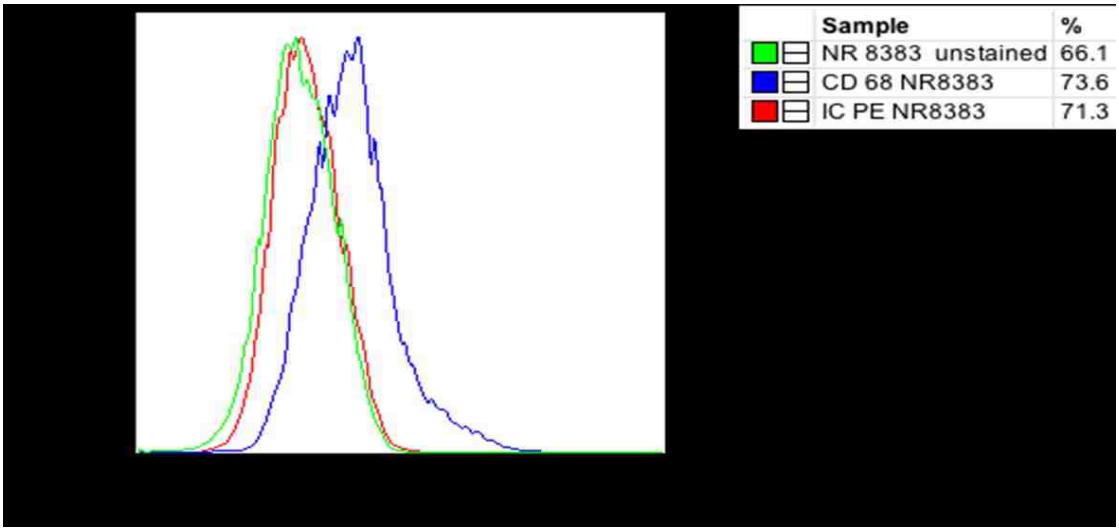

Figure 9. Histogram of CD68-PE stained NR8383 cells

Histograms of unstained NR8383 cells overlaid with CD68 stained cells and matched isotype control (IC-PE)

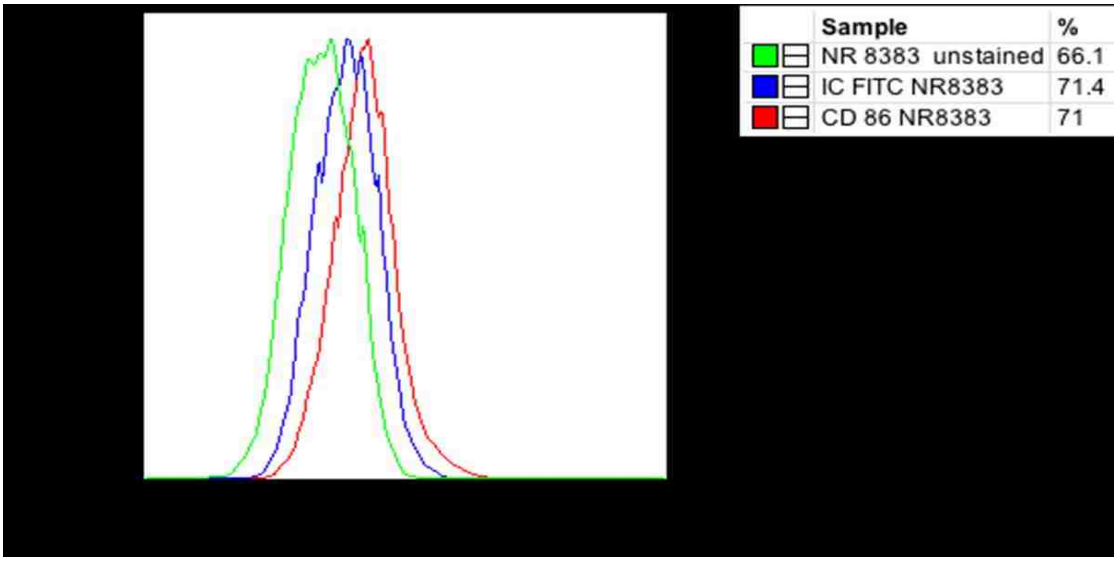

Figure 10. Histogram of CD86-FITC stained NR8383 cells

Histograms of unstained NR8383 cells overlaid with CD86 stained cells and matched isotype control (IC-FITC)

At this point, it was decided to begin optimizing experiments with primary peritoneal derived macrophages as ultimately goal was to use primary cells for differential activation, derivation and characterization. However, this flow cytometry experiment requires usage of high cell number but due to low yield of peritoneal derived macrophages (roughly 10^6 per sample which is the approximate yield from one rat) spleen derived macrophages (~10^7 cells per spleen) were adopted for further analysis. Histograms (Figure 11) below show single stain profile of spleen derived macrophages for CD68-PE (A), CD163-FITC (B), CD86-FITC (C), CD206-AF647 (D) and MHCII-APC (E).

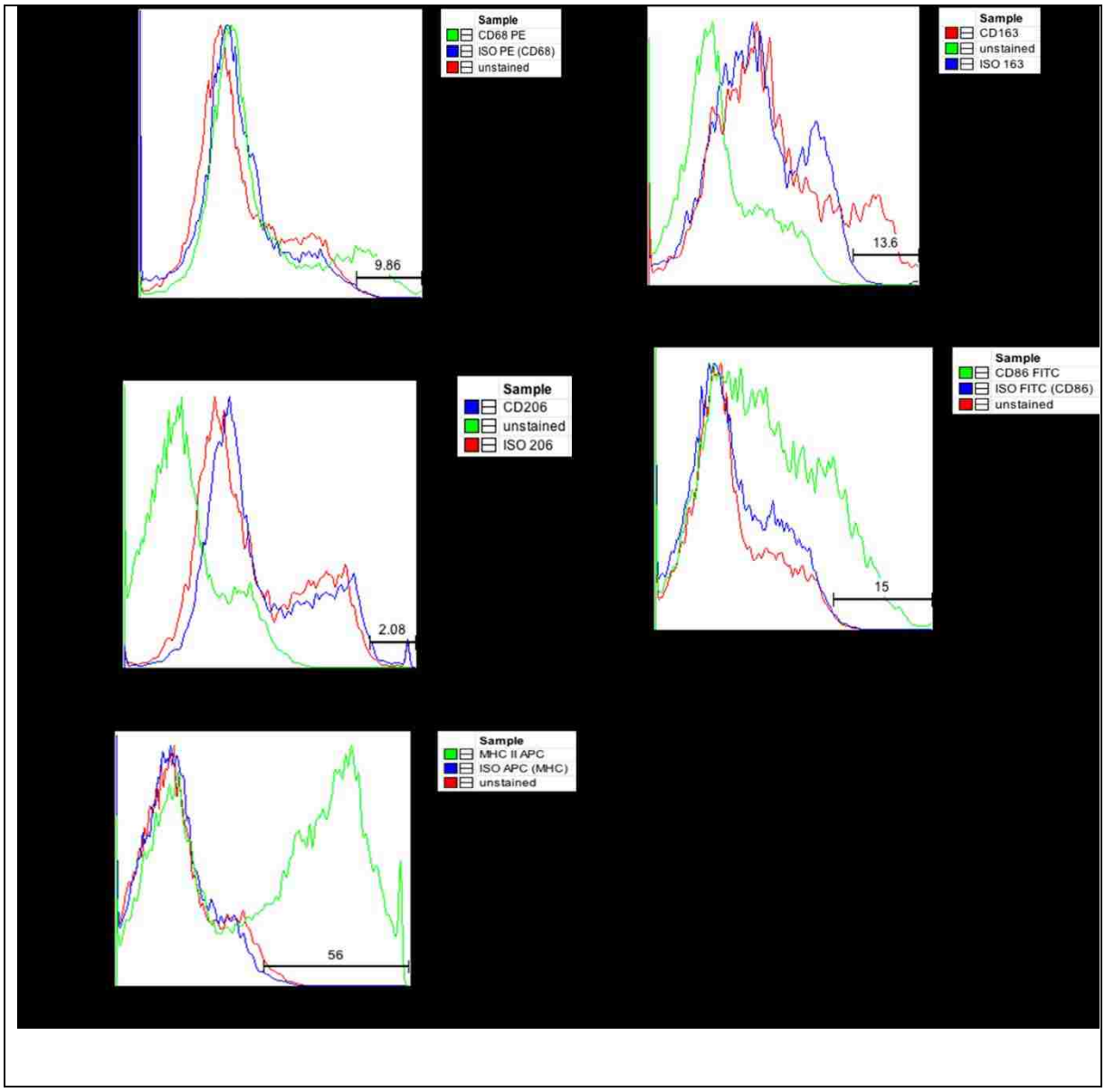

Figure 11. Histograms of single stained spleen derived macrophages

Histograms show the CD68-PE (A), CD163-FITC (B), CD86-FITC (C), CD206-AF647 (D) and MHCII-APC (E) staining of spleen derived macrophages overlaid with the matched isotype control.

CD68 while measurable, results in a faint signal. Later it was found out that optimal staining of CD68 antibody required intracellular staining that called for solubilization technique of the cell membrane using saponin (amphipathic glycoside). Next, multi-color (triple staining) flow cytometry experiments were performed to differentiate between cell surface receptor profiles of spleen derived macrophages activated in response to LPS, IL-4, IL-10, Dexamethasone and control cells grown in media alone without any stimulant.

3.3.2 Cell Surface Receptor Expression Analysis with CD68 as Macrophage Marker

Spleen derived macrophages were treated with 50 ng/mL LPS, 50 ng/mL IL-4, 50nM Dexamethasone and 50 ng/mL IL-10. M0 or control cells (not stimulated) were grown in the media alone. Incubation times were 16 hours (16 to 20 hrs time window).

For analysis of macrophage surface receptor expression, anti-rat CD68-PE, anti-rat CD 86-FITC, anti-rat MHC II-APC, anti-rat CD163-FITC and rabbit anti-MRC1/CD206 polyclonal antibody were used. Appropriate isotype controls were run for each antibody. Triple stains were performed for each treatment. CD68 positive population was analyzed for CD163 and CD206 signal in FL1 and FL4 channel, respectively. These were initial triple-stain experiments demonstrating that some shifts in the overall cell population have occurred (Figure 12).

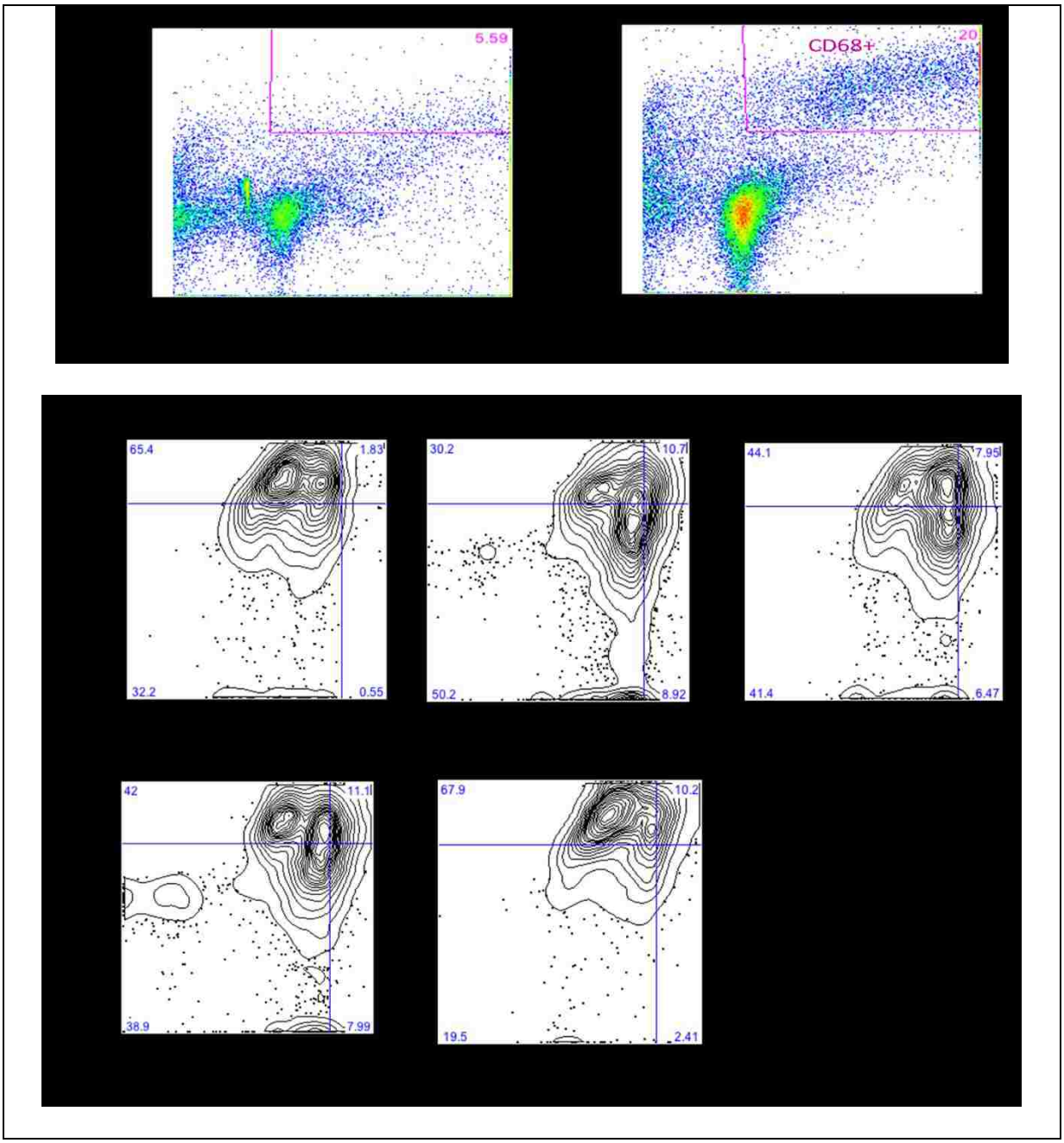

Figure 12. Contour plots of CD68+ (positive) population analyzed for CD163 (FL-1) and CD206 (FL-4)

Top (color) dot plot shows the gate for CD68 positive population. Left: Isotype Control. Right: CD68+ cells. **Bottom:** The contour plots above show the shift in CD68+ population between the FL1 (CD163) and FL4 (CD206) channel for different treatments. From top left to bottom right the populations are as follows: Control, LPS, Dexamethasone, IL-4 and IL-10.

Based on a careful look at the epicenters of the population in contour plots, IL-10 causes maximum shift of the population towards the FL1 region showing higher CD163 positives. For LPS treatment, the epicenter has moved below in the low FL-1 positive region. This is the expected shift with the treatments. There is change in the percentage positives for CD206 (FL4 channel) signal. IL-4 treated cells have high CD206 positives than IL-10 treatment. However, LPS and dexamethasone treatments resulted in comparable CD206 positives. All the treatments differ in CD206 highs when compared to control population.

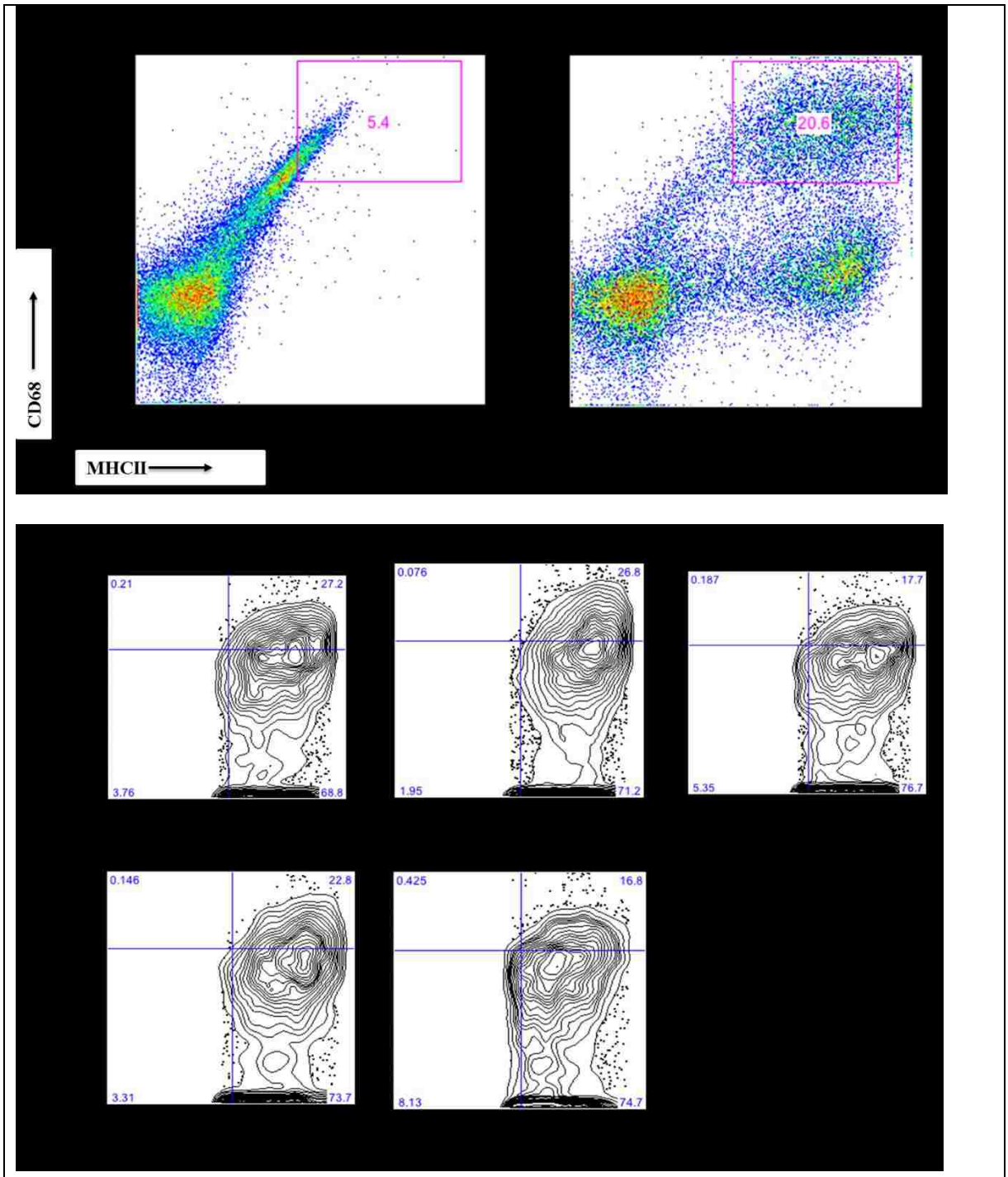

Figure 13. Contour plots of CD68+ MHCII+(positive) population analyzed for CD86 (FL-1) and MHCII (FL-4)

Top (color) dot plot shows the gate for CD68 positive population. Left: Isotype Control. Right: CD68+ cell. **Bottom:** The contour plots above show the shift in CD68+ population between the FL1 (CD86) and FL4 (MHCII) channel for different treatments. From top left to bottom right the populations are as follows: Control, LPS, Dexamethasone, IL-4 and IL-10.

Figure 13 shows the profile for CD68 and MHCII double positive macrophages with various treatments. Double positive population was analyzed in FL1 and FL4 channel for CD86 and MHC II positives, respectively. The top colored dot plot shows the selection of MHCII and CD68 double positive cells based on matched isotype controls. The selected population was then analyzed for CD86 and MHCII profile for each treatment. Bottom contour plots show the shift in populations between FL1 (CD86) and FL4 (MHCII) channel. From the contour plots (Figure 11), LPS causes maximum shift of the population in high FL1 positive zone indicating high CD86 population when compared to other treatments. This is expected in response to LPS. Dexamethasone decreases the signal in F1.

3.3.3 CD11b as Pan Macrophage Marker for Macrophage Identification

Previous preliminary experiments (Figure 12 and 13, N=1 for all treatments) were performed with CD68 as pan macrophage marker. Usage of this antibody marker involved intracellular staining which makes the experiment time consuming and labor intensive. Thus, it was decided to use CD11b as a pan macrophage marker and test whether it would also enhance the fluorescence signal intensity. CD11b is also known as macrophage-1 antigen (Mac-1 antigen), is a part of heterodimeric integrin $\alpha_M\beta_2$ protein expressed on myeloid cells and monocytes. It takes part in adhesive role of macrophages and uptake of complement coated particles [118]. CD11b has widely been used in flow cytometric analysis of monocytes and macrophages [119-121].

Figure 14 shows the histogram comparing the staining of CD11b and CD68 with matched isotype controls. It is clear from the histogram that CD11b staining is brighter than CD68. Signal for CD11b goes to the log decade 4 whereas for CD68 it goes only to the log decade 3. Also,

CD11b staining did not require additional steps of intracellular staining thus saving time and labor. Final set of experiments with N=3 were performed with CD11b as Pan macrophage marker.

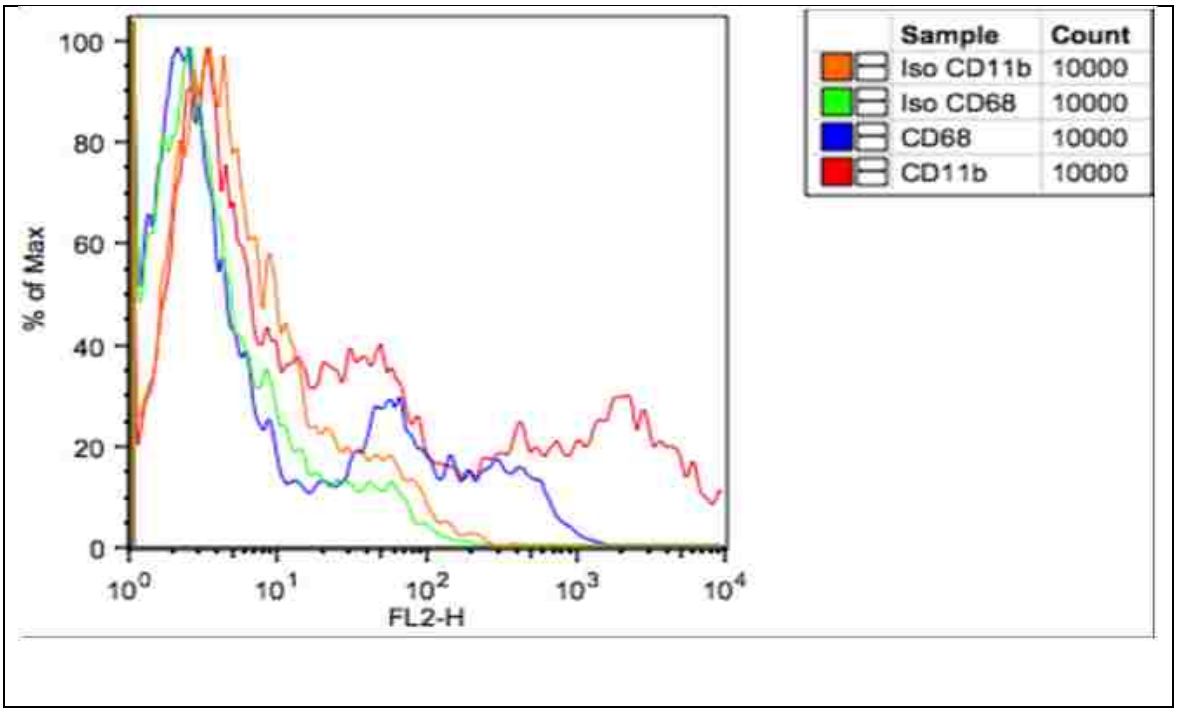

Figure 14. Histogram shows the comparison of PE conjugated CD11b and CD68 markers

The histogram shows the overlay comparison of single staining profiles of CD68 and CD11b stained spleen-derived macrophages matched with their isotype control. CD11b staining (red) is brighter than CD68 staining (blue).

3.3.4 Cell Surface Receptor Analysis of Activated Macrophages using CD11b as Macrophage Marker

Again, cells were treated with IL-4, IL-10 at 50 ng/mL, LPS (100 ng/mL), dexamethasone (100 nM), and control cells were grown in media alone. All the treatments were set up in triplicates. After 18 hours of incubation (16 to 20 hrs time window was chosen), cells were detached and stained for CD11b, CD86, MHCII, CD163, and CD206 markers. Figure 15 shows the selection of CD11b+ cells based on matched isotype control.

Figure 16 shows the representative contour plots of CD11b+ differentially activated macrophages from triplicate experiments. The blue boxes on contour plot show the percentage of highs for CD86 and MHCII double positives. From the contour plots, LPS has caused mild shift of the population in the FL1 (CD86-FITC) region while FL4 (MHCII-APC) positive zone seems to be unaffected when compared to the control cells (cells grown in media alone). Dexamethasone has resulted in epicenter of the population to move down from FL1 and FL4 double positive quadrant. IL-10 treatment does not seem to have much effect on CD86 and MHCII markers when compared to the control cells. The IL-4 treatment has resulted in movement of the epicenter towards FL4 high or MHCII high region. This seemed contrary to certain published studies from mouse bone marrow derived macrophages (BMDM). However, it is in line with previously published data where IL-4 enhances MHCII expression. This could be the difference when activating splenic macrophages with IL-4 in rats [39, 122].

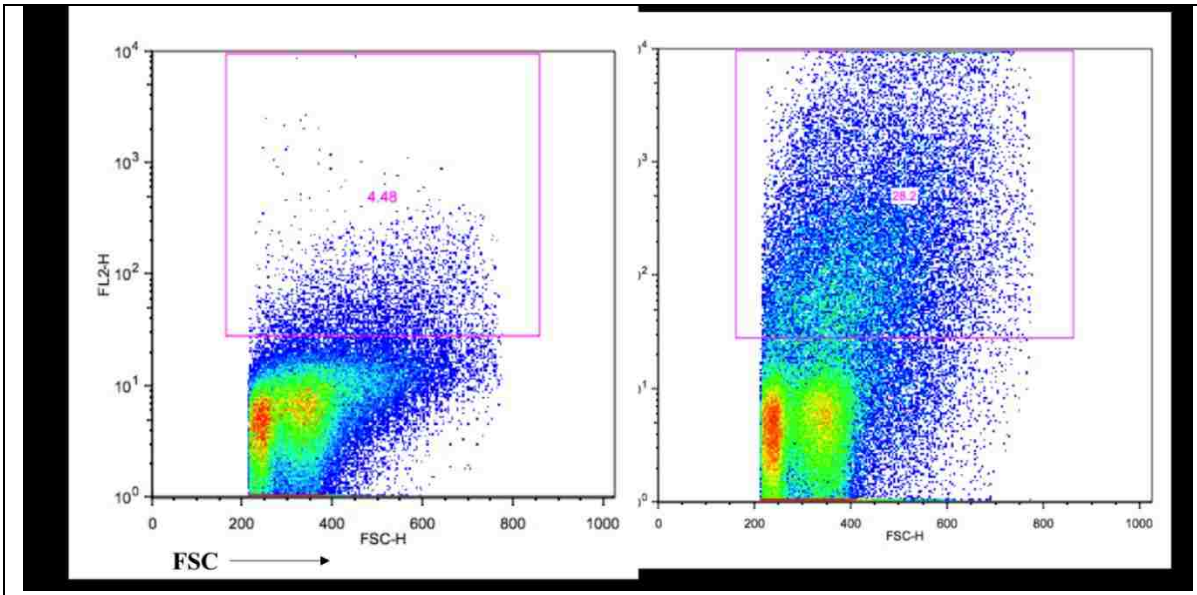

Figure 15. Dot Plot showing the selection of CD11b+ cells based on matched isotype control

Figure shows the selection of CD11b positive cells. Dot plot on left shows the profile of cells stained with the isotype. Dot plot on right side shows the cells stained with CD11b. Pink square gate shows the selected population of macrophages positive for CD11b staining.

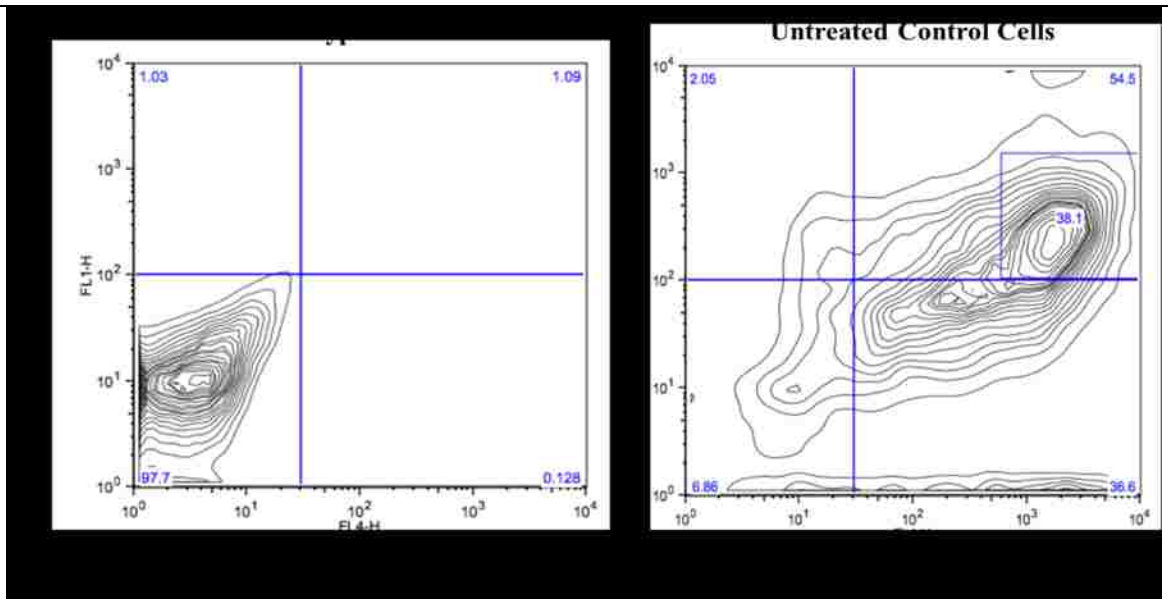
1.03
1.09
97.7
0.128
FL1-H
Untreated Control Cells
2.05
54.5
38.1
6.86
36.6

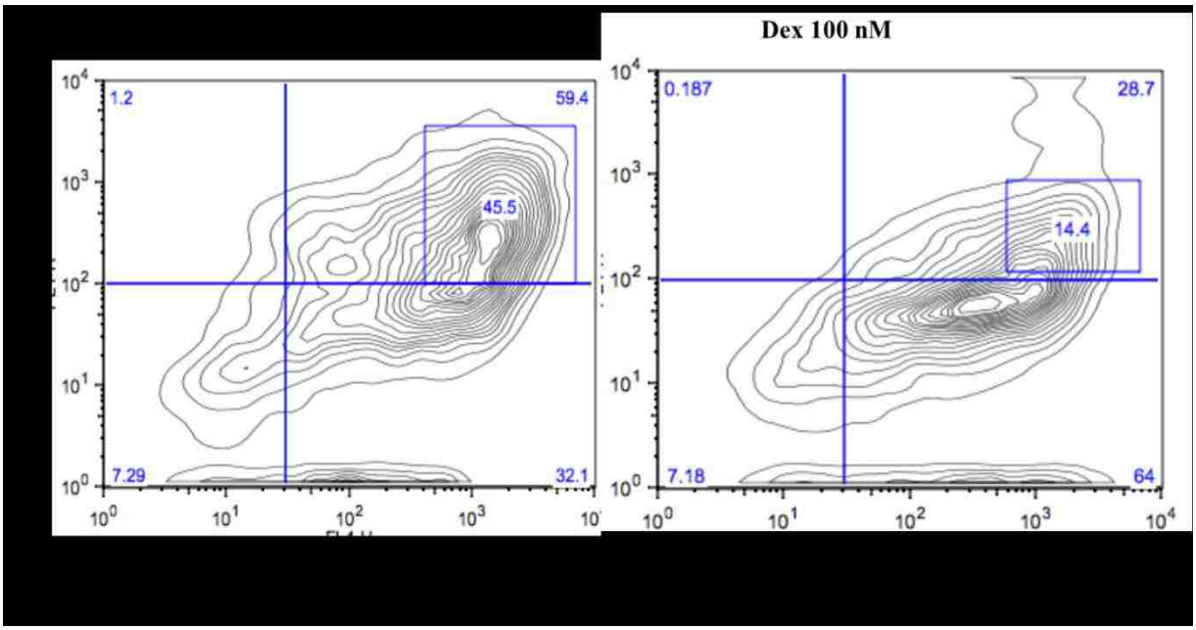
1.2
59.4
45.5
7.29
32.1
Dex 100 nM
0.187
28.7
14.4
7.18
64

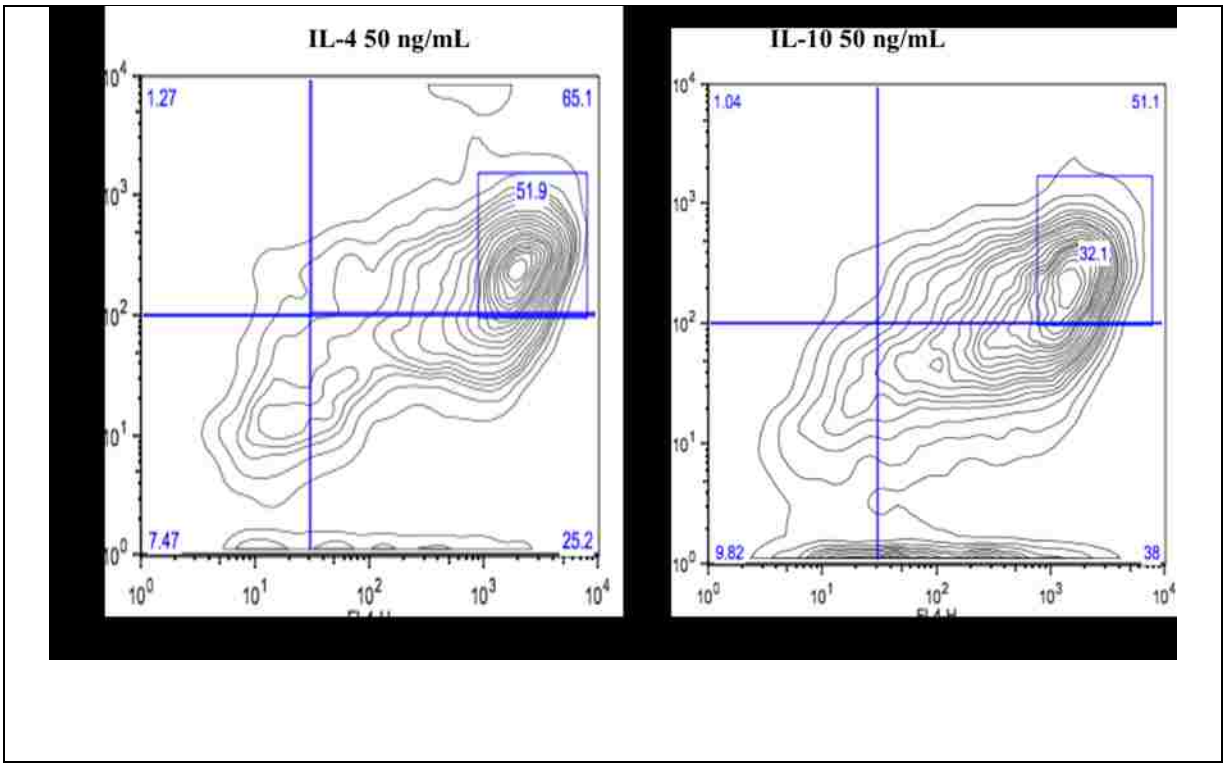

Figure 16. Contour plot showing shift in CD11b+ macrophage population between FL1 (CD86-FITC) and FL4 (MHCII-APC) channel.

The contour plots above show the shift in CD11b+ population (from Figure 15) between the FL1 (CD86) and FL4 (MHCII) channel for different treatments. From top left to bottom right the populations are as follows: Control, LPS, Dexamethasone, IL-4 and IL-10.

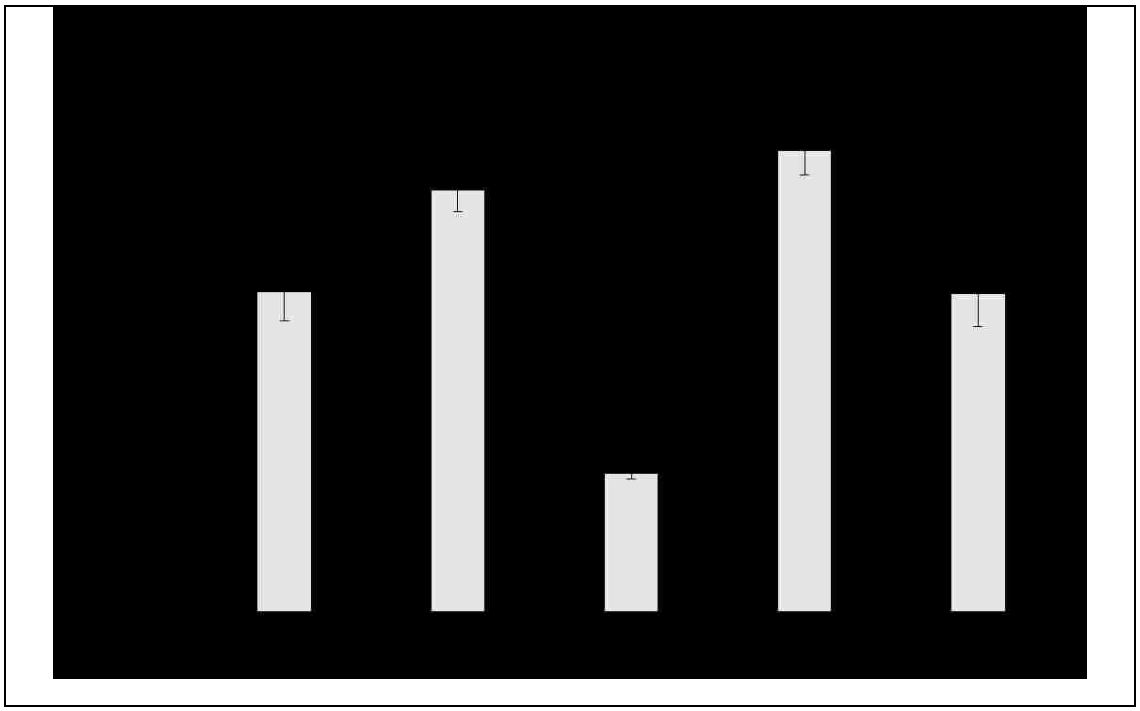

Figure 17. Graph shows the % MHCII CD86 double positives

The graph shows the Data plotted as mean ±SD, N=3. ANOVA with Bonferroni post hoc test was performed to test for significance. Significance denoted by * $p<0.05$. Dexamethasone generated profile was found to be significantly different from Control, LPS, IL-4 and IL-10 generated profiles. IL-4 generated profile was found to be significantly different from Control, LPS, Dex and IL-10 generated profiles.

Figure 17 shows the % of MHCII CD86 double positive highs from CD11b gated macrophage populations in various treatments. Difference between LPS treatment and control cells are not significant at $p<0.5$. Dexamethasone treatment has significantly ($p<0.5$) brought down the double positive highs when compared to the other treatments. IL-4 has significantly ($p<0.5$) raised the population of double positive highs due its enhancing effect on MHCII receptor.

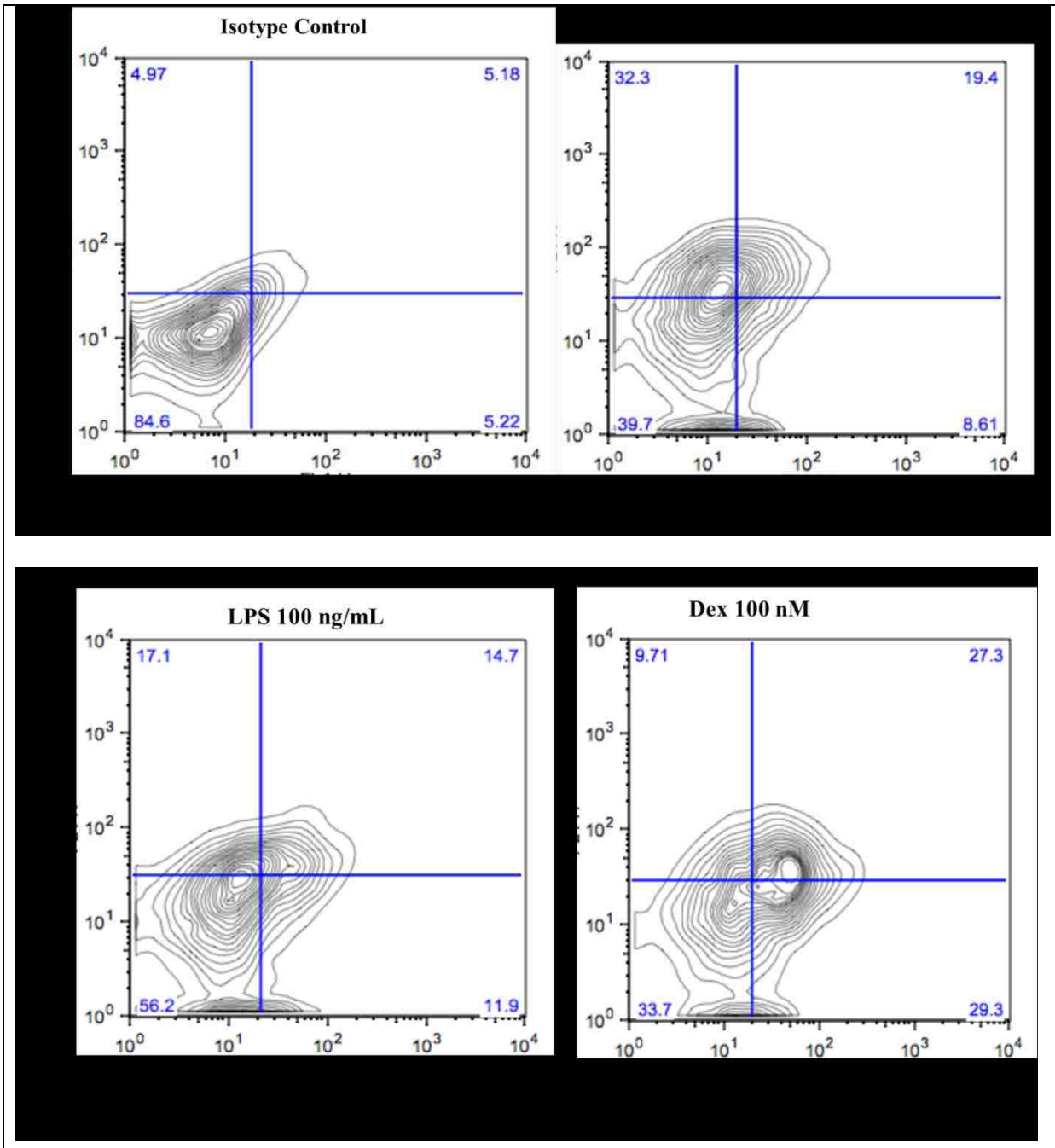
Isotype Control
4.97
5.18
84.6
5.22
32.3
19.4
39.7
8.61
LPS 100 ng/mL
17.1
14.7
56.2
11.9
Dex 100 nM
9.71
27.3
33.7
29.3

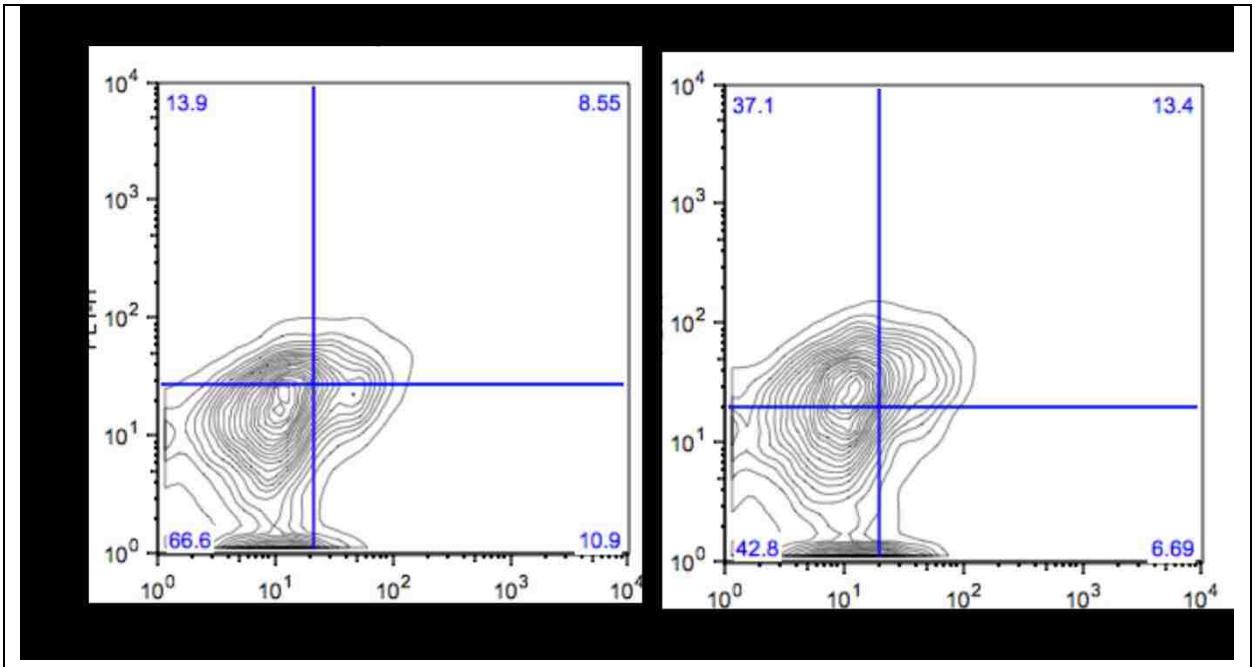

Figure 18. Contour plots showing shift in CD11b+ macrophage population between FL-1 (CD163-FITC) and FL-4 channel (CD206-AF647)

The contour plots above show the shift in CD11b+ population (from Figure 15) between the FL1 (CD163) and FL4 (CD206) channel for different treatments. From top left to bottom right the populations are as follows: Control, LPS, Dexamethasone, IL-4 and IL-10.

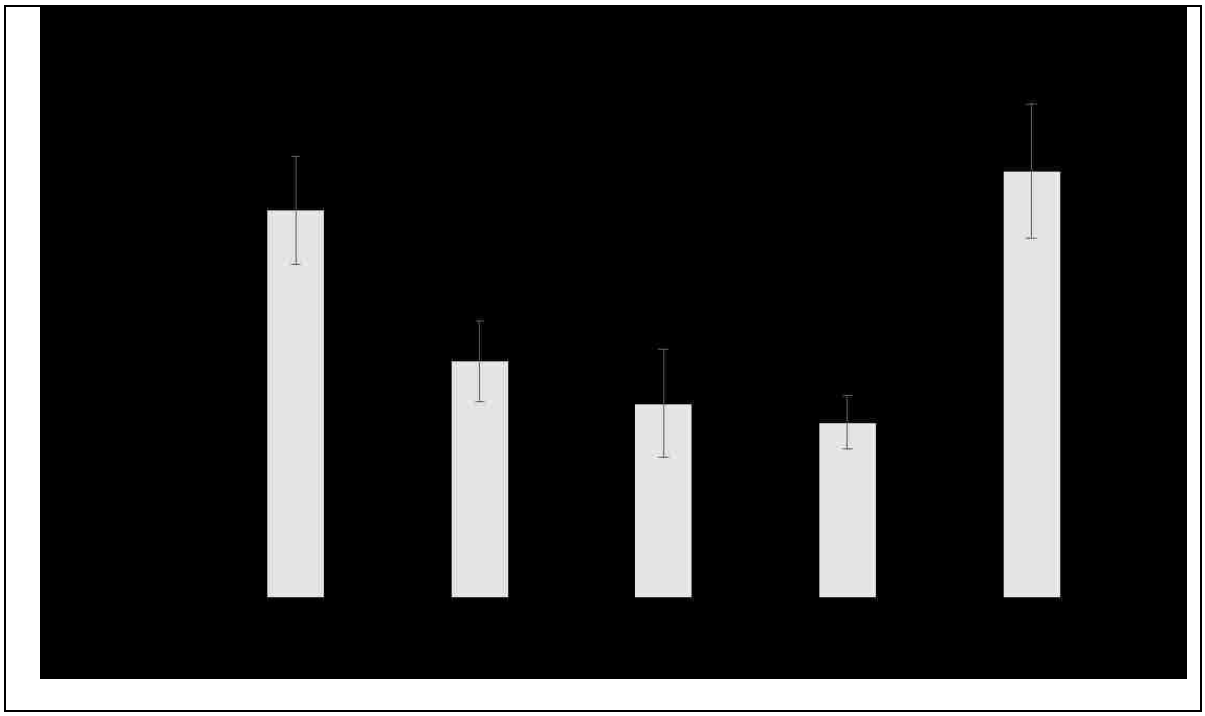

Figure 19. Graphs shows the % of CD163 positive population among different treatments

Data plotted as mean ±SD, N=3. ANOVA with Bonferroni post hoc test was performed to test for significance. Significance denoted by * $p<0.05$. LPS, Dex and IL-4 treated populations are significantly different from Control and IL-10 populations. No significant differences among LPS, Dex and IL-4 populations were found. No significant differences between control and IL-10 generated profiles were found.

Figure 18 shows the representative contour plots of CD163 and CD206 profile of CD11b+ differentially treated macrophages from triplicate experiments. The CD206 and CD163 stains were weak as the signal only goes to the Log decade 2. However, profile changes based on the epicenter shifts can be observed. Dexamethasone treatment has brought the maximum shift in the epicenter moving it more towards the CD163CD206 double positive quadrant. IL-10 treatment has resulted in the epicenter shift more towards the CD163 positive quadrant above the signal cut-off. IL-4 treatment has resulted in the down shift of the epicenter towards CD163CD206 double negative quadrant. LPS treatment has not caused any dramatic shift in CD163 population when compared to IL-4 towards double negative quadrant. However, when compared to untreated cell, a shift seems to have occurred in LPS treated cells.

Figure 19 shows the percentage of CD163 positive population among various treatments. Significant ($p<0.05$) differences were found among the treatments. Untreated control cells have significantly higher population of CD163 positive cells when compared to LPS, IL-4 and dexamethasone treatment. Although, IL-10 treatments appears to have higher CD163 positive population than control cells, data could not reach statistical significance at $p<0.05$. However, IL-10 has highest CD163 positive population when compared to other treatments which is expected. LPS and IL-4 seem to have lower the expression of CD163 and thus % of CD163+ population is significantly ($p<0.05$) less when compared to control cells and/or IL-10 treated cells.

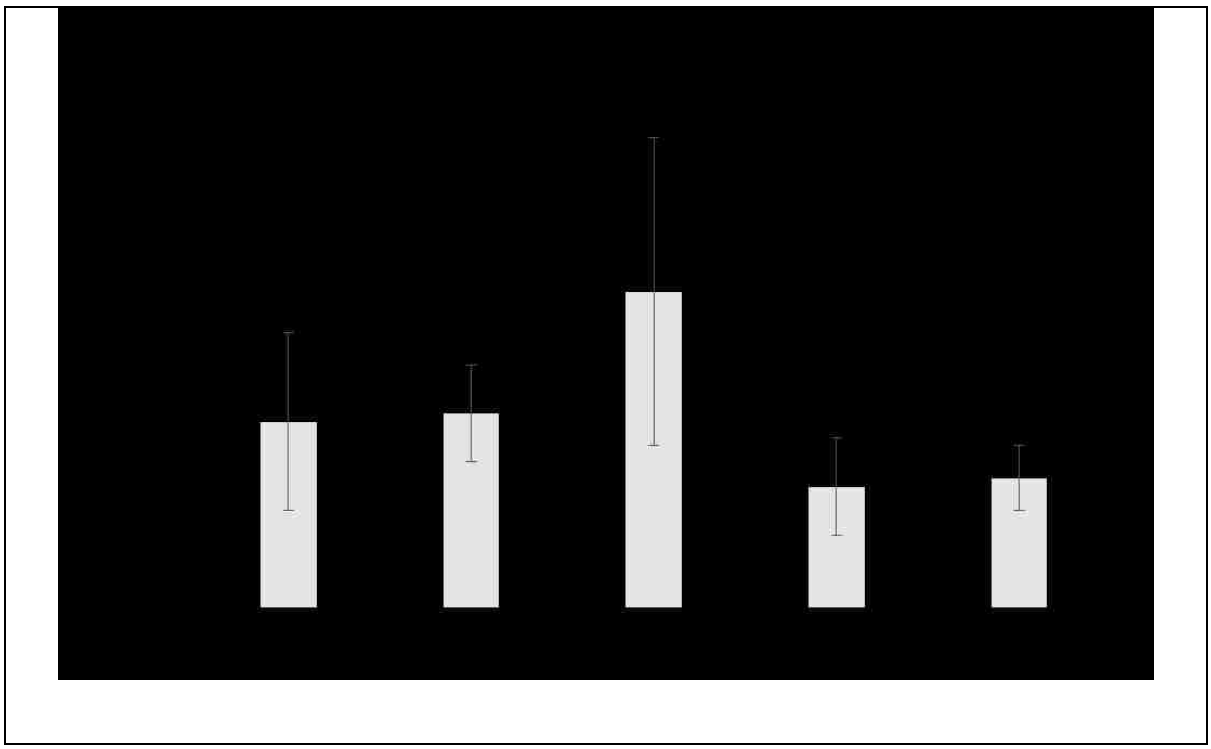

Figure 20. Graph shows the percentage of CD206 positive population among treatments

Data plotted as mean ±SD, N=3. ANOVA with Bonferroni post hoc test was performed to test for significance. Significance denoted by * $p<0.05$. Dexamethasone treated population is significantly different from Control, LPS, IL-4 and IL-10 treated populations.

Figure 20 shows the percentage of CD206 positive population among various treatments. Dexamethasone treatment has resulted in significantly ($p<0.05$) high percentage of CD206+ population when compared to control cells or IL-10 treated cells which would be expected. LPS, IL-4 and IL-10 do not seem to affect CD206 receptor expression when compared to the control cells.

Thus overall, LPS treatment resulted in only mild increase in CD86 expression while MHCII expression appears unaffected. IL-10 did not affect CD163 or CD206 expression. IL-4 treatment enhanced the expression of MHCII and decreased CD163 expression while CD206 remained unaffected. Dexamethasone has resulted in most dramatic shift compared to all other treatments. Dexamethasone enhanced CD206 expression and lowered CD86 and MHCII expression. Dexamethasone is a broad range anti-inflammatory agent. Its mechanism of action, which are still not very clear, involve shut down of major signaling pathways in the cell [123, 124]. It could be the concentration of IL-10 may not have been optimal for a dramatic effect on splenic macrophages. Similarly, the concentration of LPS used might not have been high enough for any dramatic shift in M1 markers CD86 and MHCII as rats are the most resistant species in terms of responsiveness to LPS.

The development of the flow cytometry assay allowed for assessment of protein expression in individual cells within complex populations of activated macrophages. It appears that untreated (control) splenic macrophages abundantly express the cell surface markers CD86, MHCII, CD163 and CD206 receptors. Thus, dramatic changes in receptor expression profile are not evident when compared to other treatments. Splenic macrophages are also quite heterogeneous as discussed in Chapter 1 (macrophage heterogeneity section). As mentioned before, most of the studies have been done on mice bone marrow derived macrophages (BMDM) which are relatively naïve, less

heterogeneous and undifferentiated compared to macrophages extracted from the spleen [125]. Thus, immunomodulation of BMDM seem to have dramatic shift in receptor expression profiles. Nonetheless, it is evident that splenic macrophages do respond to the modulators.

The data provides interesting insight into receptor expression modulation in response to modulators. IL-4 mediated enhanced MHCII expression is contrary to murine macrophages. From chapter 2 and 3, through various assays including flow cytometry assays immunomodulation of rat macrophages can be established *in vitro* with few possible interspecies differences from murine macrophages. Taken together, the data so far obtained provides a roadmap for *in vivo* experiments in terms of expectations for markers in response to IL-4 and IL-10 treatment.

3.4 Conclusion and Significance

To conclude, an in-house developed flow cytometry assay provided an alternative tool to profile differentially activated states of macrophages. IL-4 mediated enhanced MHCII expression is contrary to what is typically observed with murine macrophages where decreased MHCII expression is observed. IL-4 decreased CD163 expression and did not affect CD206 expression. Dexamethasone showed the most dramatic shift in both CD86 and CD206 receptor expression which was expected. LPS slightly increased CD86 expression which was expected, but did not affect MHCII and CD206 expression which was unexpected. IL-10 was expected to significantly enhance CD163 receptor expression but appears to cause no effect. IL-10 mediated CD163 upregulation has been observed in murine peripheral blood macrophages and bone marrow derived macrophages in vitro. CD163 upregulation has also been observed in vivo in wound macrophages. Gene expression data suggest upregulation of CD163 in response to IL-10. The time point of maximal CD163 receptor expression remaining off while samples were harvested, or high CV

between the triplicates resulting in statistically insignificant results could explain the lack of observed significant enhanced CD163 receptor expression in response to IL-10 in flow cytometry assays. The IL-10 treatment did not affect MHCII and CD86 expression as well.

Overall Significance: Assessment of surface receptor expression by flow cytometry is another tool for further characterization of phenotypic profiles of macrophages. The motivation to perform flow cytometry assays was to gain information on MHCII, CD28, CD68 and CD86 receptors of differentially polarized macrophages that could not be established through ELISA. The qRT-PCR assays were performed on only two of the surface receptor protein (CD163 and CD206) targets. Thus, flow cytometry assays were performed to validate qRT-PCR mRNA transcript data on CD163 and CD206 at protein level as well as to gain insight on above mentioned other surface protein markers.

Specific Points of Significance

1. Flow cytometry assays on splenic macrophages demonstrate that resting (control) cells are positive for MHCII, CD86, CD163 and CD206. Dramatic enhancement of receptor expression in response to IL-4 and IL-10 may not have been observed as splenic macrophages are relatively more differentiated (with positive expression for markers under investigation) than bone marrow macrophages or peripheral blood monocytes. This again highlights the point that depending on the source of macrophage derivation, variations in data can arise. Thus, it is crucial to perform studies on macrophages derived from various sources for in-depth understanding of macrophage activation biology. Use of rodent splenic macrophages in the present study is new and adds to the growing knowledge base in the field of macrophage activation.

2. Gene expression data suggests upregulation of CD163 in response to IL-10 and CD206 in response to IL-4. However, any significant differences in receptor expression using flow cytometry assays were not found. The gene expression could be transient without the significant enhanced receptor protein translation. This is a significant result as this highlights the known problem of correlation between gene expression and protein expression data due to different control mechanisms at transcription and translational levels. Thus, combination of various assays are used for the characterization of macrophages. Although, it is important to point out that lack of positive expression in flow cytometry may not mean no change in phenotype. It could also be due to reagents not being bright enough, and rare events remaining undetectable due to poor resolution as parent population (CD11b+ macrophages) was only ~28%.

3. Direct analysis of receptor expression using flow cytometry provided further insights on response to modulators. Significant enhancement of MHCII and down-modulation of CD163 in response to IL-4 was observed. Significant enhancement of CD206 and down-modulation CD86 in response to dexamethasone was observed. Direct assessment of receptor expression provide insights into translational level modulation by modulators. Taken together results from Chapters 2 and 3 provide various methodologies for characterization of differentially activated macrophages.

References

36. Varin, A., Mukhopadhyay, S., Herbein, G., Gordon, S. (2010) Alternative activation of macrophages by IL-4 impairs phagocytosis of pathogens but potentiates microbial-induced signalling and cytokine secretion. *Blood* 115, 353-362.

41. Ambarus, C. A., Krausz, S., van Eijk, M., Hamann, J., Radstake, T., Reedquist, K. A., Tak, P. P., Baeten, D. L. P. (2012) Systematic validation of specific phenotypic markers for in vitro polarized human macrophages. *J Immunol Methods* 375, 196-206.

118. Rosen, H. and Gordon, S. (1987) Monoclonal antibody to the murine type-3 complement receptor inhibits adhesion of myelomonoctytic cells-in vitro and inflammatory cell recruitment in vivo *J Exp Med* 166, 1685-1701.

119. Repo, H., Jansson, S. E., Leirisalorepo, M. (1993) Flowcytometric determination of CD11b up-regulation in vivo. *J Immunol Methods* 164, 193-202.

120. Barclay, A. N. (1981) The localization of populations of lymphocytes defined by monoclonal antibodies in rat lymphoid tissues. *Immunology* 42, 593-600.

121. Lagasse, E. and Weissman, I. L. (1996) Flow cytometric identification of murine neutrophils and monocytes. *J Immunol Methods* 197, 139-150.

122. te Velde, A. A., Yard, B. A., Klomp, J. P., de Vries, J. E., Figdor, C. G. (1989) Modulation of phenotypic and functional properties of human peripheral blood monocytes by interleukin-4 (IL-4). *Agents Actions* 26, 199-200.

123. Tsurufuji, S., Kurihara, A., Ojima, F. (1984) Mechanism of anti-inflammatory action of dexamethasone- blockade by hydrocortisone mesylate and actinomycin-D of the inhibitory effect of dexamethasone on leukocyte infiltration in inflammatory sites. *J Pharmacol Exp Ther* 229, 237-243.

124. Distelhorst, C. W. (2002) Recent insights into the mechanism of glucocorticosteroid-induced apoptosis. *Cell Death Differ* 9, 6-19.

125. Wang, C., Yu, X., Cao, Q., Wang, Y., Zheng, G., Tan, T. K., Zhao, H., Zhao, Y., Wang, Y., Harris, D. C. H. (2013) Characterization of murine macrophages from bone marrow, spleen and peritoneum. *BMC Immunol* 14.

Chapter 4: Directing Macrophage Activation with Microdialysis Probe Implants

4.1 Introduction

In previous chapters, the activation of macrophages *in vitro* in response to various stimulants was demonstrated for rodent macrophages. The data suggest important differences with respect to arginase isoform expression, and phenotype obtained in response to chitohexaose treatment. These differences could be due to species and/or source of the macrophage derivation. Nonetheless, these results demonstrate the efficacy of stimulants in driving macrophages to respective activation states. Although it is well known that *in vitro* results may not translate *in vivo*, these crucial *in vitro* experiments also serve as a roadmap in terms of what to expect when trying immunomodulation *in vivo* and to understand how well data translate *in vivo*. As mentioned in chapter 1, the long term aim of the research is in modulating the FBR around the implant site to reduce fibrosis and enhance the longevity of the implant. The hypothesis is immunomodulation of the macrophages toward pro-wound healing and tissue remodeling phenotype at the implant site may result in better FBR outcome.

This chapter explores the *in vivo* efforts to immunomodulate macrophages in response to localized delivery of IL-4 and IL-10 at the implant site. As described in chapter 1, microdialysis is a diffusion-based sampling technique. A microdialysis probe has a semipermeable membrane and an inlet and outlet tubing. A microdialysis probe can also be used to deliver the drug of interest based on diffusion. The subcutaneous insertion of a microdialysis probe causes trauma and subsequent FBR. In this regard, use of microdialysis serves as a model of FBR where drug can be

delivered and sampling can be performed simultaneously as well over time, allowing for monitoring of the microenvironment in response to drug.

The aim of these experiments was to locally deliver IL-4 or IL-10 *in vivo* via microdialysis probes inserted in subcutaneous tissue and perform sampling of cytokines. The idea was that differences in cytokine concentration between control and treatment would reflect modulation of macrophages at the implant site. Additionally, histological analysis of tissue around the implant would also be indicative of whether modulation was brought about by IL-4/IL-10 treatment. According to the literature, IL-4 is a pro-fibrotic cytokine, and delivery of IL-4 would result in more collagenous deposition around the implant. This chapter presents the results of IL-4/IL-10 delivery *in vivo* using microdialysis probes subcutaneously implanted in male Sprague-Dawley rats.

4.2 Materials and Methods

4.2.1 Animals

Male Sprague-Dawley rats (Harlan Laboratories Inc.) weighing between 275 to 350 grams were used in all experiments. All animals were housed in an environmentally-controlled facility with a 12-hour on/off light cycle and had *ad libitum* access to food and water. Surgical procedures followed approved protocols by the University of Arkansas, Institutional Animal Care and Use Committee in compliance with National Institutes of Health guidelines for the care and treatment of animals.

4.2.2 Microdialysis Supplies and Perfusion Fluid

CMA-20 (10 mm (length) x 0.5 mm (outer diameter, o.d.)) 100 kDa molecular weight cutoff (MWCO) polyethersulphone (PES) microdialysis probes (CMA Microdialysis, North Chelmsford, MA, USA) were used for all experiments. The Baby Bee single channel (BASi, W. Lafayette, IN) syringe pump was used with a 1000 µL BAS glass syringe (BASi, W. Lafayette, IN, USA) to deliver the perfusion fluid through the microdialysis probe. The perfusion fluid used was Ringer's solution containing 150 mM NaCl, 4 mM KCl, and 2.4 mM $CaCl_2$, and 0.1% (w/v) bovine serum albumin, BSA, (Sigma-Aldrich, St. Louis, MO, USA). Dextran 70 (6% w/v) or 500 (4% w/v) was added to prevent fluid loss across the high MWCO membranes during sampling. Perfusion fluids were prepared as needed and filter sterilized with a 0.2 µm PES membrane filter (Whatman, Florham Park, NJ, USA).

4.2.3 In vitro Relative Recovery for IL-4 and IL-10

Three CMA20 probes were immersed in the standard cocktail from Luminex multiplex kit. The outside probe concentration for IL-10 was 3650 pg/mL and the outside probe concentration for IL-4 was 2540 pg/mL. The *in vitro* recovery experiment was performed under stirred conditions, and perfusion fluid used was Ringer's solution with BSA (0.1% W/V) and Dextran 70 (6%W/V). Samples were collected for 4 hours. Dialysates samples were then analyzed on a Luminex Magpix multiplex platform using Luminex multiplex kit (Luminex Corp. Austin, TX, USA)

4.2.4 Surgical Implantation of the Microdialysis Probe in Subcutaneous Tissue

The animals were anesthetized with 5% isoflurane and were maintained under anesthesia at 2.5% isoflurane during the procedure. The dorsal side of the animals was shaved. Iodine was applied to the shaved area and wiped off with a clean alcohol gauge pad. With the help of a sterile surgical blade and forceps, T-shaped incisions were made. A subcutaneous pocket was created following the incision. With the help of the needle and the introducer, microdialysis probes were implanted on the dorsal subcutaneous tissue on either side of the midline in a symmetrical manner. Microdialysis probe lines were tunneled through a subcutaneous pocket and were pulled out from behind the neck. Lines were tucked under the subcutaneous pocket behind the neck after sampling procedures were done with the help of sterile forceps and sterile wound clips. For long term sampling from the same animals, animals were anesthetized, wound clips removed and lines pulled out. Animals were brought out of anesthesia to perform delivery and sampling in awake and freely moving animals.

4.2.5 Delivery of IL-4 and Sampling from Subcutaneous Implants

4.2.5.1 Set up 1

Two CMA 20, 100 kDa MWCO, 10 mm PES microdialysis probes were implanted into the dorsal subcutaneous space in male rats. The treatment probe included 50 ng/mL of recombinant rat (rr) IL-4 in the perfusion fluid. Ringer's solution was used as perfusion fluid supplemented with dextran 70 as an osmotic agent and 0.1% BSA. Sampling was performed on the day of

implantation (day 0) and on day 3 post-implantation with a flow rate of 1 µL/min for a total of 4 hours in awake and freely-moving animals. Samples were collected every hour. On days 0, 1, 2 and 3, a flow rate of 0.5 µL/min was used for delivery of rrIL-4. Luminex™ multiplex assays (Millipore) were used for the quantification of cytokines (IL-1β, IL-6, IL-10) in the dialysate samples. On day 4, the rats were euthanized and tissues surrounding the implanted probes were harvested for histological and immunohistochemical analysis.

4.2.5.2 Set up 2

Two CMA 20, 100 kDa MWCO, 10- mm PES microdialysis probes were implanted in the dorsal subcutaneous space in male rats. The treatment probe included 50 ng/mL of rrIL-4 in the perfusion fluid. Ringer's solution was used as perfusion fluid supplemented with dextran 500 as an osmotic agent. Sampling was performed on the day of implantation (day 0) and day 4 post-implantation with a flow rate of 1 µL/min for a total of 5 hours in awake and freely-moving animals. Samples were collected every hour. On days 0, 1, 2 and 3, a flow rate of 0.5 µL/min was used for delivery of rrIL-4. Luminex™ multiplex assays were used for the quantification of cytokines (IL-1β, IL-6) in the dialysate samples. On day 4, the rats were euthanized and tissues surrounding the implanted probes were harvested for histological and immunohistochemical analysis.

4.2.5.3 Set up 3

Two CMA 20, 100 kDa MWCO, 10 mm PES microdialysis probes were implanted into the dorsal subcutaneous space in male rats. The treatment probe included 1500 ng/mL of rrIL-4 or 1200ng/mL of rrIL-10 in the perfusion fluid. Ringer's solution was used as perfusion fluid supplemented with dextran 500 as an osmotic agent. Sampling was performed on day 2 post-implantation with a flow rate of 1 µL/min for a total of 5 hours in awake and freely-moving

animals. Samples were collected every hour. On days 0 (day of implantation) and 1, a flow rate of 0.2 µL/min was used for delivery of rrIL-4. CCL2 ELISA (BD OptEIA) was performed for the measurement of CCL2 concentrations in the dialysates. On day 2, after sampling was over, the rats were euthanized and tissues surrounding the implanted probes were harvested for gene expression assays.

4.2.6 Microdialysis Perfusion Effects on Wound Healing

To determine perfusion fluid effects, Two CMA 20, 100 kDa MWCO, 10-mm PES microdialysis probes were implanted into the dorsal subcutaneous space in male rats. Ringer's solution was perfused in one probe for 4 days at 0.5 µL/min. The control probe was not perfused. On day 7 post-implantation, the rats were euthanized. Tissues surrounding the implanted probes were harvested for histological analysis. Extreme care was taken to excise ~ 1 cm tissue surrounding the probe each time following aseptic techniques using sterile scalpel blades, forceps and scissors.

4.2.7 Histology

Explanted probes and sponges were preserved and fixed in 10% neutral buffered formalin at room temperature. Samples were processed and prepared by the Histology Laboratory at the University of Arkansas. Samples were embedded in paraffin and sections 5-8 µm were cut. Sections were stained with Masson's Trichrome for examination of collagen and fibrous deposition. Hematoxylin and eosin staining was also performed on the sections for the assessment

of cellular infiltration. Prepared sections were imaged on a Zeiss Axioplan 2 microscope with 10X /30 mm ocular lenses. Both 10X and 40X objective lenses were used. Images were recorded with a high resolution charged couple device camera. Images were processed with the help of ImageJ software (NIH).

4.2.8 Quantitative Real Time PCR Assays

Total RNA was extracted by a phenol/chloroform phase separation process from tissues with the help of TRIzol® reagent (Life Technologies) followed by column clean-up using RNeasy mini kit (Qaigen). RNA concentration was assessed by measuring the absorbance at 260 nm using a Nanodrop spectrophotometer (Thermo Scientific). An RNA quality and integrity check was performed by measuring the 260 nm/280 nm ratio and by agarose gel electrophoresis (Sigma, 1.2% gel). RNA was converted to cDNA using the High Capacity RNA to cDNA kit (Applied Biosystems). Techne TC-3000 thermocycler was used to perform the reverse transcriptase reaction for 60 min at 37ºC, followed by 5 min at 95ºC. Quantitative real time PCR was performed in duplicates. Each reaction was performed in a total volume of 50 µL using TaqMan® Gene Expression Master Mix and pre developed TaqMan® probe/primer assay reagents (Life technologies) using ABI prism 7500 sequence detection platform (Applied Biosystems). Relative expression was normalized to the reference condition and to the levels of TAF9b gene.

4.3 Results and Discussion

4.3.1 IL-4 Delivery Effects – Set up 1 Experiments

In vitro relative recovery for IL-10 was found to be 0.6% (±0.2%, N=3) and in vitro relative recovery for IL-4 was found to be 3.5 % (±0.3%, N=3). *In vivo* delivery experiments were initiated after getting the estimates of in vitro relative recovery for IL-4 and IL-10.

The treatment probe included rrIL-4 at 50 ng/mL concentration in Ringer's solution that had dextran 70 as an osmotic agent. Probes were perfused on day 1 and 2 at 0.5µL/min for 1 hour. Sampling was performed on day 0 and on day 3. After sampling was over on day 4, the animals were euthanized and the probes were harvested for histological analysis. Figure 21 shows the whole set up of live and freely moving delivery and sampling. Figure 16 shows the Masson's Trichrome staining and Figure 22 shows the Hematoxylin and Eosin (H&E) staining of control and treatment probes.

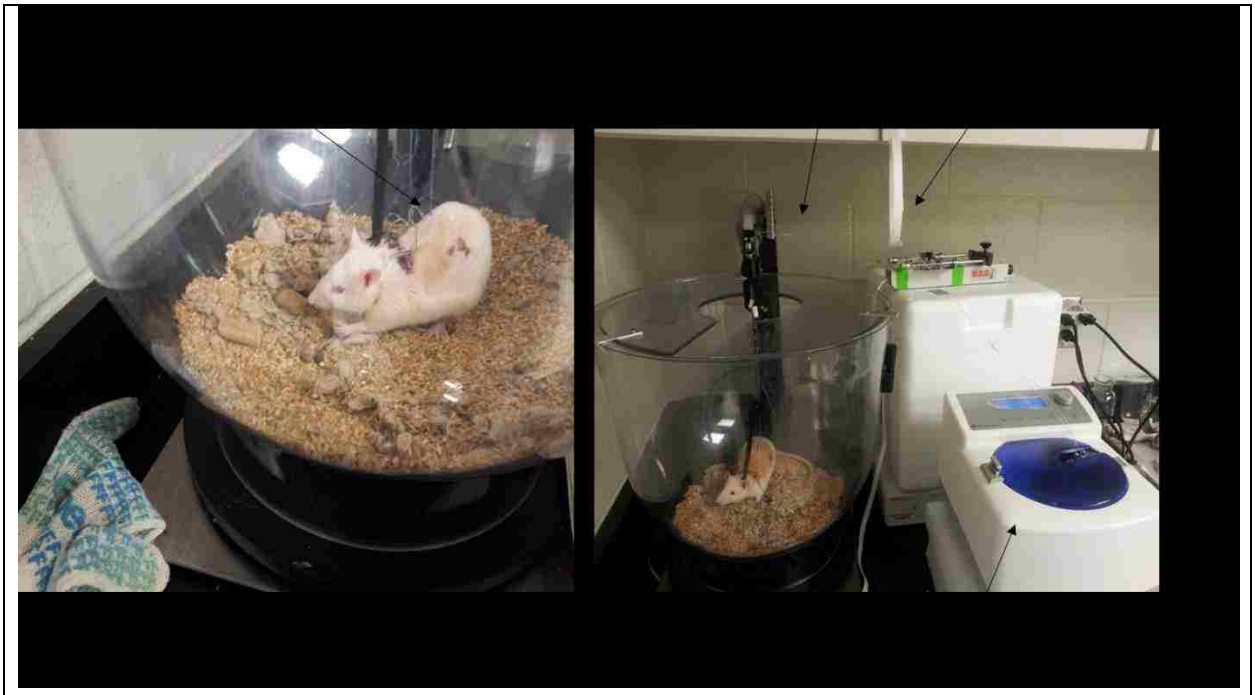

Figure 21. The set up showing live and freely moving delivery and sampling of analytes in rat

The figure shows entire set up of microsialysis delivery and sampling. The picture on the left shows the rat with subcutaneously implanted microdialysis probe placed inside the rat bowl. Black arrow indicates the implant location. The picture on the right shows the implanted probe hooked up to the syringe pumps. Outlet tubing connects to the vials in the automated sampler.

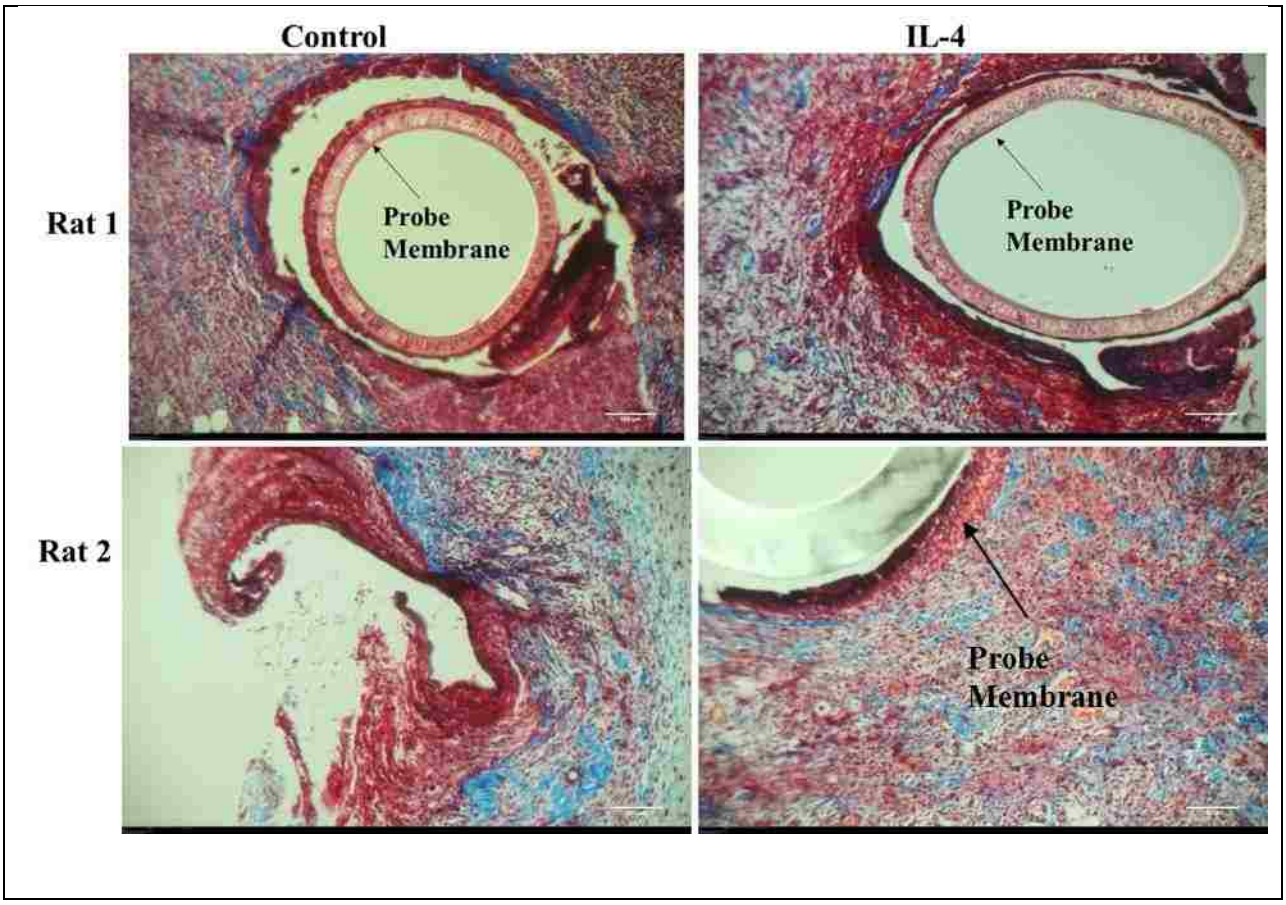

Figure 22. Masson's Trichome staining of tissue section surrounding the probe

Tissue surrounding the probes were harvested on day 3 and prepared for histological analysis. Collagen strands have been stained blue. Any noticeable differences with respect to collagen deposition between the control probe and IL-4 (50 ng/mL) perfused probe were not found.

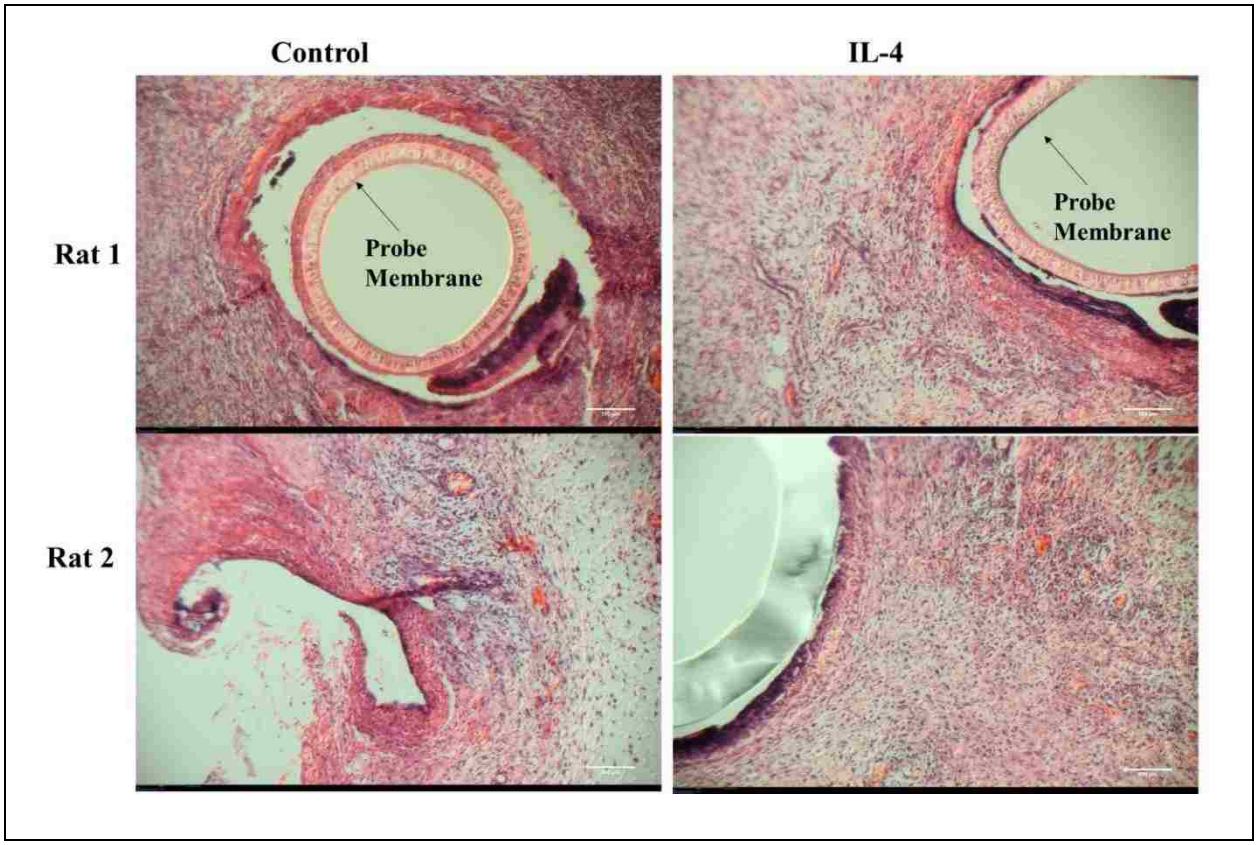

Figure 23. Hemoatoxylin and Eosin staining of tissue section surrounding the probe

Tissue surrounding the probes was harvested on day 3 and prepared for histological analysis. Collagen strands have been stained light pink. Cells have been stained as purple. Any noticeable differences with respect to collagen deposition or cellular infiltration between the control probe and IL-4 (50 ng/mL) perfused probe were not found.

As evident from Figures 22 and 23, any noticeable difference in histological sections between control and IL-4 treated tissue sections is not present. Masson's Trichrome stains the collagen in blue; thus, based on the implicated role of IL-4 in fibrosis, it would be expected to see more collagen deposition in IL-4 treated tissue. Hematoxylin and Eosin staining is mainly performed to gain insight into cellular infiltration. The nuclei of the cell are stained blue and red blood cells are stained bright orange or cherry red. Collagen fibers are stained pinkish in this stain. There is no marked difference between the control and IL-4 treated probe. The images shown here are representative images. A total of six rats were used in the experiment. At 50 ng/mL IL-4 infusion per hour every day for 3 days, any noticeable differences in histology were not found. It could be that IL-4 did not diffuse out of the probe, or it could be the dose was not high enough to cause modulation.

Microdialysis sampling of cytokines was performed on day 0 and day 3. Tables 2, 3 and 4 show the concentration of IL-6, IL-1β and IL-10, respectively, in the dialysate samples.

Table 2. Concentration of IL-6 in pg/mL on day 0 and day 4

IL-6 (pg/mL)				
Day 1	**Rat 1**		**Rat 2**	
Hour	**Treatment**	**Control**	**Treatment**	**Control**
1	50	50	70	Low
2	35	70	Not Available† (NA)	20
3	35	50	NA	Low
4	70	35	NA	Low
5	70	Low	NA	Low
Day 4 (hours)				
1	Low	290	20	Low
2	Low	100	Low	Low
3	Low	145	Low	Low
4	Low	180	Low	Low
5	Low	100	Low	Low

†Not Available (NA): indicates no dialysate collection due to random probe malfunctioning. Low indicated dialysate value being below detection of the assay limit.

Table 3. Concentration of IL-1β in pg/mL in dialysate samples

IL-1β (pg/mL)				
Day 1	**Rat 1**		**Rat 2**	
Hour	**Treatment**	**Control**	**Treatment**	**Control**
1	8	Low	Low	Low
2	Low	Low	NA†	Low
3	20	5	NA	Low
4	30	10	NA	Low
5	30	12	NA	Low
Day 4 (hours)				
1	Low	20	0	22
2	Low	Low	Low	Low
3	Low	Low	Low	8
4	Low	20	Low	45
5	Low	Low	Low	40

†Not Available (NA): indicates no dialysate collection due to random probe malfunctioning. Low indicated dialysate value being below detection of the assay limit.

Table 4. Concentration of IL-10 in pg/mL in dialysate samples

IL-10 (pg/mL)				
Day 1	**Rat 1**		**Rat 2**	
Hour	**Treatment**	**Control**	**Treatment**	**Control**
1		1265	1750	485
2	140	2610	NA†	275
3	60	2620	NA	230
4	65	4130	NA	110
5	38	3510	NA	NA
Day 4 (hours)				
1	190	55	305	305
2	90	40	Low	Low
3	75	30	80	13
4	120	50	Low	110
5	130	35	Low	75

†Not Available (NA): indicates no dialysate collection due to random probe malfunctioning. Low indicated dialysate value being below detection of the assay limit.

The IL-10 concentration seems to be higher in all the control samples in Table 4. The source of this anomaly was cross contamination from syringes that were used for other IL-10 delivery experiments. It is clear from Tables 2, 3 and 4 that no comparison could be drawn between samples obtained from control probes and IL-4 perfused probes to determine whether perfusion of IL-4 brought any changes in the cytokine microenvironment of the probe implant. Probe failure and analyte remaining below detection limit were the main constraints.

4.3.2 Perfusion Effects at the Implant Site

At this point it was also imperative to figure out if constituents of the perfusion fluid and perfusion itself were causing an inflammatory response. A series of experiments were undertaken in which major components of the perfusion were compared to control, viz Ringer's perfused probe vs non perfused probe, Ringer's with the dextran 70 vs Ringer's alone and Ringer's with BSA vs Ringer's with RSA (rat serum albumin). It was found out that dextran 70, which was being used an osmotic agent, was leaking out of the probe causing inflammation, thus inclusion of dextran 500 as an osmotic agent was opted [126]. Results of perfusion and no perfusion (control) are presented in this section. Figure 24 shows the Masson's Trichrome staining of tissue sections surrounding the probes that were perfused with Ringer's solution only (not including dextran or BSA) compared with the probe that was implanted as control and was not perfused at all. A total of three rats were used in this experiment. Probes were explanted on day 7. Figure 25 shows the normal subcutaneous tissue histology. It is clear from the Figures 24 and 25 that control probe histology is much more like normal subcutaneous tissue histology.

The normal subcutaneous tissue (non-traumatized, far away from the probe) histology shows that the tissue had ample supply of blood vessels and has collagen fibrils. The non-perfused probe at day 7 is also surrounded by collagen fibril deposition, and vasculature (blood vessels) is developing.

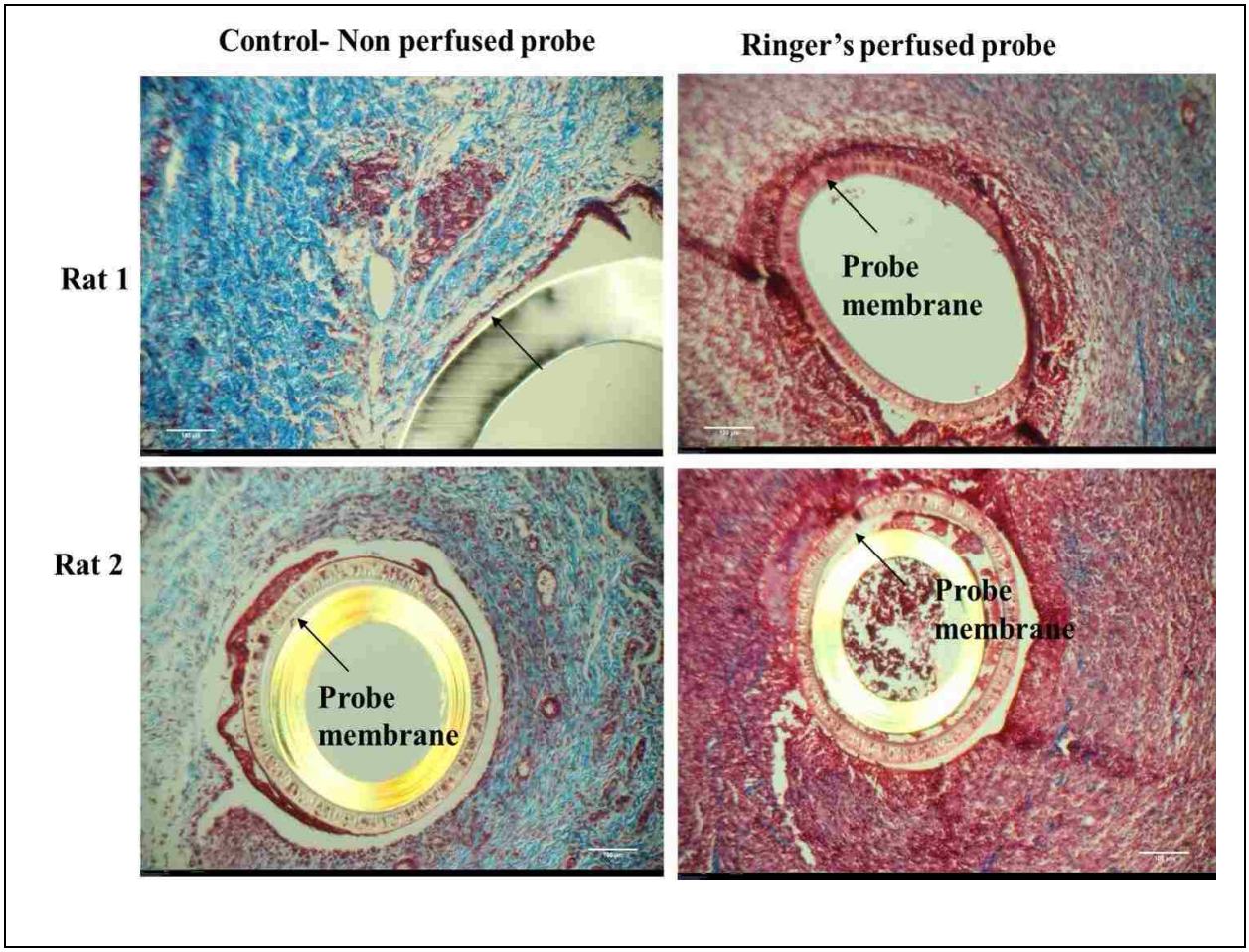

Figure 24. Masson's Trichrome staining of tissue surrounding control non perfused probe vs Ringer's perfused probe (10X resolution)

Tissue surrounding the probes were harvested on day 7 and prepared for histological analysis. Collagen strands have been stained blue. Noticeable differences with respect to collagen deposition between the control non-perfused probe and perfused probe can be observed. The perfused probe has less collagen fibril deposition and appear dense in cellular infiltration.

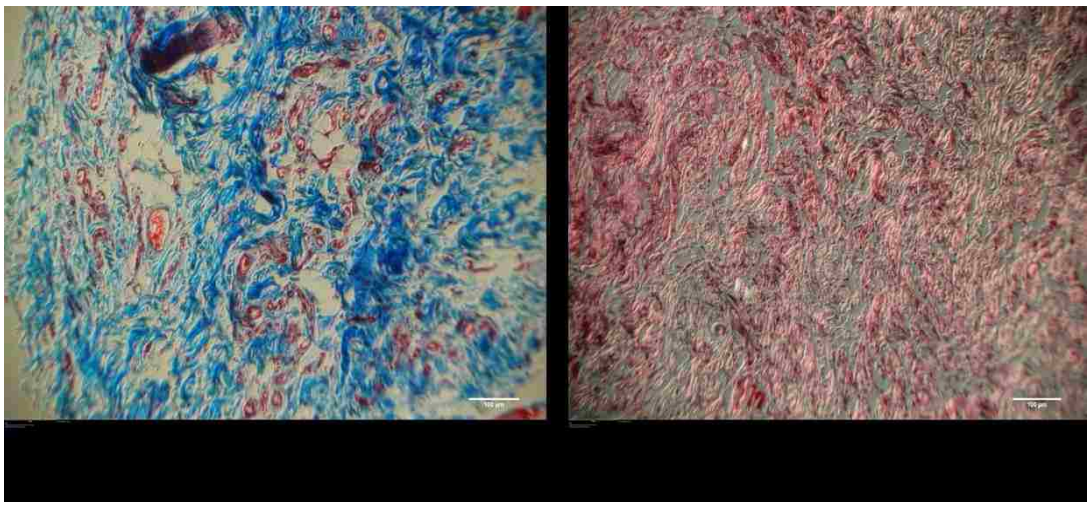

Figure 25. Normal subcutaneous tissue histology

The Figure represents the normal subcutaneous tissue (non-traumatized, far away from probe) histology stained with both Masson's Trichrome, and Hematoxylin and Eosin stains. There is ample collagen fibril network and abundant blood vessel supply (concentric ring like structures) with sparse cellular presence.

Overall, the comparison indicates that the non-perfused probe is healing in its natural course after implantation to appear more like the normal subcutaneous tissue histology. On the other hand, tissue surrounding the perfused probe still appears inflamed with less collagen fibril networking. Dense cellular infiltration is clearly visible with little developed vasculature, present only in areas away from the probe where collagen fibril deposition is seen.

It is clear that even the process of perfusion causes inflammation. However, perfusion is necessary for sampling and delivery of the drug. These experiments gave insight on how natural response to the implanted microdialysis probe looked like at day 7 when compared to normal subcutaneous tissue histology and how it differed when the probe is perfused. Overall, the conclusion was to stop the usage of dextran 70 as an osmotic agent.

4.3.3 IL-4 Infusion with Dextran 500 in Ringer's fluid – Set up 2 Experiments

IL-4 infusion experiments were again initiated. This time, dextran 500 was used in the perfusion fluid as an osmotic agent, as it was found dextran 70 was leaking out of the membrane, leading to additional inflammation. It was anticipated that effects of IL-4 might be observed in this set of experiments, as the inflammation due to dextran 70 that might be overwriting the effects of IL-4 infusion has been taken care of. In this set of experiments, a total of 6 rats were used. A dose of 50 ng/mL was infused on day 0 following sampling, and then on days 1, 2 and 3 a dose of 100ng/mL of IL-4 was infused for 1 hour at 0.5 µl/min, followed by sampling on day3. Animals were euthanized on day 7 and tissue surrounding the probe was harvested on day 7. Figure 26 shows the day 7 explants of control and IL-4 treated probe. Again, the problem of random probe failure on various time points of the study led to inconclusive data. In animals (N=2), where both

the control and treatment probes worked, no differences in histology could be established. Multiplex assays performed on dialysate samples obtained in these animals, also remained undetectable for IL-1β and IL-6 leading to inconclusive data.

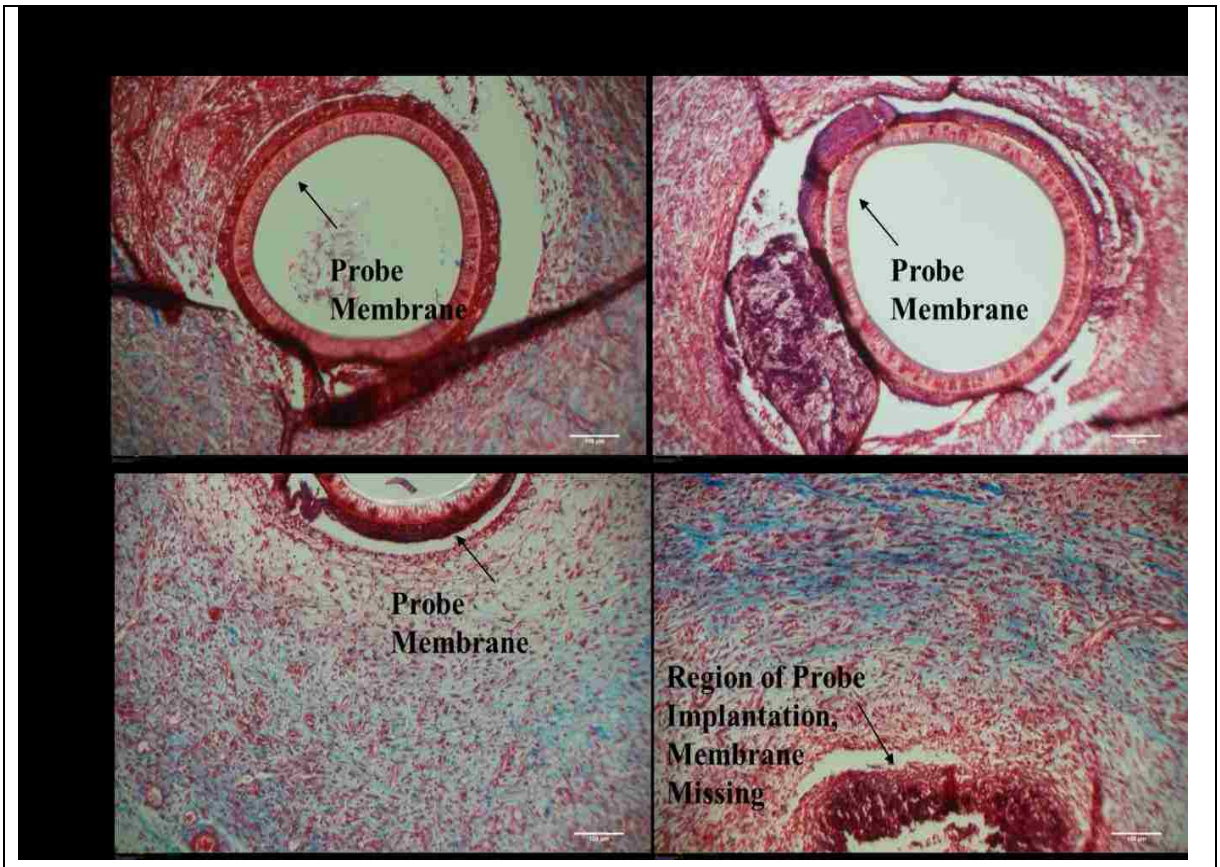

Figure 26. Masson's Trichrome staining of tissue sections surrounding the probe. (10X magnification)

Tissue surrounding the probes was harvested on day 7 and prepared for histological analysis. Collagen strands have been stained blue. Any noticeable differences with respect to collagen deposition and cellular infiltration between the control probe and the IL-4 (50 ng/mL, in Ringer's with dextran 500 as an osmotic agent) perfused probe were not found.

4.3.4 IL-4/IL-10 Infusion at Higher Dose – Set up 3 Experiments

The challenges with the previous experiments led to this set of experiments in which the major motivation was to test infusion of a higher dose of IL-4 or IL-10 at a very slow flow rate (0.2µl/min) for a total of 1.5 hours at time points 0 (right after probe insertion), 24 hours, 48 hours and termination at 72 hours. Slow flow rate was chosen to enhance the concentration of analyte around the probe, as the slower the flow rate, the more time for analyte to diffuse across the probe. Thus, slow flow rate increases the local concentration, but decreases the total amount delivered. IL-4 at 1500 ng/mL was included in Ringer's solution without dextran and BSA. The rationale was to avoid any kind of non-specific binding/clogging of membrane region with dextran and BSA. At the 72 hour time point, animals were euthanized and probes were harvested for gene expression analysis. Previous methods of multiplex cytokine assays and histology comparison did not yield any conclusive results. Thus, the idea was to measure changes at the transcript level to ascertain whether IL-4/IL-10 did affect the microenvironment at all. Figure 27 shows the gene expression analysis of tissue surrounding the control probe and IL-4 (1500 ng/mL) infused probe. Taf9b was used as a reference gene and normal subcutaneous tissue (far away from probe insertion area) was used as a reference condition.

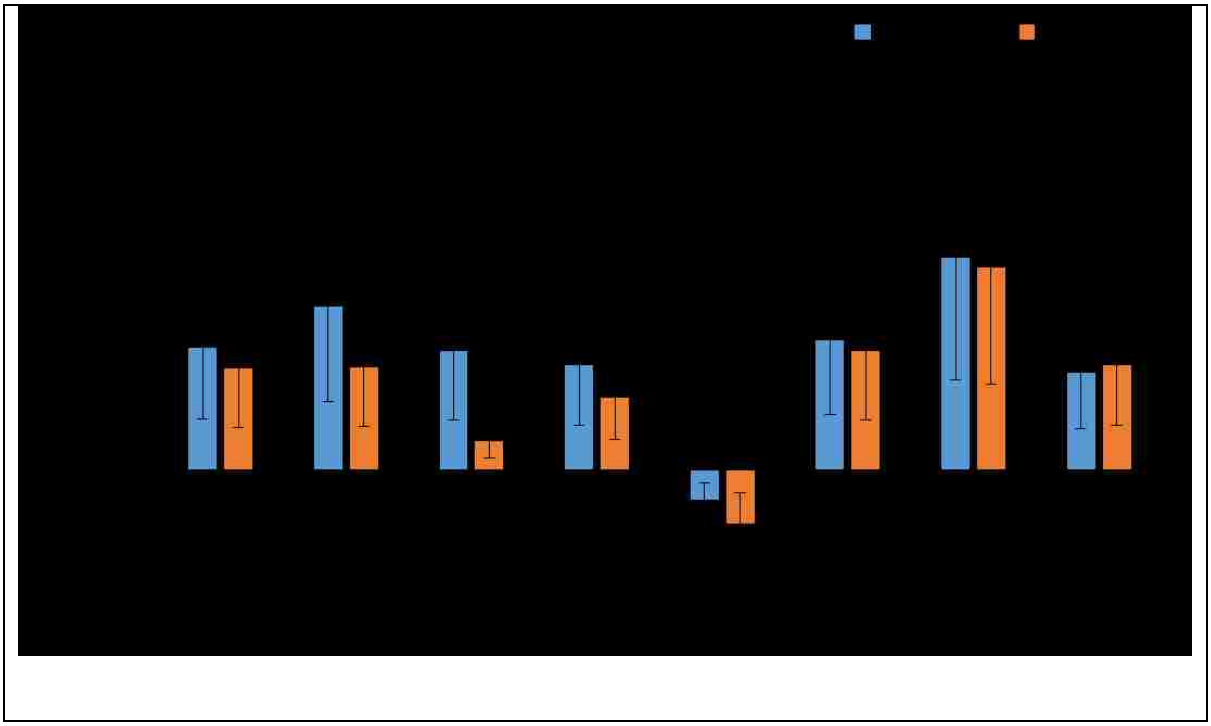

Figure 27. Gene expression profile of tissue surrounding the control and IL-4 infused probe

Gene expression profile of IL-4 (1500 ng/mL) infused tissue and control tissue around the microdialysis probe. The log base 2 transformed expression ratios (fold change) represent the mean values from 3 animals. (±SD represented by error bars). Normal subcutaneous tissue (far away from probe) as reference sample and TAF9B gene was used as a reference gene. Significance is denoted by * $p<0.05$.

CCL2, NOS2 and IL-6 are significantly upregulated ($p<0.05$) in control probe tissue when compared to the un-traumatized reference tissue. In IL-4 treatment tissue, only NOS2 is significantly ($p<0.05$) upregulated when compared to the reference tissue. It is interesting to note that inflammatory cytokines IL1β, IL6 and CCL2 are not upregulated in IL-4 probe tissue. This suggests that there could be some effects of IL-4 on the probe site. Placement of both the probes involved surgery, perfusions, osmotic effects and inflammation. The only variable was infusion of IL-4 at 1500 ng/mL, as opposed to just Ringer's solution in control probe. It is possible that at concentration of 1500 ng/mL (with only ~3% diffusion across ie 45 ng/mL), changes might not be stark enough to be picked up when directly comparing the control probe and IL-4 probe tissue.

4.3.4.1 IL-4 Infusion and Sampling at 72 hours

Based on above gene expression analysis in response to IL-4 infusion, a small pilot study comprising of 3 rats was conducted. In this set of experiments, all the procedures were done the same as above, except at the 72 hour time point microdialysis sampling (for 5 hours) was also performed with both the control and IL-4 infused probe before euthanizing the animals. Based on the results from gene expression studies (Figure 27), CCL2 was chosen for analysis.

Table 5. CCL2 (pg/mL) levels in dialysates obtained from control and IL-4 probe

Animal 1 (CCL2 pg/mL)				Animal 2 (CCL2 pg/mL)		
Hours	**Control**	**IL-4**		**Hours**	**Control**	**IL-4**
0	NA	200		0	580	240
1	170	400		1	410	260
2	70	220		2	190	140
3	70	225		3	150	100
4	60	220		4	110	140
5	50	250		5	85	110

Table 5 shows the CCL2 levels obtained from control probe and IL-4 infused probe from two animals. Levels of CCL2 obtained from animal 1 appear to be higher in the treatment probe. However, CCL2 levels obtained from animal 2 appear to be lower in the treatment probe than would be expected from the gene expression assays. However, it could be possible that implantation trauma might have been pronounced in animal 1 which could have let to the higher levels of CCL2 in the dialysates. At this point, with N value of only 2, no conclusion can be drawn. More experiments are needed to be performed to have enough statistical power.

4.3.4.2 IL-10 infusion and gene expression analysis at 72 hour time point

In this set of experiments 3 rats were used. A similar experimental set up was used as for IL-4 infusion in the above experiment. Briefly, two probes were implanted, one as a control probe perfused with Ringer's solution alone and a treatment probe perfused with 1200 ng/mL of IL-10 in Ringer's solution. A flow rate of 0.2 µL/min was used and perfusions were done for a total of 1.5 hours on time points 0, 24, 48 hours followed by termination of animals at 72 hours and extraction of tissue surrounding the probes for gene expression analysis. Figure 22 shows the gene expression profile of control probe tissue and IL-10 probe tissue. TAF9B gene was the reference gene, and non-traumatized normal subcutaneous tissue was used as reference condition. It is interesting that CCL2 is mildly upregulated in IL-10 infused probe tissue. The log ratio for control CCL2 is 9.6 (±5.6) and that for IL-10 treated probe is 9.9 (±5.7).

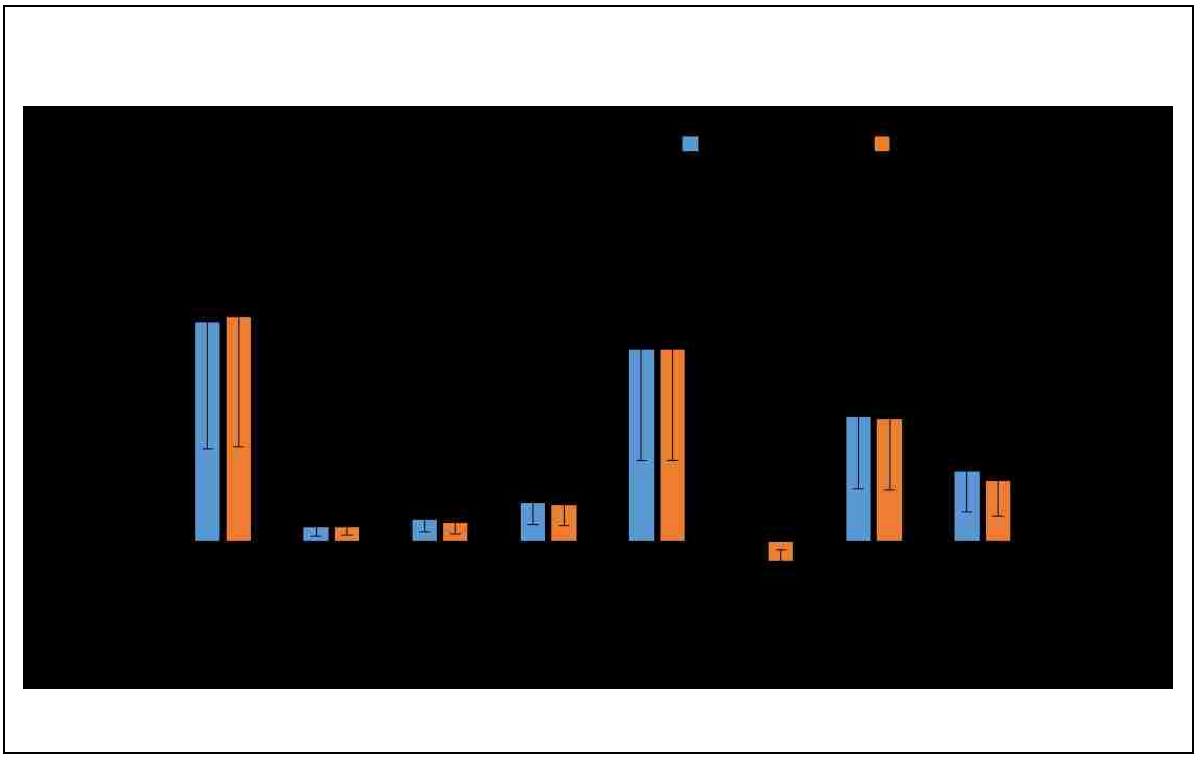

Figure 28. Gene expression profile of tissue surrounding the control probe and IL-10 infused probe

Gene expression profile of IL-10 (1200ng/mL) infused tissue and control tissue around the microdialysis probe. The log base 2 transformed expression ratios (fold change) represent the mean values from 3 animals. (±SD represented by error bars). Normal subcutaneous tissue (far away from probe) as reference sample and TAF9B gene was used as reference gene. Significance is denoted by * $p<0.05$.

It could be that IL-10 infusion resulted in transient CCL2 expression, but at this stage any conclusive remarks cannot be made. It is clear that more experiments are required to have confidence in the data. It may be possible that concentration of cytokines, especially IL-10 used for infusion, were not enough to affect genes CD163, Arg2 and CD206, or it may be that early infusion of cytokine followed by analysis at the 72 hour time point may not be as efficacious as opposed to delayed infusions on later days as FBR/wound healing progresses. It could be that IL-10 when introduced from the day of surgery and analyzed at the 72 hour time point may only modulate the expression of CCL2 alone. As discussed in chapter 1 (progression of wound healing and FBR) neutrophils infiltrate the site from 24 hour onwards and they remain on the site till 48 hours. Macrophages begin to infiltrate from 48 hours to 72 hours onwards. Thus, infusion at early time points may give quite different modulation responses as opposed to the introduction of drugs at later stages when macrophages dominate the site from 48 hours onwards.

More studies are needed to fully optimize, and ensure less variability and confidence in the data. Initial pilot experiments with IL-4 infusion at higher dose suggest significant downregulation of CCL-2 expression. The sample size needed for further experiments can be determined by power analysis. Below are the results of power analysis for this pilot study of IL-4 infusion (1500 ng/mL)

		Sample Size Needed in Each Group			
alpha level			**Power**		
("p" value)		**95%**	**90%**	**80%**	**50%**
0.10		10	8	6	3
0.05		13	10	8	4
0.02		15	13	10	5
0.01		17	14	11	6

The above power analysis show appropriate sample sizes to have required statistical power. Usually, 80% power is acceptable. If the differences are small, then the sample size required would be large.

Most importantly, experiments are needed to confidently show diffusion of IL-10 (also, IL-4) across the probe that could cause a biological response. It is very important to mention that these experiments are completely novel with respect to the delivery of cytokine as drugs using a microdialysis probe to cause immunomodulation around the implant site. There are several constraints and challenges associated with these experiments.

The delivery of the analyte is estimated based on the *in vitro* RR% of that analyte. It is assumed that diffusion of analyte out from the probe would be same as its RR%. *In vitro* relative recovery of IL-4 and IL-10 was determined to be ~3.4% and 1% respectively. Thus, if 1500 ng/mL concentration of IL-4 is used, then it would be estimated that delivered concentration would be

roughly 50 ng/mL. Similarly, *in vitro* RR% of IL-10 is ~1%; thus, at a concentration of 1200 ng/mL, it would be estimated that roughly 12 ng/mL is being delivered. These are only estimates based on the assumption that diffusion in and across the probe is the same but determination of the exact concentration of the drug being delivered is an important factor and needs to be addressed. Also, whether the drug/cytokine remains biologically active from the time it is filled in the syringe, runs through the long FEP tubings (~15 inches) and reaches the microdialysis membrane region is also a concern.

The advantage of a microdialysis system is that it can be employed for long term sampling over time, on different days and the animal serves as its own control. However, it needs to be established that targeted cytokines and chemokines relevant to these studies (that are affected by IL-4 and IL-10 modulation) can be sampled effectively and reproducibly. Another major concern is the variability of recovery between the control and treatment probes due to differences in surgical implantation of the probes. There are inherent diffusion resistances to cytokines in the microdialysis sampling process which can further vary between the probes due to differences in surgical trauma. This could lead to question if the observed differences in the cytokines levels from treatment probe and control probe are actually due to the changes brought about by the infused drug or due to inherent diffusion constraints of the cytokines. This could be answered through skilled surgical implantation of the probes, and the reproducibility of the data can ensure modulation in response to the drug. Another concern is the recovery of the target analyte/cytokine. In the microdialysis sampling process, the collected analyte is only a certain percentage of what is present in the extracellular space. Thus, if the changes brought about by the drug between control and treatment are not vast enough, it might be hard to be picked up as the recovery might not be very different.

It is important to be aware of and acknowledge the above-mentioned concerns while optimizing the experiments. Overall, it could be concluded from this chapter that these experiments are novel and challenging, needing a lot more optimization. Based on the gene expression profile of tissues surrounding the IL-4/IL-10 infused probe and control probe, it seems that there are effects; however, concentration of IL-4/IL-10, length of IL-4/IL-10 infusion and time points for end point analysis also need careful consideration for future studies.

4.4 Conclusion and Significance

To conclude, microdialysis mediated delivery of IL-4/IL-10 to modulate the macrophage responses at the implant site is novel. The gene expression profile of tissues surrounding the IL-4/IL-10 infused probe and the control probe suggest modulation in IL-6, CCL2 and iNOS transcripts. However, concentration of IL-4/IL-10 for delivery, length of IL-4/IL-10 infusion and time points for end point analysis need further optimization for future studies.

Overall Significance: Macrophage activation and modulation is a new area and extensive exploration is necessary, both *in vitro* and *in vivo* on a case-by-case basis to fully elucidate the macrophage activation dynamics. Especially, there is a lack of *in vitro* to *in vivo* translational research in this area. Studies attempting to characterize macrophage phenotypes in response to modulators in vivo in the biomaterials field are not available as of now. Based on *in vitro* data, there are speculations and hypotheses about utilizing macrophage immunomodulation for clinical purposes. To be able to utilize the clinical potential of macrophage plasticity, basic *in vivo* translational studies are imperative. This study is completely novel in attempting localized immunomodulation at the implant site using the microdialysis technique in rats as model organisms.

As mentioned in Chapter 1, the advantage of microdialysis lies in the fact that it allows for the simultaneous localized delivery of a modulator and sampling of target analyte/s. This can provide information about effects or changes brought about by the modulator over time. Cytokines are signaling proteins and govern the progression of FBR. Thus, knowledge of localized changes in the cytokine's profile in response to modulators is of particular significance. Unexpected probe failures and the sampled analytes remaining below detection were major constraints. However, the significance of the work lies in its novelty and attempt to understand *in vitro* to *in vivo* translation of the data. Preliminary gene expression data comparing IL-4 infused tissue and control tissue is promising. As mentioned before, optimizations are required to successfully employ a microdialysis model of delivery for immunomodulation.

Specific Points of Significance

1. Once fully optimized, microdialysis will allow for the direct sampling of cytokines released at the implant site in response to the modulators. This will provide valuable knowledge of localized cytokine profiles that play crucial roles in the progression of FBR.

2. The microdialysis model, together with cytokine sampling and tissue end-point analysis of modulator infused versus control tissue, will provide a means to investigate *in vitro* to *in vivo* translation of macrophage activation data.

References

126. Keeler, G. D., Durdik, J. M., Stenken, J. A. (2014) Comparison of microdialysis sampling perfusion fluid components on the foreign body reaction in rat subcutaneous tissue. *Eur J of Pharm Sci* 57, 60-67.

Chapter 5: Directing Macrophage Activation with Polyvinyl alcohol (PVA) Sponge Implantation Model

5.1 Introduction

The use of the PVA-sponge as a model for immunomodulation of macrophages was undertaken to have a rapid turnaround of the information about modulators with respect to FBR. As mentioned in Chapter 1, the use of sponges allows for the extraction of wound fluid from an explanted sponge at a chosen time point which can provide cytokine information present in the local milieu. Wound cells of interest can be harvested from the sponges at a chosen time point and analyzed for phenotypes using gene expression assays or flow cytometry alone or in combination (depending on the cell yield). This provides a rapid screening method for the macrophage modulator of interest in the wound healing/FBR model.

The aim of this chapter was to assess the effects of IL-4 and IL-10 on the cytokines IL-1β, CCL2 and IL6, obtained from sponged wound fluid at day 3 and day 7. A secondary goal was to analyze the phenotypic profile of macrophages extracted from the sponges in response to IL-4 and IL-10 as compared to the control sponges.

5.2 Materials and Methods

5.2.1 Animals

Male Sprague-Dawley rats (Harlan Laboratories Inc.) weighing between 275 to 350 grams were used in all experiments. All animals were housed in an environmentally-controlled facility with a 12-hour on/off light cycle and had *ad libitum* access to food and water. Surgical procedures followed approved protocols by the University of Arkansas Institutional Animal Care and Use Committee in compliance with National Institutes of Health guidelines for the care and treatment of animals.

5.2.2 Preparation of PVA Sponges

PVA sponge disks were sourced from PVA Unlimited (Warsaw, IN, USA) measuring 12 mm × 3 mm in size. Sponges were soaked in 0.9% saline overnight and then sterilized by autoclaving at 121ºC for 30 minutes. Afterwards the remaining preparatory procedures were performed in a sterile culture hood. Sponges were taken out in a sterile tissue culture plate and excess saline was allowed to be drained, and sucked out with the help of sterile pipettes and sterile forceps. To load with the modulator of interest (IL-4, IL-10 in this case), sponges were then soaked in either IL-4 or IL-10 (200 ng/mL) solution in PBS in sterile Lobind Eppendorf™ vials and kept on ice. IL-4 and IL-10 come as sterile tissue culture tested lyophilized powder. IL-4 and IL-10 powders were reconstituted with sterile PBS in their original vials at 50 µg/mL concentration, according to the manufacturer's instructions (R&D systems). Aliquots were made in sterile Eppendorf LoBind™ and stored at -80º C. All the steps were performed under the tissue culture hood.

5.2.3 Subcutaneous Implantation of the Sponges

Animals were maintained under isoflurane anesthesia as described in chapter 4. The ventral side was shaved and sterilized with the help of iodine solution and further cleaned with the alcohol swab. Incisions were made and subcutaneous pockets were created with the help of sterile scissors and forceps. Sponges were implanted in the subcutaneous pockets. Incisions were then sealed with the help of Vetbond surgical glue. Animals were then returned to housing. Animals were euthanized either at day 3 post implantation or day 7 post implantation with day 0 being the day of surgical implantation. In experimental set ups where sponge incubation times were 7 days, a booster of dose of either IL-4 or IL-10 (200 ng/mL, a total of 150µL) was given on day 3 by direct injection into the treatment sponge. A vehicle (sterile PBS) was injected into the control sponges.

5.2.4 Harvest of Wound Fluid and Cells from Sponges

The PVA-sponge-implanted rats were euthanized at specified (day 3 or 7) time points by CO_2 asphyxiation. Sponges were explanted with the help of sterile scissors, scalpels and forceps. Sponges were squeezed into sterile Eppendorf tubes with the help of forceps to extract the accumulated wound fluid. Sponges were stored in 10% neutral buffered formalin for fixing and were later sectioned and processed for histological studies. Extracted wound fluid was stored at -80ºC until analyzed.

For the extraction of cells, sponges were squeezed and fluid was centrifuged at 1500 rpm for 5 minutes to pellet the cells in the fluid. Cell-free wound fluid was stored at -80ºC for ELISA

analysis (no more than 3 days). Sponges were minced into small sections in sterile petri dishes with sterile PBS. Minced sections were pushed through 10 mL syringes (no needle) to push cells out embedded in sponge sections by the help of compression. Cells from the minced sponge and fluid were then pooled (of same sponge sample) and treated with ACK lysis solution to lyse the red blood cells for 10 min on ice. The pellet was washed with PBS and finally resuspended in 1 mL of PBS. A cell count was then performed at this stage by trypan blue dye exclusion method using an automated cell counter, Countess™ (Life technologies, Grand Island, NY, USA). Cells were then resuspended in Ham's F12k media (supplemented with 10% FBS and 1% antibiotic/antimycotic solution). These cells were allowed to adhere for hours and adherent cells were selected for subsequent gene expression assays.

5.2.5 RNA Extraction and qRT-PCR Assays

Sponge-derived macrophages were lysed by Trizol™ reagent and RNA was separated by chloroform-based phase separation. The RNA was cleaned up using RNeasy column kit. RNA concentration was assessed by measuring the absorbance at 260 nm using a Nanodrop spectrophotometer (Thermo scientific). The RNA quality and integrity check was performed by measuring the 260 nm/280 nm ratio and by agarose gel electrophoresis (Sigma, 1.2% gel). RNA was converted to cDNA using the High Capacity RNA to cDNA kit (Applied Biosystems). A Techne TC-3000 thermocycler was used to perform the reverse transcriptase reaction for 60 min at 37ºC, followed by 5 min at 95ºC. Quantitative real time PCR was performed in duplicates. Each reaction was performed in a total volume of 50 µL using TaqMan® Gene Expression Master Mix and pre-developed TaqMan® probe/primer assay reagents (Life Technologies) using the ABI

prism 7500 sequence detection platform (PE Applied Biosystems). Relative expression was normalized to the reference condition (cells extracted from control sponges) and to the levels of TAF9B. The following TaqMan® probe/primer assay reagents were used

1) Arg2: Rn00567522_m1
2) CD163: Rn01492519_m1
3) CD206: Rn01487342_m1
4) IL-10: Rn01483987_m1
5) IL-12a: Rn00584538_m1
6) NOS2: Rn00561646_m1
7) TGF-β: Rn00572010_m1
8) TNF-α : Rn01525859_g1

5.2.6 ELISA

IL-6 and CCL2 OptEia ELISA kits were sourced from BD Biosciences (San Jose, CA, USA) and IL1-β was sourced from Rand D systems (Minneapolis, MN, USA). Assays were according to the manufacturer's protocol. Typical sample volume obtained from the pooling of two sponges yielded approximately 100 to 125 µL volume. ELISA measurements were done in duplicates per sample. Total protein content was also measured using Nanodrop (Thermo Scientific) by A280 measurement using 2µL of the sample volume. Quantified cytokine levels were normalized to the total protein levels in the wound fluid.

5.3 Results and Discussion

5.3.1 Preliminary Data with PVA sponges

In these preliminary experiments sterile PVA sponges were implanted for two different time points: that is, at 65 hours and day 7. The 65 hour time point is not indicated as day 3 as explants were made 8 hours early. Only 3 rats were used for the preliminary experiment. Two sponges per rat were implanted. At the 65 hour time point, only one rat was used and for day 7 two rats were used. Both the sponges were pooled in each rat to have enough wound fluid for further analysis. Multiplex cytokine assays and histological analysis of sponge sections were performed. Table 6 shows the concentration of cytokines obtained from sponges in each rat. The N value is 1 here with measurement performed in duplicates. From the cytokine profile, it appears that IL-10 is present (105 pg/mL) in collected wound fluid at 65 hours but was below detection on day 7. VEGF is present at a higher concentration on day 7 but is also present at the 65 hour time point. This is expected, as published literature suggests expression of VEGF at later stages of wound healing. Concentration of IL-6 at 90 pg/mL is present at 65 hours but is not detectable in both the rats at day 7.

Table 6. Cytokines levels in wound fluid extracted from sponges

	IL-10 (pg/mL)	VEGF (pg/mL)	IL-1β (pg/mL)	IL-6 (pg/mL)	CCL2 (ng/mL)
Rat 1 (65 hours)	105 (±20)	1440 (±200)	2385 (±440)	90 (±10)	800 (±1)
Rat 2 (Day 7)	Not Detected	1070 (±100)	880 (±210)	Not Detected	460 (±10)
Rat 3 (Day 7)	Not Detected	1050 (±40)	770 (±52)	Not Detected	530 (±30)

The N value is 1. Measurements have been made in duplicates for each sample (represented by ±SD)

The concentration of IL-1β appears to be lower on day 7 in both the rats than at 65 hours. Concentration of CCL2 appears to decrease at day 7, as opposed to the 65 hour time point.

Figure 29 shows the Masson's Trichrome staining of sponge sections. At time point 65 hours, cellular infiltration seems to be sparse as compared to the day 7 time point. At day 7, cellular encapsulation in and around the sponge section can be clearly seen (indicated by the black arrow on the Figure). This is expected and is in line with previously published studies as discussed in Chapter 1.

Preliminary data with treated PVA sponges

In this experiment one rat was used. Two sponges treated with IL-10 (200 ng/mL) were implanted in the dorsal and ventral subcutaneous pockets. One sponge treated with IL-4 (200 ng/mL), one sponge with LPS (200 ng/mL) and control sponge with just PBS alone were also implanted in the ventral subcutaneous pocket of the rat. On day 2, a booster dose of all the analytes at same 200 ng/mL concentration was given. Sponges were explanted on day 8 post implantation, wound fluid was extracted and sponge sections were prepared for histological analysis. Figure 30 shows the cytokine profile of wound fluid extracted from differently treated sponges.

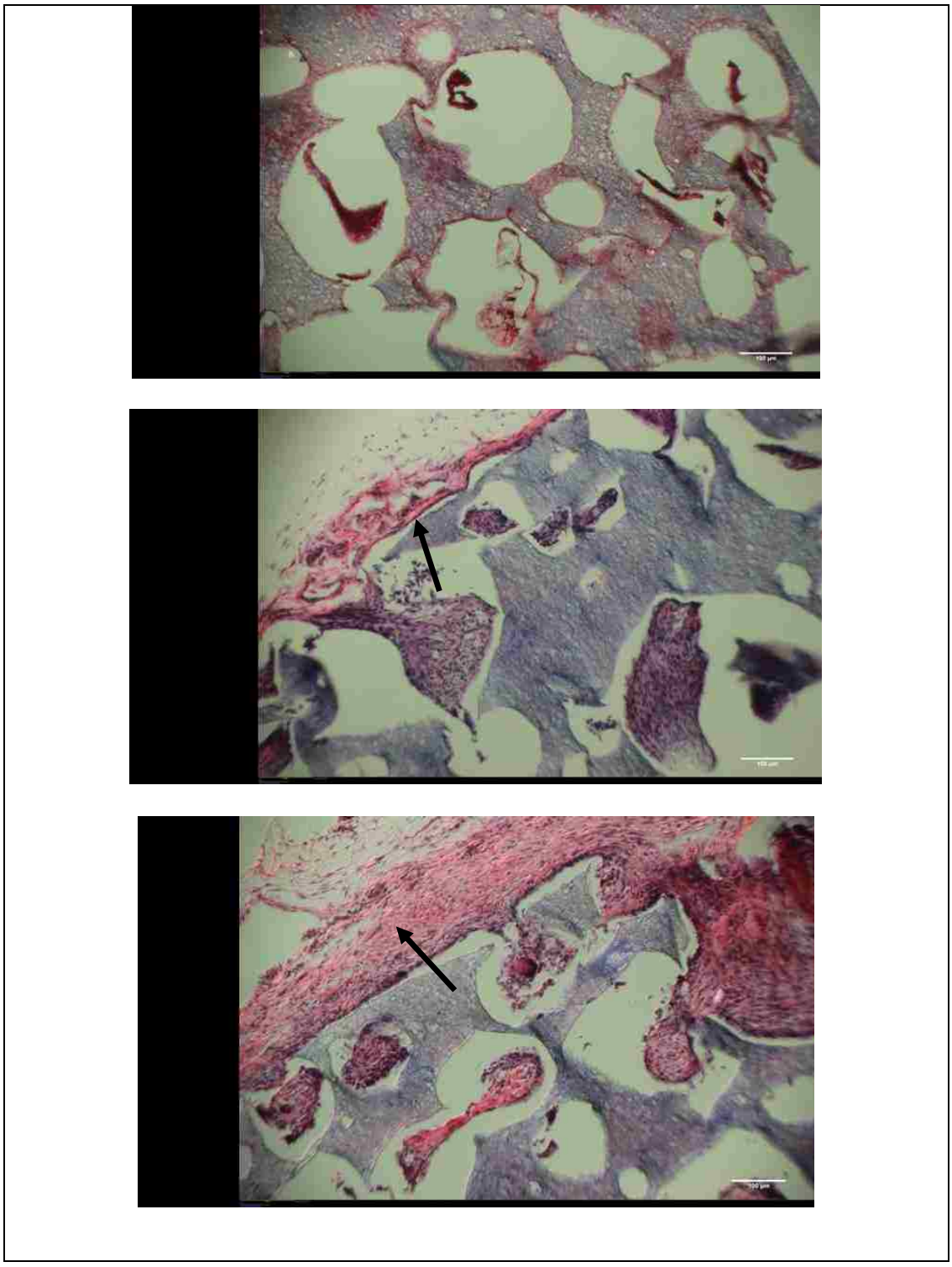

Figure 29. Masson's Trichrome staining of sponge sections harvested at different time points.

Sponges were harvested at the 65 hour or day 7 time points. The black arrow indicates the dense cellular infiltration at day 7 time point.

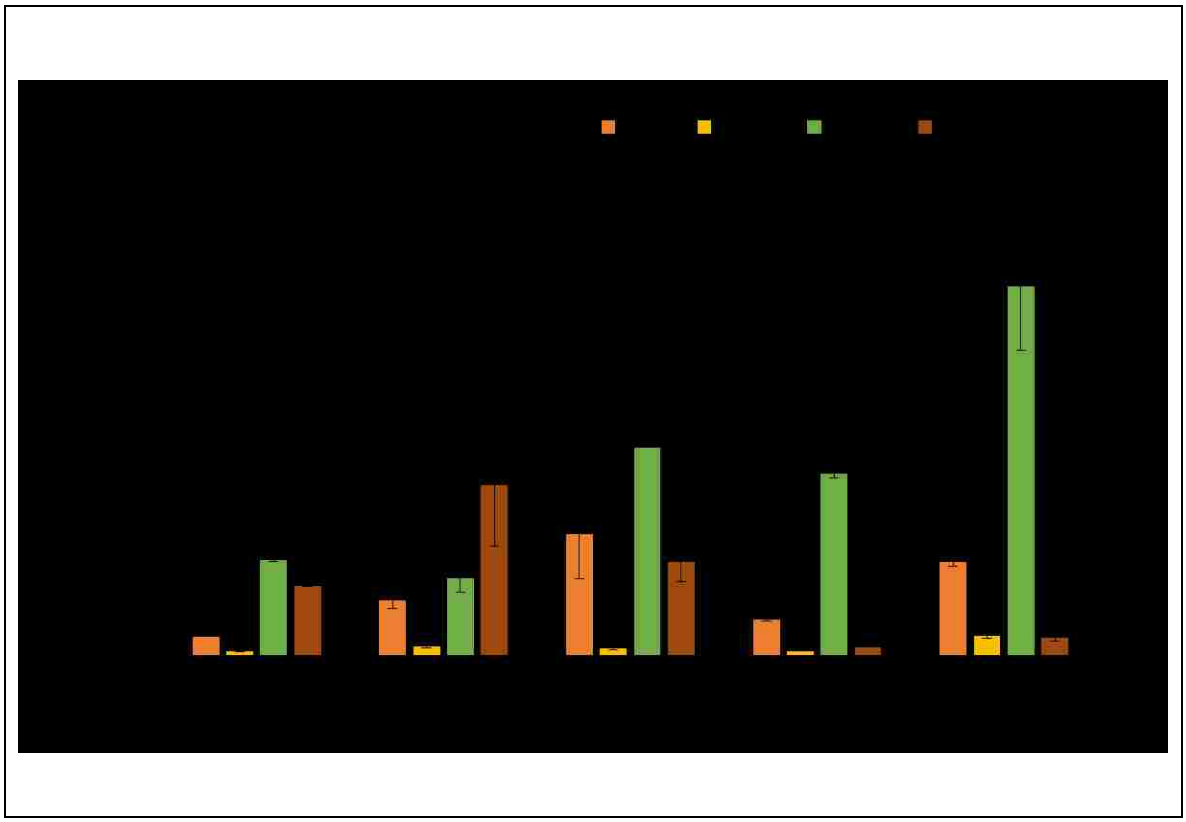

Figure 30. Cytokine profile of wound fluid extracted from treated sponges.

The graph shows the concentration of IL-1β, VEGF, IL-6 and IL-10 in wound fluid extracted from the LPS, IL-4 and IL-10 treated sponges (200 ng/mL) at day 8. Control sponge had PBS alone. N value is 1 (One sponge for each treatment in one rat). Error bars represent the ±SD of duplicate measurements of each sample.

The concentration of inflammatory cytokine IL-1β appears to be highest in the LPS treated sponge sample (2000 pg/mg of total protein) compared to all other sponge samples, which would be expected as LPS is an inflammatory mediator. The IL-4 treated sponge sample has less concentration of IL-1β around 990 pg/mg of total protein, when compared to the LPS treated or control sponges (1130 pg/mg of total protein). IL-1β concentration is the lowest in IL-10 treated sponges (520 and 420 pg/mg of total protein), which would be expected, as IL-10 is a potent anti-inflammatory cytokine. Concentration of IL-6 is highest in the control sponge (660 pg/mg of total protein) and the LPS treated sponge (510 pg/mg of total protein). Concentration of VEGF seems to be highest in IL-10 treated sponges at around 920 pg/mg of total protein.

Figure 31 shows the Masson's Trichrome staining of sponge sections from different treatments. The LPS and control sponge sections appear inflamed with dense cellular infiltration (shown by the black arrow). The IL-4 treated sponge section appears less dense in terms of cellular infiltration and has collagen deposition developing. Cellular infiltration appears to be sparse in the IL-10 treated sponge when compared to the LPS, control and IL-4 treated sponge sections. The preliminary histology data combined with cytokine profile of wound fluid collected from treated sponges provided encouraging data indicating modulation of the microenvironment in response to treatments occurred.

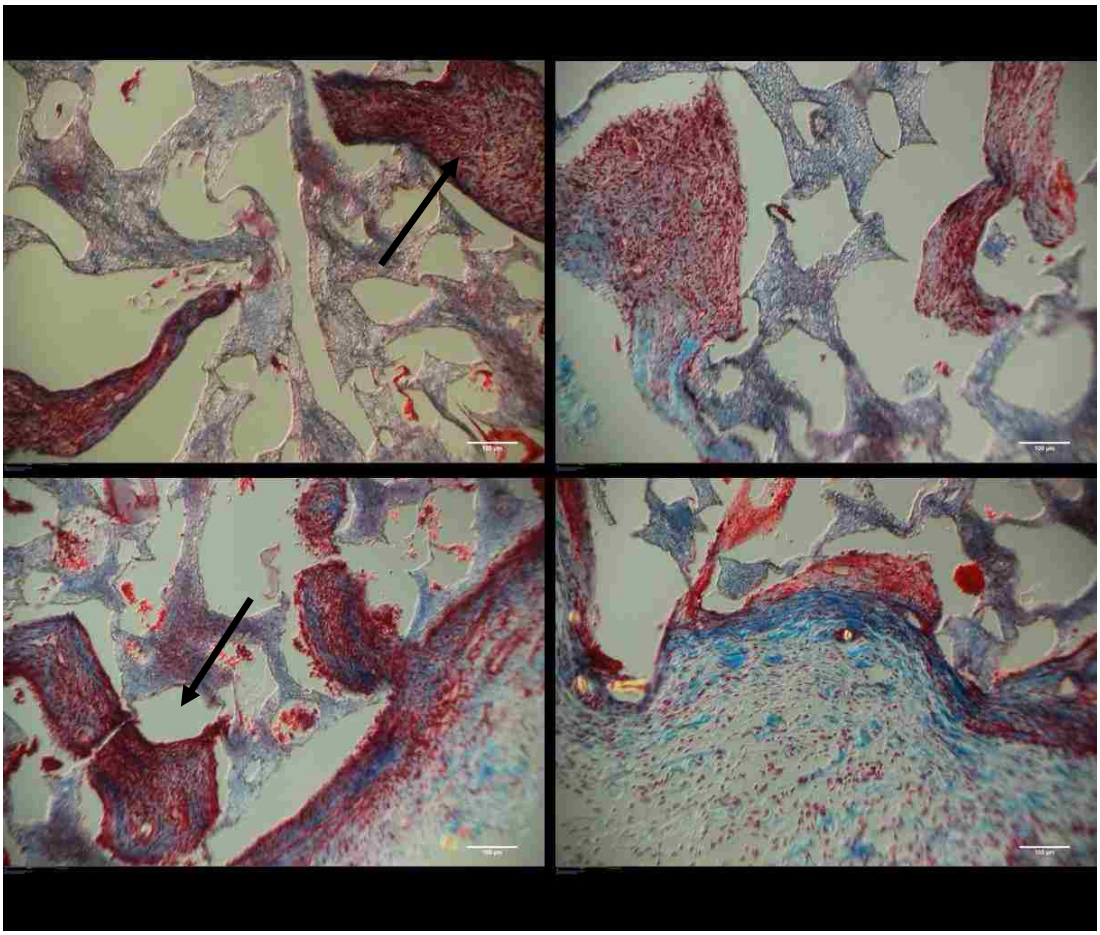

Figure 31. Masson's Trichrome staining of treated sponge sections

The Figure shows the histological sections of sponges implanted in one rat. Sponges were treated with LPS, IL-4 and IL-10 at 200 ng/mL. Control sponge had PBS alone. Sponges were harvested at day 8. The black arrows indicate the area of dense cellular infiltration in LPS and control sponges.

Next steps were to repeat the experiments with IL-4 and IL-10 treatment, that involved wound fluid analysis as well as gene expression analysis of macrophages extracted from the sponge at day 7 time point and day 3 time point.

5.3.2 Effects of IL-4 on Wound Microenvironment at Day 7

In this set of experiments a total of 6 rats were used. IL-4 loaded (200 ng/mL) sterile PVA-sponges were implanted in the ventral subcutaneous pockets (2 per rat). Control sponges were soaked in PBS alone (2 per rat). On day 3, a booster dose of IL-4 (150 µL of 200 ng/mL) was injected directly into the sponges. PBS (150 µL) was injected into the control sponges. On day 7, sponges were explanted and processed as described in methods section. Wound fluid and cells from both the IL-4 sponges were pooled in each rat. Similarly, wound fluid and cells from both the control sponges were pooled in each rat. Thus, providing one treatment and one control sample each rat.

Table 7 shows the count of cells extracted from the control and IL-4 sponges. Figures 32, 33 and 34 show the CCL2, IL-1β and IL-6 levels in the wound fluid, respectively. CCL2 levels in control samples were found to be 10 (±3, N=6) pg/µg of total protein. In the IL-4 treated sample, CCL2 levels were 9 (±2, N=6) pg/µg of total protein. Only CCL2 levels have been expressed as pg/µg due to high concentrations obtained from wound fluid. The control sample IL-6 levels were 13 (±3, N=3) pg/mg of total protein and the IL-4 treated sample IL-6 levels were 17 (±4, N=3) pg/mg of total protein. Difference in the concentration of CCL2 and IL-6 levels between the control and IL-4 treated sponges did not reach any statistical significance. IL-6 levels were lowest and only samples from 3 rats gave detectable concentration during ELISA. Levels of IL-1β in the

wound fluid extracted from IL-4 treated sponges (112 ±30 pg/mg total protein, N=5) are significantly lower at $p<0.05$ when compared to the levels in the control sponges (160 ±40 pg/mg of total protein, N=5).

Figure 35 shows the gene expression profile of macrophages extracted from control and IL-4 treated sponges. Any statistically significant differences between the control and the IL-4 treatment were not found. Although IL-1β protein levels are significantly lower in IL-4 treated sponges, the gene expression data for IL-1β did not reach statistical significance value. Correlation between gene expression and protein expression may not occur due to differences in regulatory mechanisms of genes and proteins. This has to be kept under consideration. Lower concentrations of IL-1β in IL-4 treated sponges when compared to control sponges are consistent with the preliminary experiment detailed in the previous section.

Table 7. Total number of cells extracted from sponges

	Control	**IL-4**
Rat 1	Total = 1.4×10^6 Viability = 62 %	Total = 4.7×10^5 Viability = 67 %
Rat 2	Total = 1.4×10^6 Viability = 70 %	Total = 1.2×10^6 Viability = 70 %
Rat 3	Total = 2.3×10^6 Viability = 61 %	Total = 1.2×10^6 Viability = 72 %
Rat 4	Total = 1.9×10^6 Viability = 71 %	Total = 8.5×10^5 Viability = 73 %
Rat 5	Total = 1.9×10^6 Viability = 70 %	Total = 1.1×10^6 Viability = 60 %
Rat 6	Total = 1.6×10^6 Viability = 72 %	Total = 4.4×10^5 Viability =81 %
Average	1.7×10^6 ($\pm3.5\times10^5$)	8.7×10^5 ($\pm3.5\times10^5$)

Each rat was implanted with two control and two treatment sponges. Both the control and treatment sponges were pooled in each rat to have enough cells. Thus, one control and one treatment sample from each rat.

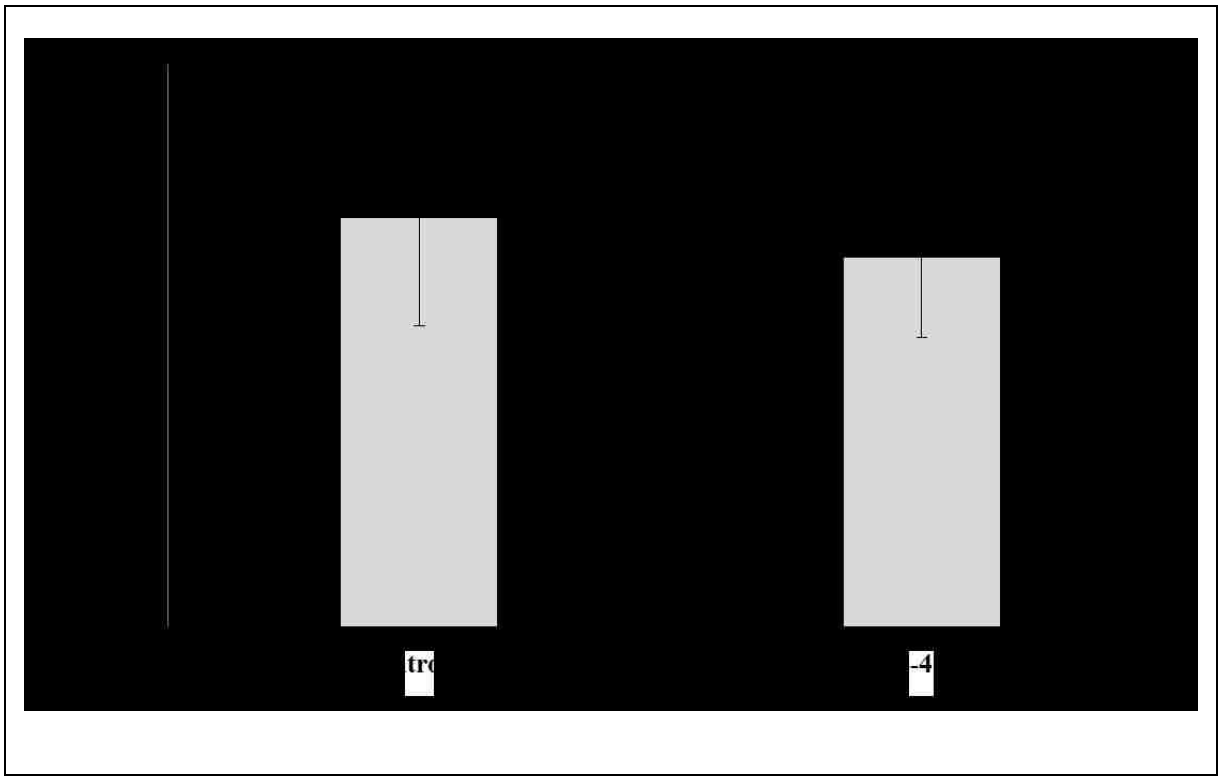

Figure 32. CCL2 levels in wound fluid from control and IL-4 treated sponges

Wound fluid was extracted from the control and IL-4 (200 ng/mL) treated sponges on day 7. CCL2 levels were determined through ELISA and were normalized to total protein concentrations. Data has been plotted at the mean value of samples from 6 rats. Error bars represent the ±SD.

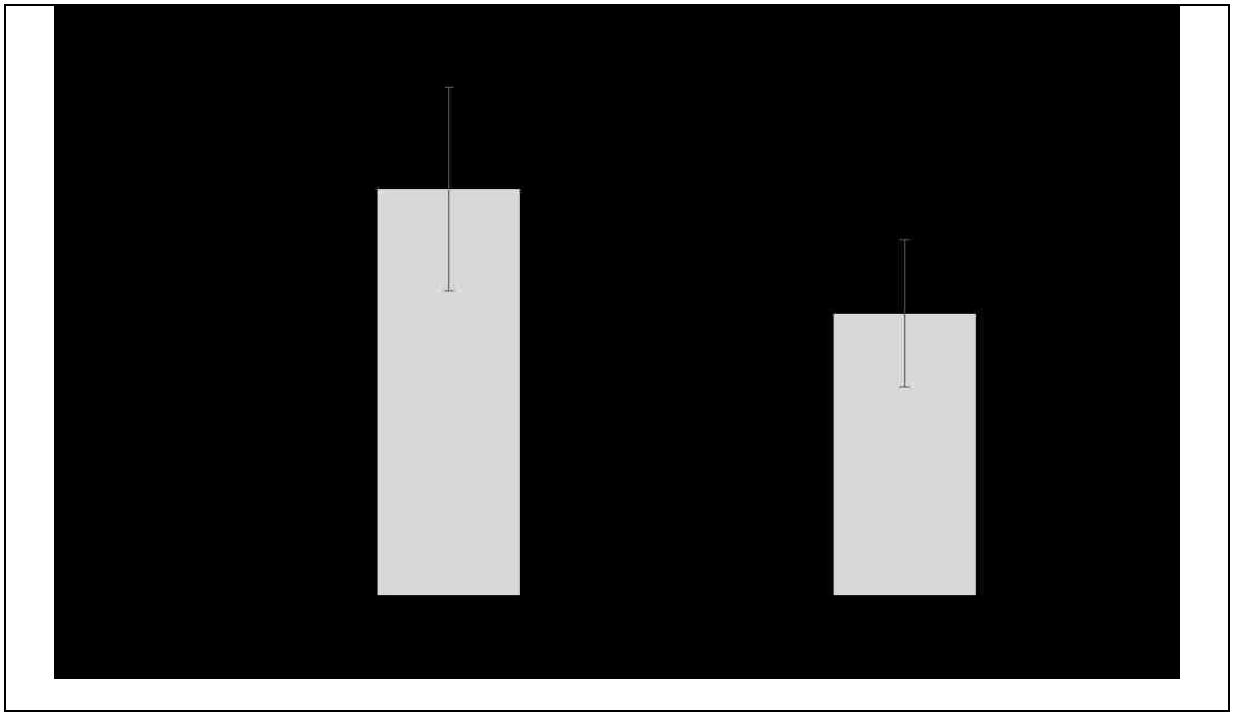

Figure 33. IL-1β levels in wound fluid extracted from control and IL-4 treated sponge

Wound fluid was extracted from the control and IL-4 (200 ng/mL) treated sponges on day 7. IL-1β levels were determined through ELISA and were normalized to total protein concentrations. Data has been plotted at the mean value of samples from 5 rats. Error bars represent the ±SD. Significance is denoted by * $p<0.05$

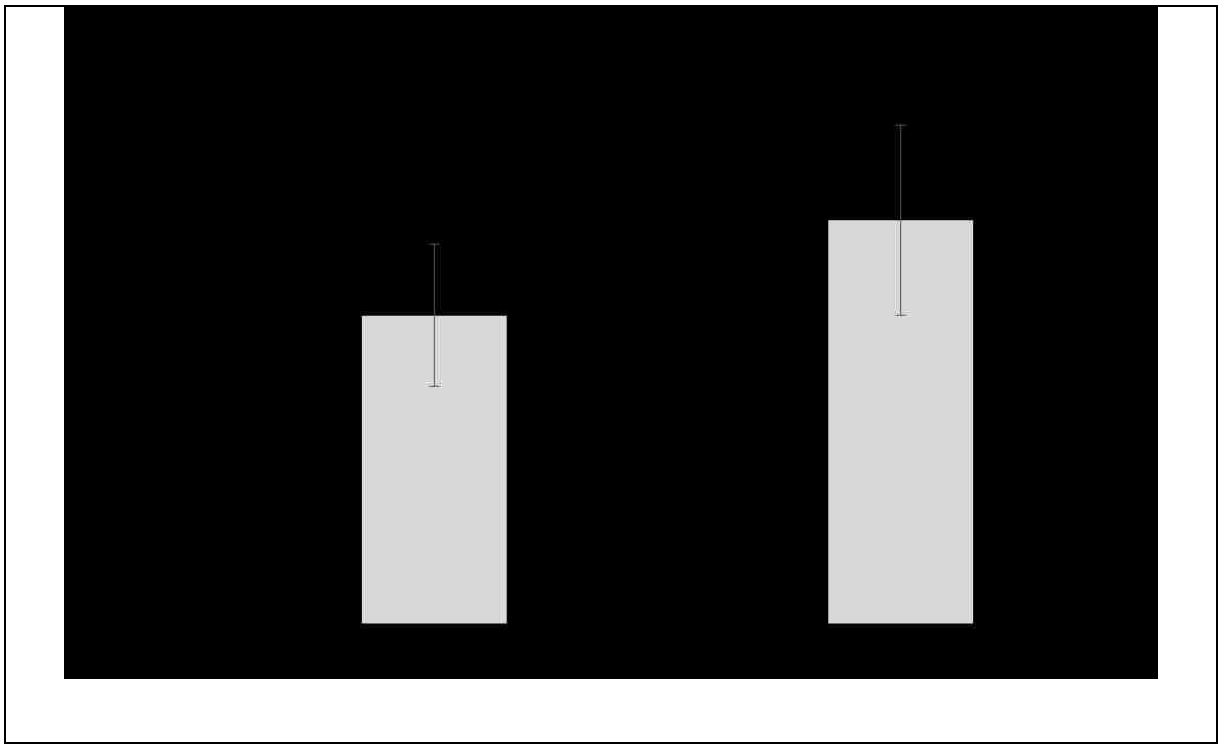

Figure 34. IL-6 levels in wound fluid extracted from control and IL-4 treated sponge

Wound fluid was extracted from the control and IL-4 (200 ng/mL) treated sponges on day 7. IL-6 levels were determined through ELISA and were normalized to total protein concentrations. Data has been plotted at the mean value of samples from 3 rats. Error bars represent the ±SD.

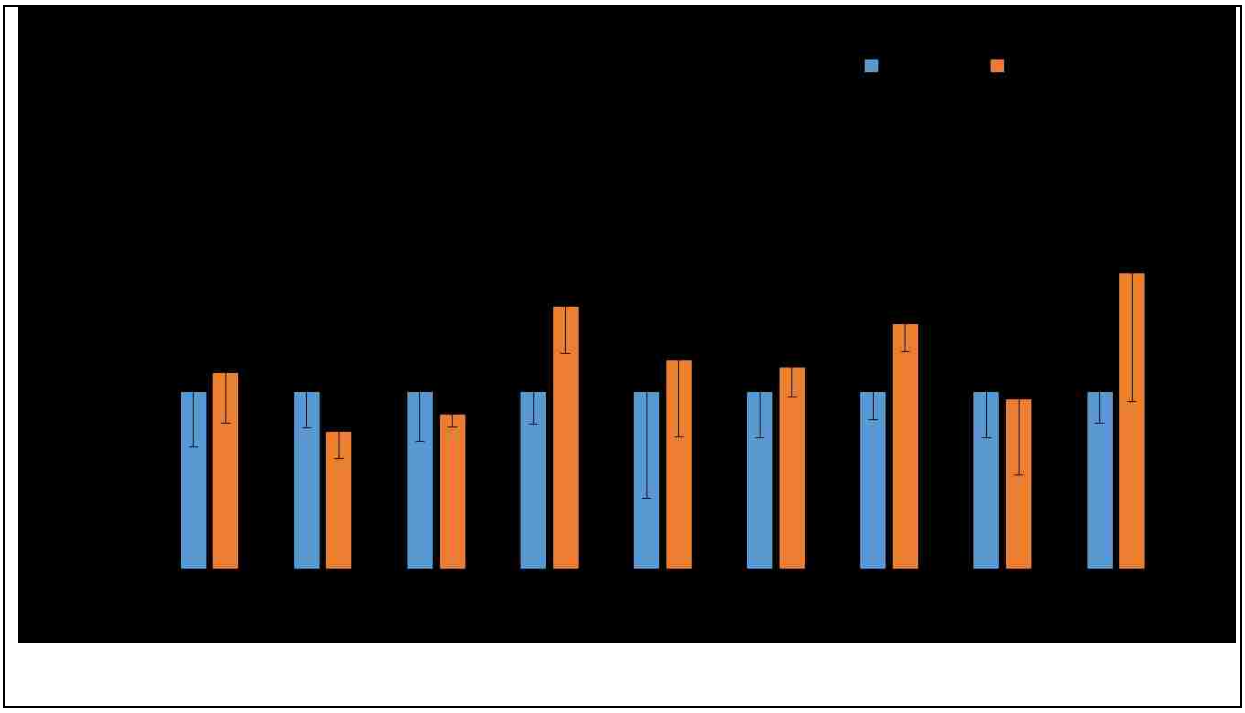

Figure 35. Gene expression profile of macrophages extracted from control and IL-4 treated sponge

Gene expression profile of macrophages extracted from control and IL-4 (200 ng/mL) treated sponges at day 7. The log base 2 transformed expression ratios (fold change) represent the mean values from 4 animals (±SD represented by error bars). TAF9B gene was used as a reference gene.

5.3.3 Effects of IL-10 on Wound Microenvironment at Day 7

Similar experimental set up was used as described in previous section for IL-4 treated sponges. IL-10 (200 ng/mL) loaded sponges (total of 2 per rat) were implanted in a total of six rats. Control sponges had PBS alone (total of 2 per rat). On day 3 a booster dose of IL-10 (150µL at 200 ng/mL) was given and PBS was injected in the control sponges. The Total volume of injection was 150µL in each sponge. Sponges were explanted on day 7. Wound fluid and macrophages were extracted from the sponges for further analysis. Samples were pooled from both the control and the IL-10 treated sponges in each rat. Table 8 shows the number of cells extracted from the sponges. Figure 36 shows the CCL2 and Figure 37 shows the IL-6 profile in the wound fluid.

Table 8. Total number of cells extracted from the sponges

	Control	IL-10
Rat 1	Total = 1.2×10^6 Viability = 76%	Total = 1.2×10^6 Viability = 67 %
Rat 2	Total = 7.8×10^5 Viability = 77 %	Total = 9.6×10^5 Viability = 70 %
Rat 3	Total = 1.3×10^5 Viability = 66 %	Total = 1.6×10^5 Viability = 72 %
Rat 4	Total = 5.5×10^5 Viability = 60 %	Total = 7.5×10^5 Viability = 54 %
Rat 5	Total = 1.2×10^6 Viability = 74 %	Total = 1.4×10^6 Viability = 70 %
Rat 6	Total = 1.2×10^6 Viability = 70 %	Total = 1.4×10^6 Viability = 67 %
Average	8.4×10^5 ($\pm4.4\times10^5$)	9.7×10^5 ($\pm4.7\times10^5$)

Each rat was implanted with two control and two treatment sponges. Both the control and treatment sponges were pooled in each rat to have enough cells. Thus, one control and one treatment sample from each rat.

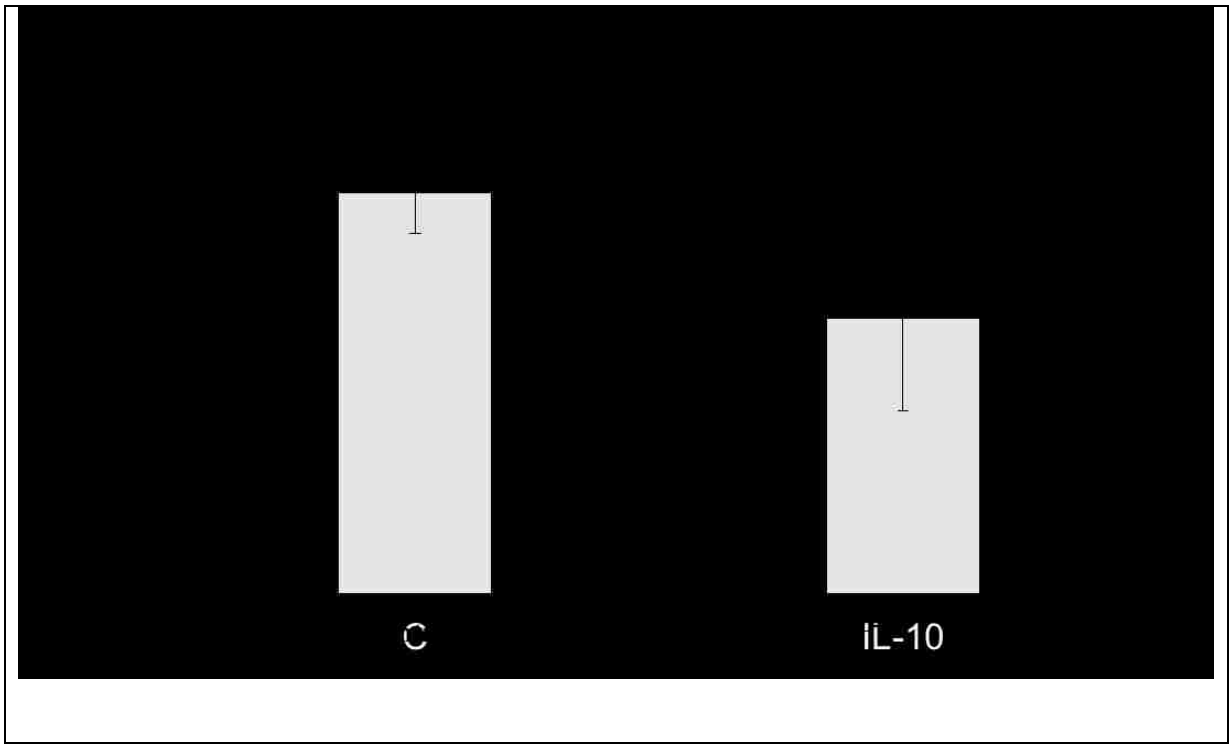

Figure 36. CCL2 levels in wound fluid extracted from control and IL-10 treated sponges

Wound fluid was extracted from the control and IL-10 (200 ng/mL) treated sponges on day 7. CCL2 levels were determined through ELISA and were normalized to total protein concentrations. Data has been plotted at the mean value of samples from 5 rats. Error bars represent the ±SD. Significance is denoted by * $p<0.05$

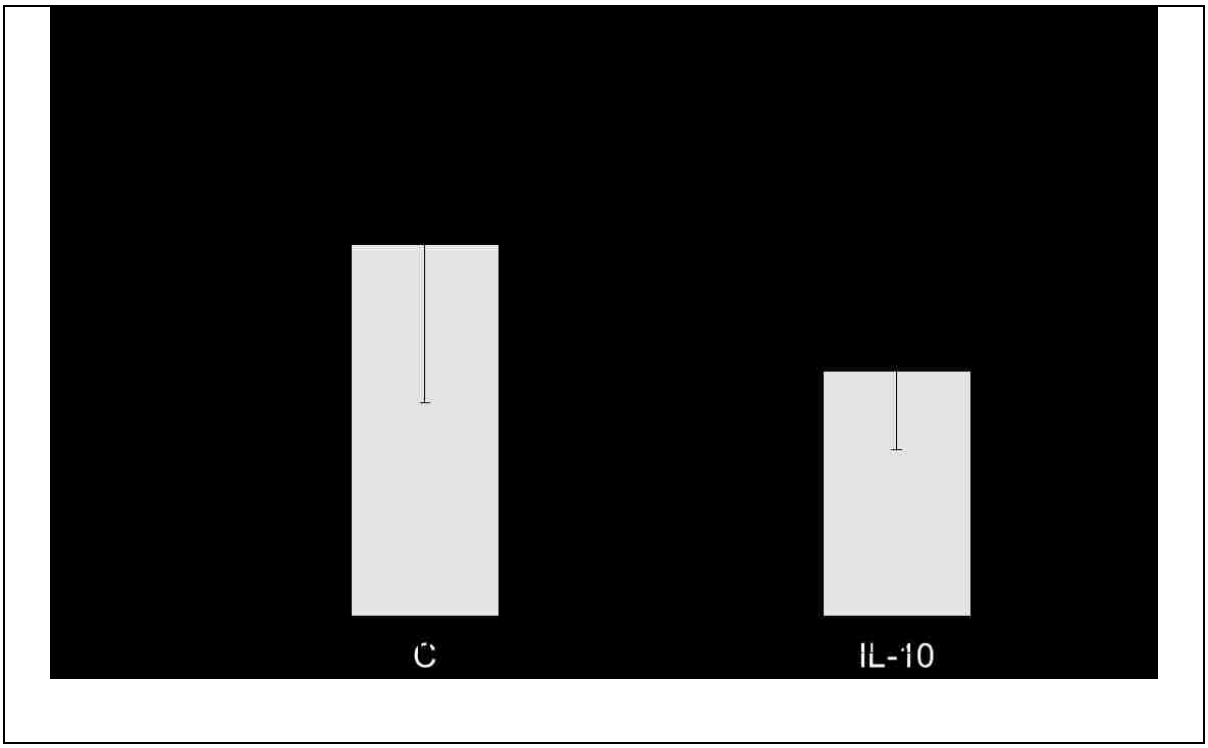

Figure 37. IL-6 levels in wound fluid extracted from control and IL-10 treated sponge

Wound fluid was extracted from the control and IL-10 (200 ng/mL) treated sponges on day 7. IL-6 levels were determined through ELISA and were normalized to total protein concentrations. Data has been plotted at the mean value of samples from 5 rats. Error bars represent the ±SD.

Administration of IL-10 resulted in significantly lower concentrations of CCL2 (13 pg/µg of total protein) in the wound fluid compared to that of the control sponges (18 pg/µg of total protein). From Figure 37, IL-6 levels obtained from IL-10 treated sponges and control sponges were not statistically different. IL-6 levels were lower in all experiments at day 7, and no statistically significant difference between the control sponges and IL-4 or IL-10 treated sponges was found. This suggests that expression of IL-6 protein at this time point might not be influenced by either IL-4 or IL-10. Also, the early appearance of IL-6 during FBR between day 0 to day 3 has been documented [127, 128]. This could also be the reason for lower levels of IL-6 in the wound fluid at this time point which remain unaffected by either IL-4 or IL-10 administration.

Figure 38 shows the gene expression of the profile of macrophages extracted from control and IL-10 treated sponges. IL-10 administration resulted in the significant down-regulating of IL-1β, CCL2 (which correlates with the protein concentration too), IL-12a and NOS2 genes.

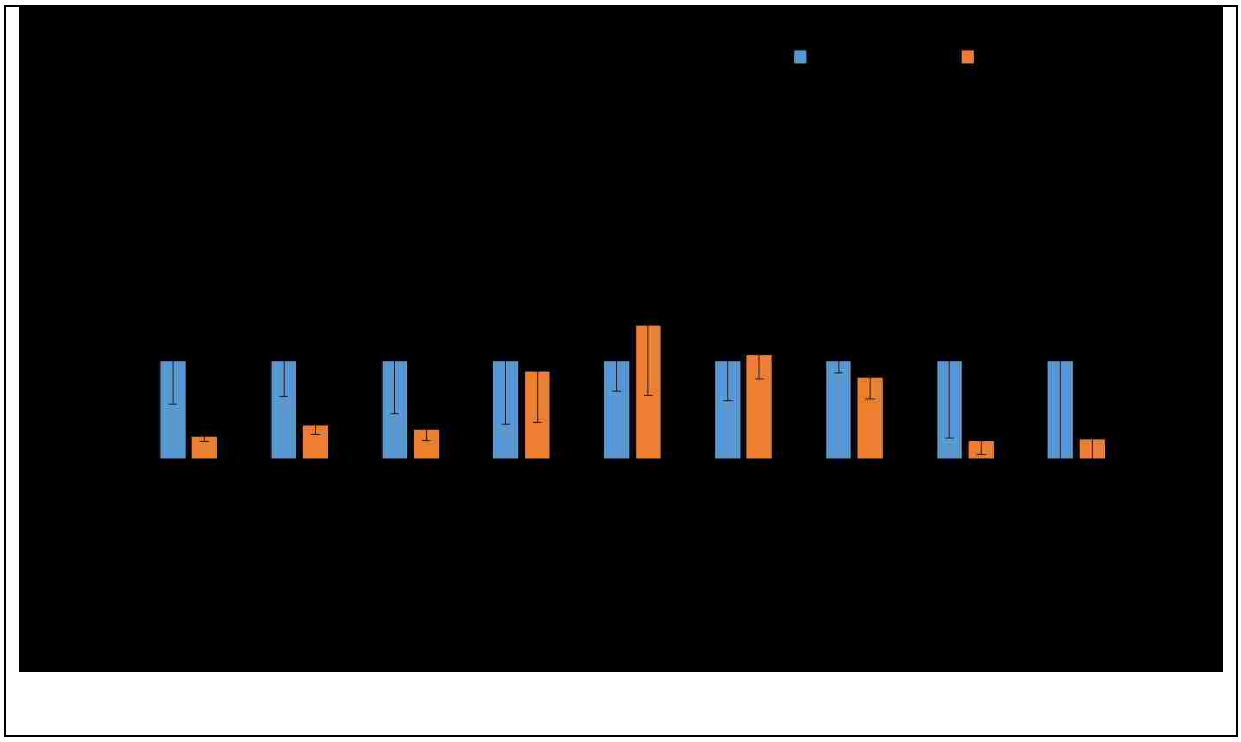

Figure 38. Gene expression profile of macrophages extracted from control and IL-10 treated sponges

Gene expression profile of macrophages extracted from control and IL-10 (200 ng/mL) treated sponges at day 7. The log base 2 transformed expression ratios (fold change) represent the mean values from 4 animals (±SD represented by error bars). TAF9B gene was used as a reference gene. Significance is denoted by * $p<0.05$.

Recalling from Figure 4 (TNF-α dampening in response to IL-4/IL-10) in Chapter 2, it was concluded that at same molar concentrations, IL-10 was more effective in dampening the TNF-α release from the LPS induced macrophages. IL-10 is a known potent anti-inflammatory cytokine; thus, its down-regulating effects on inflammatory markers can be seen from Figure 35. However, the hallmark gene of *in vitro* IL-10 activation, which is CD163, was not found to be significantly upregulated. Similarly, the hallmark genes of *in vitro* IL-4 activation, Arg2 or CD206 were not significantly upregulated i*n vivo*.

There are differences in IL-4 and IL-10 mediated anti-inflammatory effects, as discussed above. It could be the dosage used for IL-10 (200 ng/mL), given at the time of implantation and on day 3 only, did affect the inflammatory markers, but it may not have been optimal to induce a stark shift in the CD163 expression profile. Also, it is important to point out what is known about CD163 expression in response to IL-10 comes from *in vitro* studies. How it correlates to *in vivo* delivery of IL-10 is still not known in the context of FBR. It could also be possible that IL-10 might not affect CD163 expression *in vivo* due to multiple signals present in the microenvironment that also control macrophage phenotypes.

5.3.4 Effects of IL-10 on Wound Microenvironment at Day 3 Time Point

In this set of experiments, control and IL-10 (200 ng/mL) treated sponges were explanted at the day 3 time point. A total of 7 rats were used. Four rats were implanted with a total of four sponges each that were soaked in PBS alone as controls. In the other 3 rats, a total of 4 sponges that were loaded with IL-10 were implanted in each rat as treatment. No booster dose was given during the three day incubation period after implantation. After termination of the animals, sponges

were explanted for the wound fluid and macrophage extraction. Wound fluid and cells from all four sponges in each animal were pooled to be able to have enough sample for later analysis. At the day 3 time point, it was anticipated that enough cellular infiltration would not occur to provide enough number of cells for further analysis.

Table 9 shows the total number of cells extracted from the control and IL-10 treated sponges. It is clear from the table that enough cells could be extracted from the sponges at the day 3 time point by pooling all the four sponges in each rat. As discussed before, according to the literature, migration of macrophages starts from 48 hours to 72 hours and later macrophages dominate the site. The ample number of cells extracted could be representative of this time point when cellular infiltration progresses. Figures 39, 40 and 41 show the levels of IL-1β, CCL2 and IL-6 respectively, in wound fluid extracted from the control and IL-10 treated sponges.

Table 9. Total number of cells extracted from control and IL-10 treated sponges at day 3

	Control	**IL-10**
Rat 1	Total = 5.6×10^6 Viability = 62 %	-
Rat 2	Total = 5.5×10^6 Viability = 67 %	-
Rat 3	Total = 12.4×10^6 Viability = 50 %	-
Rat 4	Total = 9×10^6 Viability = 65 %	-
Rat 5	-	Total = 8×10^6 Viability = 60 %
Rat 6	-	Total = 9×10^6 Viability =67 %
Rat 7	-	Total = 7.5×10^6 Viability =65 %
Average	8.1×10^6 ($\pm3.2\times10^6$)	8.1×10^6 ($\pm7.6\times10^5$)

A total of four sponges either as control or IL-10 treatment were implanted in each rat. All four sponges in each rat were pooled to give either one control sample per rat or one treatment sample per rat.

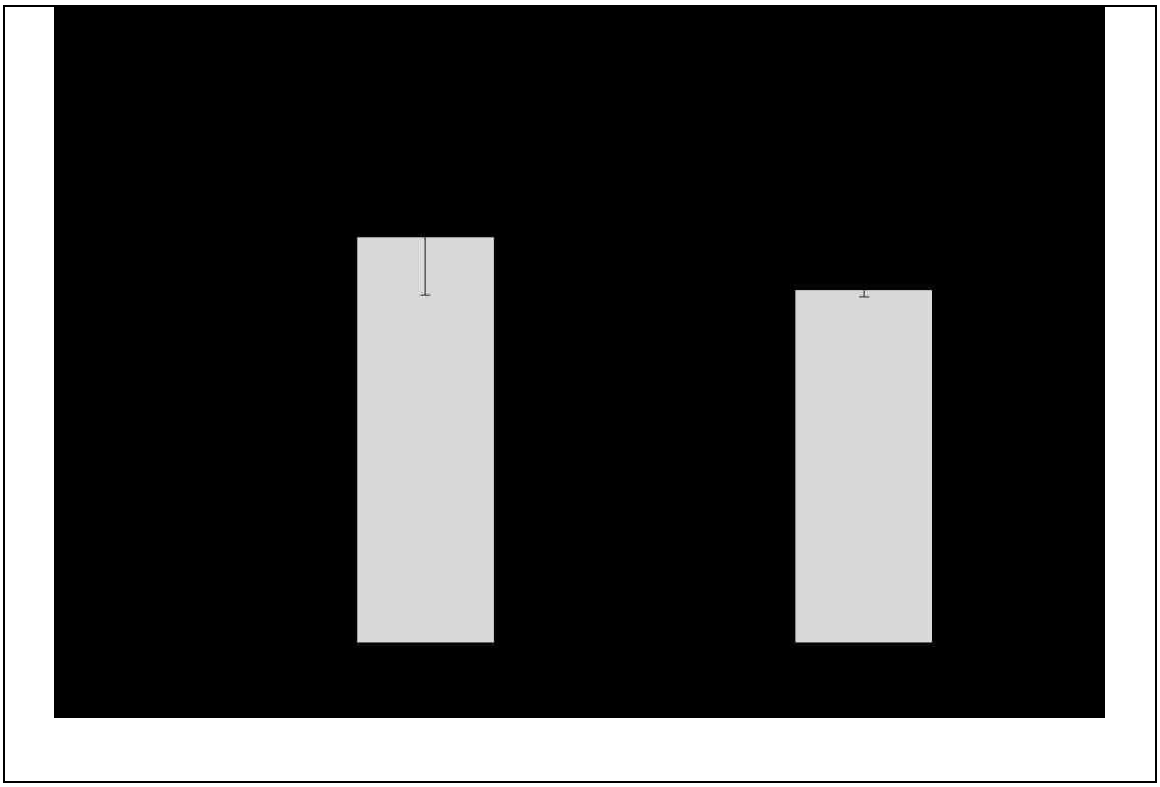

Figure 39. IL-1β levels in wound fluid extracted from control and IL-10 treated sponges at day 3

Wound fluid was extracted from the control and IL-10 (200 ng/mL) treated sponges on day 3. IL-1β levels were determined through ELISA and were normalized to total protein concentrations. Data has been plotted at the mean value of samples from 4 rats. Error bars represent the ±SD.

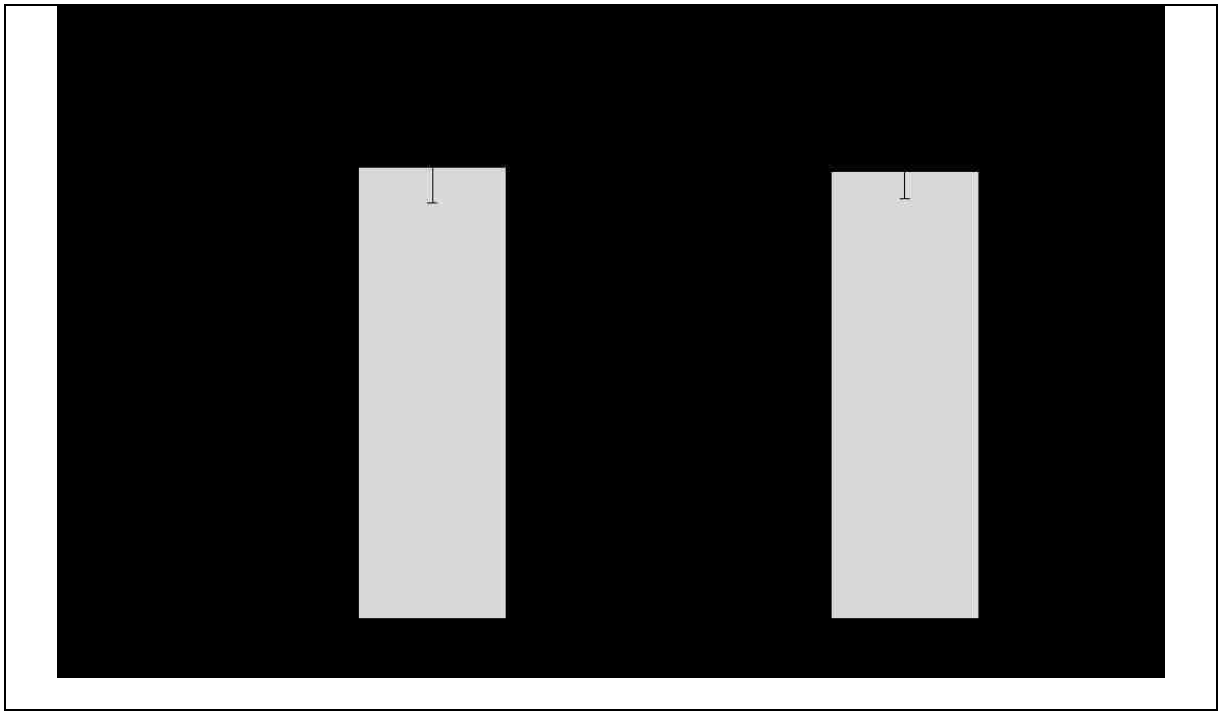

Figure 40. CCL2 levels in wound fluid extracted from control and IL-10 treated sponges at day 3

Wound fluid was extracted from the control and IL-10 (200 ng/mL) treated sponges on day 3. CCL2 levels were determined through ELISA and were normalized to total protein concentrations. Data has been plotted at the mean value of samples from 4 rats. Error bars represent the ±SD.

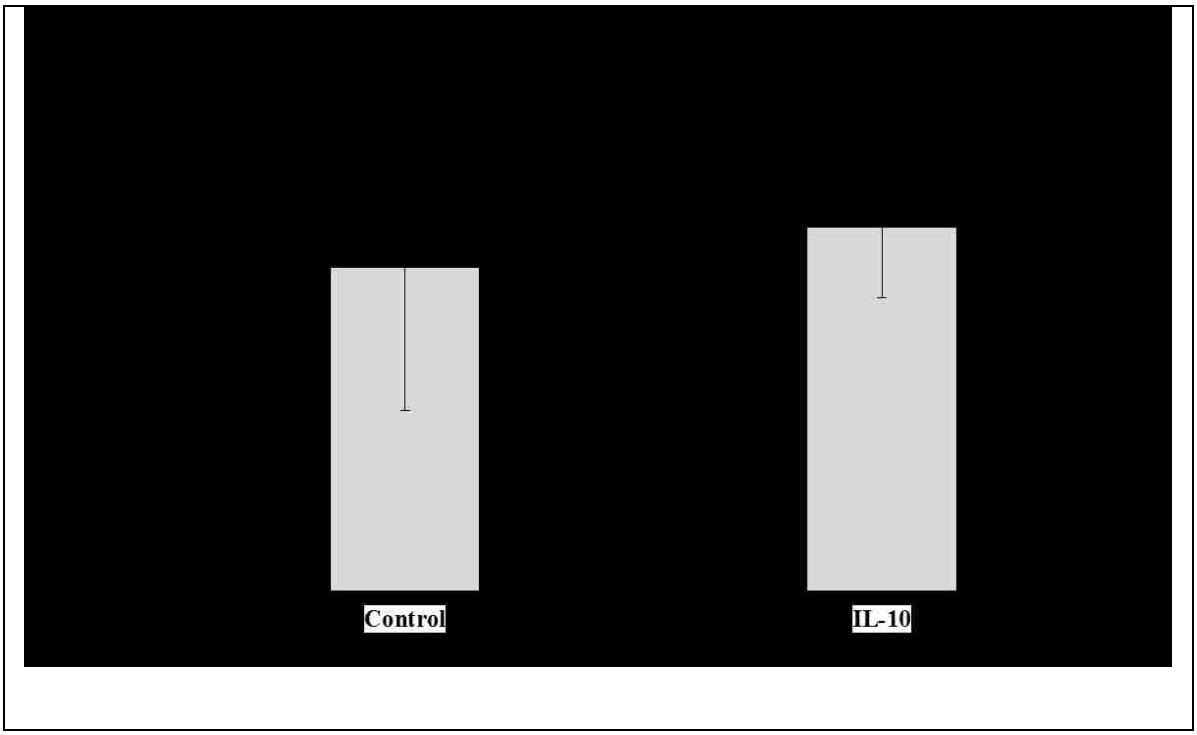

Figure 41. IL-6 levels in wound fluid extracted from control and IL-10 treated sponges at day 3

Wound fluid was extracted from the control and IL-10 (200 ng/mL) treated sponges on day 3. IL-6 levels were determined through ELISA and were normalized to total protein concentrations. Data has been plotted at the mean value of samples from 4 rats. Error bars represent the ±SD.

Levels of IL-1β are higher at day 3 in both control and IL-10 treated sponges when compared to the day 7 time point (Figure 33). Similarly, levels of IL-6 are higher at day 3 when compared to the day 7 time point (Figure 34 and 37). No statistically significant differences between cytokine levels in wound fluid from the control and IL-10 treated sponges were found for CCL2, IL-1β and IL-6 levels. Interestingly, IL-10 administration at the time of implantation without a further booster dose did not affect the levels of inflammatory cytokines in the wound fluid. There are two possible interpretations for this result. Firstly, the administration of IL-10 only at the implantation time could have been degraded by the proteases as the incubation times progressed and was not optimal to sustain the anti-inflammatory effects without the booster dose. Secondly, it could be possible that IL-10 administration might not have any effects due to early administration with the analysis time point as day 3.

Figure 42 shows the gene expression profile of macrophages extracted from the control and IL-10 treated sponges. It is interesting that CCL2 expression is significantly ($p<0.001$) up-regulated in IL-10 treated sponges compared to the control. At day 7, IL-10 significantly down-regulated CCL2 at both the gene and protein levels. However, at day 3 when the dose is given at the time of implantation (day 0, IL-10 loaded sponges), CCL2 levels are upregulated. Also, CCL2 protein levels in wound fluid from control and IL-10 treated sponges are not significantly different. Interestingly, in Figure 28 from chapter 4, the IL-10 treated probe mildly upregulated the expression of CCL2 at 72 hours. This suggests that initial delivery of IL-10 right at the time of implantation may enhance the CCL2 expression.

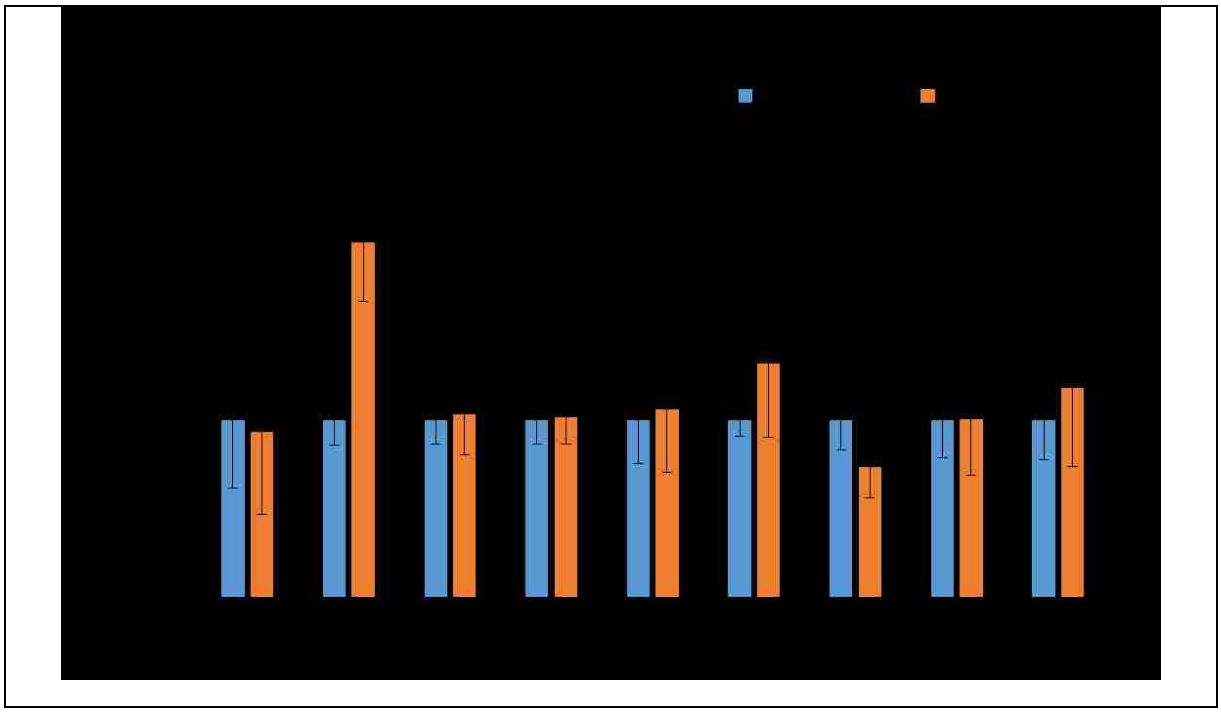

Figure 42. Gene expression profile of cells extracted from control and IL-10 treated sponges at day 3

Gene expression profile of macrophages extracted from control and IL-10 (200 ng/mL) treated sponges at day 3. The log base 2 transformed expression ratios (fold change) represent the mean values from 4 animals (±SD represented by error bars). TAF9B gene was used as a reference gene. Significance is denoted by * $p<0.001$. TAF9b gene was used as reference gene.

When a booster dose of IL-10 was given at day 3, a significant down-regulation of inflammatory mediators was observed. It could be that macrophage infiltration is maximum around 72 hours and a dose given at that time point leads to maximum effects. This suggests the importance of the time point chosen for the delivery of drugs as this leads to differential effects on the targets chosen. This also suggests possibilities of modulating the micro-environment to have different outcomes depending on the time point and concentration of the drug chosen.

Overall in this chapter, the effects of IL-4 and IL-10 at 200 ng/mL dose were studied using the PVA-sponge model. Inflammatory cytokine and gene expression was affected in response to IL-10 at day 7, but at the day 3 time point IL-10 resulted in CCL2 upregulation. IL-4 did significantly affect the IL-1β at protein level but its effects on gene expression profile of other markers were not significant. As mentioned before, in either case IL-4 and IL-10 did not significantly influence CD206 /Arg2 and CD163 which are the hallmark markers of IL-4 and IL-10 activation in macrophages *in vivo*, respectively.

Studying the effects of cytokines *in vivo* is not straightforward and is challenging due to the multitude of factors (cellular, proteins and other mediators) in the microenvironment that govern the progression of a condition. As discussed in chapter 1, alteration and activation of macrophages has emerged as a key area in the fields of biomaterials and regenerative medicine. IL-4 and IL-10 both are anti-inflammatory cytokines and have been implicated in the progression of FBR. The observation that macrophages adapt phenotypically to exogenous stimulants *in vitro* such as IL-4 and IL-10 and the chronic presence of macrophages at the implant site led to the hypothesis of modulating the response to macrophage to induce better out comes in FBR. A majority of studies have been done *in vitro* on macrophage (especially murine macrophages) activation in response to modulators. It is a new area with a lot of unknowns in terms of translation

of these studies *in vivo,* especially in the context of FBR and wound healing. It is important to emphasize that the experiments that were undertaken in chapter 4 and 5 are novel in their approach in trying to address a very challenging biological problem. Due to the novelty of these experiments, it is hard to find published studies to compare and contrast results with. There are multiple issues. First, *in vitro* to *in vivo* translation of data with respect to macrophage phenotypes, and markers needs to be addressed. Secondly, even if *in vitro* to *in vivo* translation is achieved, how it would actually influence the FBR needs to be determined.

The IL-4 is a pleiotropic cytokine affecting various cell types and mediates anti-inflammatory effects. *In vitro* studies showed the formation multinucleated FBGCs in response to IL-4 treatment in vitro in murine macrophages [56, 129, 130]. Helming et al., showed that IL-4 mediated FBGC formation is a multistep process and also depends on the source of macrophages [130, 131]. The presence of FBGC around the implant sites suggests the possible role of IL-4 in fibrosis based on *in vitro* observations. However, there is a scarcity of literature to confirm local administration of IL-4 at the biomaterial implant site will worsen the situation, leading to more FBGC formation, which in turn would have poor fibrotic outcomes.

On the contrary, there are reports that suggest accelerated cutaneous wound healing in response to IL-4 administration. Connie et al., studied the effects of local administration of IL-4 on ligament healing in rats [132]. They found that the early administration of IL-4 (100 ng/mL) up to day 5 favored the wound healing while administration up to day 11 resulted in antagonistic responses. They showed that healing was favored in response to IL-4, but it was time dependent. Veronique et al., showed positive effects of IL-4 administration (250 ng) on rat excisional wounds leading to accelerated healing [42]. They also found that expression of IL-4 was present in wounds as early as day 1, which peaked at day 4 but started to decline after day 5. In an another interesting

study by Mokarram et al., on peripheral never repair in rats showed accelerated healing in response to IL-4 administration [133]. The concentration of IL-4 used was 1 μg/mL. They attributed the accelerated healing to modulation of macrophage phenotypes brought about by IL-4. Interestingly, the ratios of CD206+ to CCR7+ macrophages were higher in the IL-4 treated scaffold.

Contrary to the above discussed beneficial roles, IL-4 helps progression of pulmonary lung fibrosis. An interesting study by Huaux et al., compared the effects of bleomycin induced pulmonary fibrosis in wild type (IL4+/+) mice and IL-4 deficient (IL-4-/-) mice. They found that in earlier stages, IL-4 mediated anti-inflammatory effects but in later stages lead to chromic fibrotic progression in wild type mice, while IL-4 deficient mice developed significantly less pulmonary fibrosis. Other studies have also pointed out the critical role of IL-4 in pulmonary fibrosis [44, 134].

A study by Daley et al., studied the phenotype of murine wound macrophages utilizing the PVA-sponge model [135]. Their results were very interesting. They could not detect IL-4, the cytokine that is considered important for alternative activation of macrophages, in the wound environment, though, they found that wound macrophages on days 1, 3 and 7 expressed markers of alternative activation. Wound macrophages were found to be complex and mice lacking the IL-4 receptor did not affect the phenotype. In experiments presented in this dissertation, the IL-4 transcript could not be detected in macrophages extracted from the sponges. Taken together, the role of IL-4 seems to be complex and its effects vary from situation to situation and are also time dependent. It is very likely that IL-4 administration on day 0 and day 3 in sponge experiments could have only affected the inflammatory cytokine IL-1β that we observed but could not influence other markers due to the timing and dosage used.

As discussed in chapter 1, IL-10 is a potent anti-inflammatory cytokine. It is pleiotropic in its action that affects various cell types. The observation that scar-less healing of fetal wounds was attributed to IL-10 led to it being a potential candidate in regenerative healing. Its role as a therapeutic agent is under investigation for various conditions including, but not limited to, psoriasis, arthritis, Crohn's disease and pulmonary fibrosis [136-139]. Kradin et al., compared the outcomes of bleomycin-induced lung fibrosis in wild type and IL-10 deficient (IL-10-/-) mice. Their finding suggested the protective role of IL-10 against inflammation but did not impart protection against fibrosis [140]. Nakagome et al., delivered the IL-10 gene to mice to alleviate bleomycin induced lung fibrosis[141]. The contrasting results from both the studies suggest that in wild type mice IL-10 did not affect fibrosis, but exogenous gene delivery attempted at over expression of IL-10 did impart protective role against pulmonary fibrosis. The point to conclude is that dosage of IL-10 might play a critical role in alleviating a condition.

In the context of biomaterials, not many published studies are available that focus on its exogenous administration *in vivo* to alleviate FBR and fibrotic encapsulation. In a recent study by Boehler et al., lentiviral mediated gene delivery of IL-10 was proposed at the implant site to sustain an alternative phenotype of macrophages that would mark down the inflammation. The study was performed *in vitro* using murine macrophages. As discussed, various *in vitro* studies have shown IL-10-mediated anti-inflammatory effects of macrophages and generation of CD163+ phenotypes that have been implicated in tissue remodeling. However, *in vivo* studies are scarce that can provide insights about *in vitro* to *in vivo* translation. The data presented here show modulation of inflammatory cytokines by IL-10 at day 7. This indicates that IL-10 at the concentration chosen causes anti-inflammatory effects. However, how it would affect the outcome of FBR with respect to fibrosis needs further evaluation through histological analysis. This would require a separate set

of experiments. It could also be possible that at this concentration (200 ng/mL), it may just cause anti-inflammatory effects and not modulate the fibrosis. No other effects were observed at day 3 except upregulation of CCL2 in response to IL-10. From recent studies, IL-10 has been shown to enhance the CCL2 expression [76, 142]. This effect could be time dependent.

In psoriasis and Crohn's disease, concentrations of IL-10 being administered were 8 µg/kg/day and 25 µg/kg/day, respectively [138, 143]. A high dose range might be required to have dramatic shift in the macrophage phenotype or a daily delivery of IL-10 dose may be required to have profound effects on macrophage modulation at day 3 or at day 7. Ultimately, how those dramatic phenotypic shifts will dictate the outcome of FBR needs further evaluation. In conclusion, it is evident that IL-4 and IL-10 function in complex ways, exerting contrasting effects in different situations. In the situation presented in this dissertation, some immunomodulation is observed at the 200 ng/mL dose tested on two different time points, but more studies are required to test these and/or other time points at higher dosages, and how it would ultimately influence the FBR and encapsulation needs evaluation.

5.4 Conclusion and Significance

To conclude, effects of IL-4 and IL-10 at a 200 ng/mL dose were studied in this chapter using the PVA-sponge model. Inflammatory cytokine gene expression was affected in response to IL-10 on day 7, but at the day 3 time point, IL-10 resulted in CCL2 upregulation. IL-4 significantly affected IL-1β at the protein level but its effects on the gene expression profile of other markers were not significant. As mentioned before, in either case IL-4 and IL-10 did not significantly affect the expression of CD206 /Arg2 and CD163, which are the hallmark markers of IL-4 and IL-10 activation in macrophages *in vitro*, respectively.

Overall Significance: As mentioned in the Significance section of Chapter 4, *in vivo* translational studies need to be performed to provide in-depth insight into *in vivo* aspects of macrophage plasticity. Without the basic *in vivo* translational studies, the full clinical potential cannot be achieved. The significance of this study lies in its attempt to understand in vivo immunomodulation in rat model organisms.

In Chapter 4, a novel localized IL-4/IL-10 delivery using the microdialysis model was employed for studies directing the *in vivo* macrophage activation. Comparative cytokine analysis could not be performed due to random probe failures. Conclusive inferences could not be drawn from tissue histological analysis. Directing macrophage activation using the microdialysis technique requires further optimization. Thus, in Chapter 5, the same questions sought to be answered utilizing a different approach. The PVA-sponge model has been used extensively in wound healing studies. The target drug/s can be injected directly into the sponge. How injected drug/s affect the wound microenvironment and infiltrating cells can then be studied. The in vivo sponge model allowed for the extraction of wound exudate for cytokine analysis and macrophages phenotype analysis that infiltrated the sponges. Again, these are novel experiments with respect to attempting in vivo IL-4/IL-10 mediated immunomodulation and characterization of macrophage phenotypes. The data obtained adds to the knowledgebase of existing sparse *in vivo* studies, and provides a fundamental framework for future studies.

Specific Points of Significance

1. The sponge infiltrated macrophages were harvested for phenotypic analysis through gene expression assays. The gene expression profile shows a mixed phenotype that expresses IL-1β, IL-10, CCR7, CD163 and CD206 transcripts, suggesting a mixed phenotype in *in*

vivo situations. Data provides assessment of macrophage phenotypic profiles directly harvested from the sponge implants. This is of high significance as knowledge of what phenotypes are actually present *in vivo* in a given condition is crucial.

2. IL-6 levels were higher in day 3 wound exudates than day 7 wound exudates. Both IL-4 and IL-10 treatments did not affect IL-6 levels, which suggests its expression may not be regulated by either of the cytokines *in vivo* in the wound model employed. This data provides new insight on IL-6 immunomodulation in the chosen model system at chosen modulator concentration.

3. The levels of IL-1β were affected by IL-4 treatment at the day 7 time point. No significant differences in other markers were found. Whereas IL-10 treatment down-modulated inflammatory markers IL-1β, CCL2, IL12a and iNOS. Data provides insight into differences in responsiveness to IL-4 and IL-10 treatments, and their affected targets.

4. At the day 3 time point, IL-10 enhanced CCL2 expression, whereas at day 7 it down-modulated the CCL2 expression both at transcriptional and translational levels. The study shows how dose timings influence the responses and have to be an important consideration in *in vivo* immunomodulation.

5. Combined together, this new study provides an initial groundwork for future in vivo immunomodulation studies with respect to IL-4/IL-10 dose concentrations, timings and their affected targets.

References

42. Salmon-Ehr, V., Ramont, L., Godeau, G., Birembaut, P., Guenounou, M., Bernard, P., Maquart, F. X. (2000) Implication of interleukin-4 in wound healing. *Lab Invest* 80, 1337-1343.

44. Jakubzick, C., Choi, E. S., Joshi, B. H., Keane, M. P., Kunkel, S. L., Puri, R. K., Hogaboam, C. M. (2003) Therapeutic attenuation of pulmonary fibrosis via targeting of IL-4- and IL-13-responsive cells. *J Immunol* 171, 2684-2693.

56. McNally, A. K. and Anderson, J. M. (1995) Interleukin-4 induces foreign body giant cell from human monocytes macrophages-differential lymphokine regulation of macrophage fusion leads to morphological variants of multinucleated giant cells *Am J Pathol* 147, 1487-1499.

127. Kondo, T. and Ohshima, T. (1996) The dynamics of inflammatory cytokines in the healing process of mouse skin wound: A preliminary study for possible wound age determination. *Int J of Legal Med* 108, 231-236.

128. Werner, S. and Grose, R. (2003) Regulation of wound healing by growth factors and cytokines. *Physiol Rev* 83, 835-70.

129. Jay, S. M., Skokos, E., Laiwalla, F., Krady, M.-M., Kyriakides, T. R. (2007) Foreign body giant cell formation is preceded by lamellipodia formation and can be attenuated by inhibition of Rac1 activation. *Am J Pathol* 171, 632-640.

130. Helming, L. and Gordon, S. (2009) Molecular mediators of macrophage fusion. *Trends Cell Biol* 19, 514-522.

131. Helming, L. and Gordon, S. (2007) Macrophage fusion induced by IL-4 alternative activation is a multistage process involving multiple target molecules. *Eur J Immunol* 37, 33-42.

132. Chamberlain, C. S., Leiferman, E. M., Frisch, K. E., Wang, S., Yang, X., Brickson, S. L., Vanderby, R. (2011) The influence of interleukin-4 on ligament healing. *Wound Repair Regen* 19, 426-435.

133. Mokarram, N., Merchant, A., Mukhatyar, V., Patel, G., Bellamkonda, R. V. (2012) Effect of modulating macrophage phenotype on peripheral nerve repair. *Biomaterials* 33, 8793-8801.

134. Izbicki, G., Or, R., Christensen, T. G., Segel, M. J., Fine, A., Goldstein, R. H., Breuer, R. (2002) Bleomycin-induced lung fibrosis in IL-4-overexpressing and knockout mice. *Am J Physiol Lung Cell Mol Physiol* 283, L1110-L1116.

135. Daley, J. M., Brancato, S. K., Thomay, A. A., Reichner, J. S., Albina, J. E. (2010) The phenotype of murine wound macrophages. *J Leukoc Biol* 87, 59-67.

136. Herfarth, H. and Scholmerich, J. (2002) IL-10 therapy in Crohn's disease: at the crossroads. *Gut* 50, 146-147.

137. Al-Robaee, A. A., Al-Zolibani, A. A., Al-Shobili, H. A., Kazamel, A., Settin, A. (2008) IL-10 implications in psoriasis. *Int J Health sci* 2, 53-8.

138. Asadullah, K., Sterry, W., Stephanek, K., Jasulaitis, D., Leupold, M., Audring, H., Volk, H. D., Docke, W. D. (1998) IL-10 is a key cytokine in psoriasis - Proof of principle by IL-10 therapy: A new therapeutic approach. *J Clin Invest* 101, 783-794.

139. Numerof, R. P. and Asadullah, K. (2006) Cytokine and anti-cytokine therapies for psoriasis and atopic dermatitis. *Biodrugs* 20, 93-103.

140. Kradin, R., Sakamoto, H., Jain, F., Zhao, L., Hymowitz, G., Preffer, F. (2004) IL-10 inhibits inflammation but does not affect fibrosis in the pulmonary response to bleomycin. *Exp Mol Pathol* 76, 205-11.

141. Nakagome, K., Dohi, M., Okunishi, K., Tanaka, R., Miyazaki, J., Yamamoto, K. (2006) In vivo IL-10 gene delivery attenuates bleomycin induced pulmonary fibrosis by inhibiting the production and activation of TGF-beta in the lung. *Thorax* 61, 886-894.

142. Musso, T., Cappello, P., Stornello, S., Ravarino, D., Caorsi, C., Otero, K., Novelli, F., Badolato, R., Giovarelli, M. (2005) Il-10 enhances CCL2 release and chemotaxis induced by CCL16 in human monocytes. *Int J Immunopathol Pharmacol* 18, 339-349.

143. Mocellin, S., Panelli, M. C., Wang, E., Nagorsen, D., Marincola, F. M. (2003) The dual role of IL-10. *Trends Immunol* 24, 36-43.

Chapter 6: *In Vivo* Microdialysis Sampling of Adipokines CCL2, IL-6 and Lepin in the Mammary Fat Pad of Adult Female Rats

Geetika Bajpai, Rosalia C.M. Simmen and Julie A. Stenken

[Bajpai, G., Simmen, R. C., and Stenken, J. A. (2014). In vivo microdialysis sampling of adipokines CCL2, IL-6, and leptin in the mammary fat pad of adult female rats. *Mol BioSyst, 10*(4), 806-812.] - Reproduced by permission of the Royal Society of Chemistry

http://pubs.rsc.org/en/content/articlelanding/2014/mb/c3mb70308h#!divAbstract

6.1 Introduction

Adiposity has been linked with increased breast cancer risk [144]. By volume, breast tissue contains approximately 90% adipocytes that comprise the white adipose tissue and 10% epithelial cells. Adipocytes within the white adipose tissue secrete signaling proteins which are collectively called adipokines [89]. Many different adipokines exist including CCL2, IL-6, IL-8, resistin, TNF-α, and VEGF [145]. Cancer is believed to start from the breast epithelial cells and growth factors and cytokines secreted by adipocytes are suspected to significantly contribute to breast cancer progression [146-148]. CCL2, a 13 kDa monomer that forms a dimer to be biologically active, plays a potent role in macrophage recruitment at the site of injury or infection [149]. IL-6 is a 20.8 kDa pleiotropic cytokine exhibiting both pro- and anti-inflammatory properties, depending on cell context [150]. The primary function of IL-6 is the initiation of acute phase response during inflammation and infection [59, 151]. IL-6 activates multiple signaling pathways to control cellular proliferation and apoptosis. Upregulation of IL-6 and CCL2 in breast cancer promote inflammation which in turn is linked to tumor progression. Leptin is a 16 kDa non-glycosylated protein hormone secreted mainly by adipose tissues in proportion to body mass index and is essential for normal mammary gland development [91]. Leptin expression occurs in normal mammary tissues, in breast cancer cell lines, and in tumors [152].

Microdialysis is a well-established diffusion-based *in vivo* sampling technique that has been used for chemical sampling from extracellular fluid space in the fields of neuroscience, drug metabolism and pharmaceutics [153, 154]. A microdialysis probe is made up of a semipermeable dialysis membrane with a defined molecular weight cut-off (MWCO) and inlet and outlet tubing. A perfusion fluid that matches extracellular fluid in ionic strength and composition is pumped (at flow rates ~ 0.5 µL to 2 µL min^{-1}) through the inlet and dialysate containing the diffusible solutes

is collected from the outlet. Relative Recovery (*RR*) or extraction efficiency (*EE*) can be defined as the ratio, $EE = C_{outlet}/C_{\infty ECF}$ where C_{outlet} is the concentration of the analyte in the outlet and $C_{\infty ECF}$ is the concentration of the analyte in the tissue extracellular fluid at far-field distance from the implanted probe [155]. Since microdialysis sampling is a diffusion-based separation process, the collected solute concentrations from any tissue will be a function of the mass transport properties for the solute through the tissue, dialysis membrane, and the dialysate [156]. Analytes with smaller diffusion coefficients such as the adipokine proteins will generally exhibit *EE* values of roughly 10% or less [154].

Microdialysis sampling has been employed for the sampling of large protein molecules such as cytokines and adipokines [157-163]. The microdialysis sampling technique has several merits, the most important being the ability to provide continuous sampling of the extracellular fluid space within tissues. The microdialysis sampling procedure is considered to be minimally invasive due to small size of the probe (500 μm), thus causing less tissue disruption when implanted. Dialysate samples obtained from the device are analytically clean, requiring no further sample clean up and can be directly subjected to immunoassays or other quantitation methods.

The goal of the present study was to employ microdialysis sampling to collect and quantify adipokines from the mammary fat pad of young adult female rats. Rats are a commonly-used animal model for human breast cancer [164-166]. While Xu *et. al.* employed microdialysis sampling technique to sample osteopontin, clusterin and cystatin-c from mammary tumors in female rats, to our knowledge no reports of microdialysis sampling in normal mammary glands of rodents has been reported [167]. CCL2, IL-6, and leptin were selected for the study as they are important mediators of inflammation underlying mammary tumor development and progression. A critical issue with microdialysis sampling, particularly with larger molecules, is the calibration

of the dialysate concentrations relative to actual tissue concentrations [168]. Dialysate concentrations are representative of a certain percentage of the tissue concentrations. While whole tissue extracts would also represent any cytokines stored in granulocytes, we chose to also compare dialysate protein concentrations with those extracted from whole tissue.

6.2 Materials and Methods

6.2.1 Microdialysis Supplies and Perfusion Fluid

CMA-20 (10 mm (length) x 0.5 mm (outer diameter, o.d.) 100 kDa molecular weight cutoff (MWCO) polyethersulphone (PES) microdialysis probes (CMA Microdialysis, North Chelmsford, MA) were used for all experiments. The Baby Bee single channel (BASi, W. Lafayette, IN) syringe pump was used with a 1000 µL BAS glass syringe (BASi, W. Lafayette, IN) to deliver the perfusion fluid through microdialysis probe. Perfusion fluids contained phosphate-buffered saline (PBS), containing 0.137 M NaCl, 2.7 mM KCl, 4.3 mM Na_2HPO_4 and 1.4 mM KH_2PO_4 with 6% (w/v) Dextran 70 (Sigma-Aldrich, St. Louis, MO) and 0.1% (w/v) bovine serum albumin, BSA, (Sigma-Aldrich, St. Louis, MO). Dextran was added to prevent fluid loss across the high MWCO membranes during sampling and BSA was used to reduce non-specific adsorption of adipokines to membrane materials. Perfusion fluids were prepared as needed and filter sterilized with a 0.2 µm PES membrane filter (Whatman, Florham Park, NJ).

6.2.2 *In vitro* Microdialysis Recovery Experiment

The calibration of the probe to determine the relative recovery of CCL2, IL-6 and leptin was conducted *in vitro*. Briefly, CMA 20 microdialysis probes (100 kDa MWCO and 10 mm length) were immersed into a solution containing 2 ng mL^{-1} of each protein, with stirring at 37°C. The perfusion flow rate was set at 2 μL min^{-1} and dialysates were collected every hour for a total of five hours. Samples were quantified as outlined below.

6.2.3 Animals and Probe Implantation Procedure

Sixteen adult female Sprague-Dawley rats (Harlan Laboratories Inc., Madison, WI) weighing between 220 to 250 g were used in this study. The first set of experiments used ten rats (Set 1) while the second set had six rats (Set 2). All animals were housed in an environmentally-controlled facility with a 12-hour on/off light cycle and had *ad libitum* access to food and water. Surgical procedures followed approved protocols by the University of Arkansas Institutional Animal Care and Use Committee in compliance with National Institutes of Health guidelines for the care and treatment of animals. The animals were anesthetized with 5% isoflurane (Butler Schein, Dublin, OH) (in oxygen). The body temperature was monitored using a rectal thermometer and maintained using a temperature-controlled heating pad (CMA microdialysis, USA). An 18-gauge needle was used to place the microdialysis probe in the abdominal mammary fat pad of the animal while under 2.5% O_2 inhalation. The needle was inserted from one side and the microdialysis probe was tunneled through the needle; the needle was then pushed out from the side of insertion leaving the microdialysis probe embedded in the mammary fat pad (Figure 43). Post mortem analysis was performed to confirm probe location in the mammary fat pad.

Figure 43. Microdialysis sampling probe implantation into the mammary fat pad

An increasing microscopic view of the probe implantation is illustrated from left to right. Farthest right: The circle indicates the location of microdialysis probe implanted in the right abdominal mammary fat pad.

6.2.4 Microdialysis Sampling

Animals remained under anesthesia (2.5 % isoflurane in oxygen) throughout the sampling procedure. Prior to implantation, microdialysis probes were perfused with perfusion fluid at a flow rate of 3 µL min^{-1} for a total of 20 minutes. The tubing lines were then flushed with perfusion fluid (flow rate of 3 µL min^{-1}) for 15 minutes. The flow rate was then reduced to 1 µL min^{-1} and samples were collected every hour for a total of three hours. Dialysates were collected into Eppendorf 0.5 mL protein LoBind™ tubes (Eppendorf, NY) in ice. To prevent protease degradation of adipokines, protease inhibitor cocktail (Halt™, Thermo Scientific, Rockford, IL) was added to the collection tubes at 2X final concentration. All dialysate samples were stored at -80°C until analysis was performed within 2 days of collection.

6.2.5 Tissue Harvest and Protein Extraction

Rats were euthanized by CO_2 asphyxiation immediately after microdialysis sampling. Mammary tissue (weighing between 0.4 to 0.5 g per rat) was harvested from right (probe implant side) and left (control side) abdominal mammary fat pad of each rat (Set 1). For Set 2, mammary tissue within ~2 mm of the region where the probe was implanted was harvested. An equivalent amount of mammary tissue was also excised from tissue with no implanted probe. Tissue samples were frozen immediately in liquid nitrogen and stored at -80°C until analysis within 2 days of tissue collection. T-PER buffer (Pierce Protein Research Products, Thermo Scientific, Rockford, IL) was used for tissue protein extraction, following the manufacturer's guidelines. Briefly, tissue samples were thawed on ice, weighed and divided into 0.25 g minced sections. T-PER buffer containing 1 X Halt Protease inhibitor cocktail was added (4 µL mg^{-1} of tissue), and tissues were

lysed by at least 5 freeze/thaw cycles, followed by homogenization using a Bullet Blender (Next Advance Inc., Averill Park, NY). Tissue homogenates supernatant was collected by centrifugation at 8000g for 15 minutes at 4°C. Total protein concentration in tissue lysates was determined using a bicinchoninic acid (BCA) assay kit (Calbiochem, San Diego, CA) as per the manufacturer's protocol.

6.2.6 Adipokine Quantification

The amounts of CCL2, IL-6, and leptin in 25 µL of dialysate samples were determined using the Multiplex MAP kit (Millipore, Billerica, MA) following the manufacturer's instructions. Sample concentrations (pg mL^{-1}) were determined by comparing median fluorescence intensity (MFI) against a standard curve of known protein concentrations, using a Luminex™ 100 IS analyzer (Luminex Corp, Austin, TX). The concentration range for the leptin assay was 2.4 – 10,000 pg mL^{-1} and 4.88 – 5000 pg mL^{-1} for the CCL2 and IL-6. *In vitro* dialysates samples and tissue extracts were quantified by ELISA using Leptin (Millipore, Billerica, MA), IL-6 and CCL2 (BD Pharmingen, San Diego, CA) ELISA kits.

6.2.7 Statistical Analysis

Origin 8 software platform (OriginLab Corp, Northampton, MA) was used for statistical analysis. The normality of the concentrations of the samples from microdialysis and protein extraction experiments was analyzed using a Shapiro-Wilk test. Data are presented as box and

whiskers plots. Comparisons between samples were made using a Kruskal-Wallis ANOVA with a Bonferroni post hoc test and were considered significant at $p < 0.05$.

6.3 Results and Discussion

6.3.1 *In vitro* Relative Recovery Values

The average relative recovery values of leptin, IL-6 and CCL2 were found to be 11.6 ± 1.2%, 3.3 ± 0.6% and 18.6 ± 9% (n = 5), respectively with a 2 μL min^{-1} flow rate. These relative values for IL-6 and CCL2 are within the range of values reported previously [154]. By contrast, the relative recovery of leptin (~12%) is an order of magnitude higher than previously described. Dostalova et al. reported *in vitro* recovery of leptin at 5.85 % (flow rate of 1 μL/min) and 5.17 % (flow rate of 2 μL min^{-1}), while Duo et al. reported recoveries of 4% and 2% using flow rates of 1 μL min^{-1} and 2 μL min^{-1} respectively [158, 169, 170]. Variations in experimental conditions (37° C under stirred conditions in our studies) which maximized *in vitro* recovery may account for these observed differences.

6.3.2 Probe Implantation in Rat Mammary Fat Pad

Given the anatomical structure of the mammary fat pad, the use of a linear microdialysis probe for collection would have been ideal [171]. In our initial studies, we attempted to use the CMA 31 PES 55 kDa MWCO linear probes. While this probe could be inserted into the fat pad and its membrane positioned within the fat pad itself, no adipokines were collected using these

probes. Additional studies using *in vitro* standards demonstrated that for the 55 kDa MWCO probes, neither CCL2 (13 kDa) or leptin (16 kDa) could be recovered in quantifiable levels across this membrane at a low flow rate of 0.5 μL min^{-1}. It is important to note that MWCO values for the membranes used here are based on the values used for standard kidney dialysis methods. Since MWCO values are obtained using bulk or equilibrium measurements performed under different conditions than microdialysis sampling, it is common with microdialysis sampling to see recovery rates far lower for solutes with molecular weights under the MWCO[172],[173]. We subsequently selected the CMA 20 microdialysis probes with the 100 kDa MWCO based on our previous experience for cytokine collection.

6.3.3 *In vivo* Microdialysis Collection and Protein Extraction from Tissue

Two sets of rats (with ten and six animals, respectively, in Sets 1 and 2) were used to compare cytokine dialysate and extracted tissue protein concentrations. In contrast to those for CCL2 and IL-6, the multiplex assay carried out for leptin in set 1 did not result in standard curves that were appropriate for quantitative measurements. This is a common problem with these bead-based assays in that they do not behave as ruggedly and reliably as standard ELISA [174]. However, given the low volumes obtained using microdialysis sampling, the bead-based assays do allow for multiplexed measurements in our low μL samples. In the second set of six rats, the multiplex assay for CCL2, IL-6 and leptin yielded standard curves that subsequently permitted the comparisons between dialysate and tissue concentrations for all adipokines.

6.3.4 CCL2, IL-6, and Leptin Concentrations in the Dialysates

Figure 44 depicts the dialysate concentrations obtained for CCL2 and IL-6 for the two independent experiments. The concentrations obtained for each adipokine between the two groups are comparable, indicating reproducibility of the experimental procedures. During the sample collection periods, the concentrations of both IL-6 and CCL2 gradually increased temporally during collection. By the end of the collection period (180 minutes), CCL2 concentrations increased from ~20 to 175 pg mL^{-1} (median values) while IL-6 concentrations increased from median values of 30 to 105 pg mL^{-1}. The increase in CCL2 and IL-6 concentrations reflects the anticipated wounding response from insertion of the microdialysis probe.

Analyses by the non-parametric Kruskal-Wallis ANOVA followed by the Bonferroni post hoc test were performed on this data giving the following results. For set 1 animals, there is a significant difference in the protein concentrations at 60 min and 180 mins for both CCL2 and IL-6 ($p < 0.05$). However, there is no significant difference in the protein levels between 60 min and 120 mins and similarly between 120 mins and 180 mins for both CCL2 and IL-6. For set 2 animals, there is no significant difference between the protein levels obtained at the different time points for CCL2, IL-6 and leptin. This is likely due to the different outlier concentrations in this smaller data set. Finally and more important, there is no significant difference in CCL-2 and IL-6 concentrations at comparable time points between set 1 and set 2 animals.

The dialysate concentrations of leptin obtained from the 2^{nd} set of animals did not change at the different collection points, with median values of 750 pg mL^{-1} (Figure 45). This result is consistent with leptin, unlike that of CCL2 and IL-6, to be unresponsive to a foreign body insult.

Thus, the lack of change in leptin concentrations after probe insertion suggests that dialysate leptin concentration may reflect basal levels within the extracellular fluid space in the mammary gland.

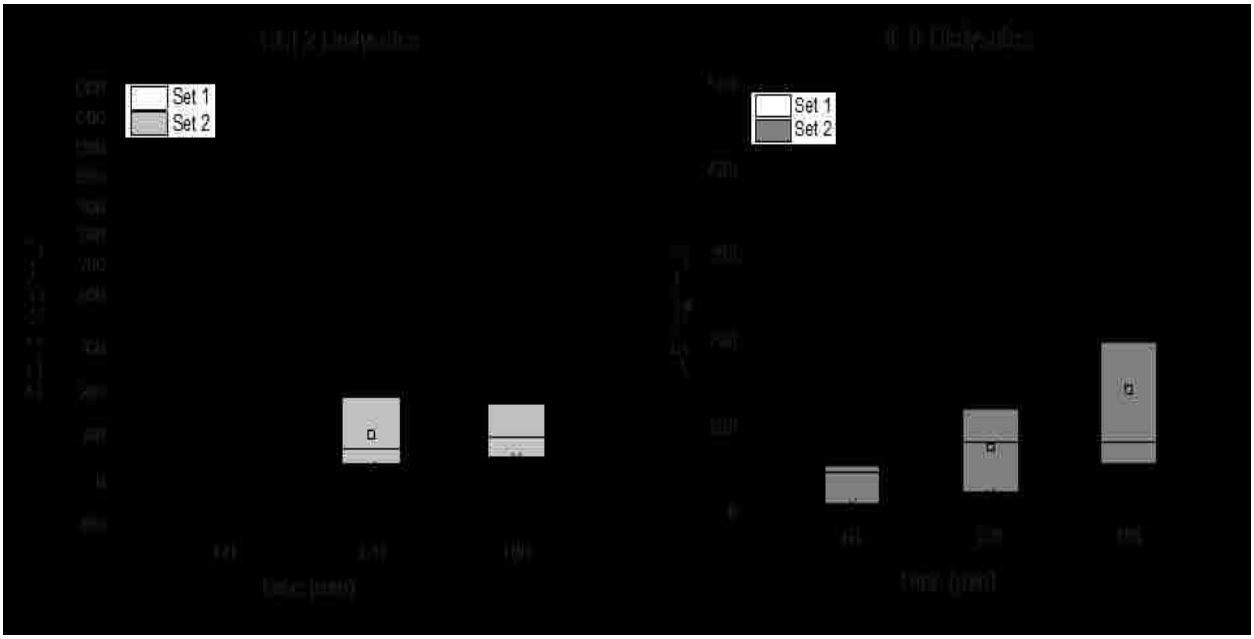

Figure 44. CCL2 and IL-6 dialysate profile

CCL2 (left) and IL-6 (right) concentrations from 1 µL min^{-1} perfused microdialysis probes in two sets of female rats during a three-hour collection period following probe implantation. The "n" value is 10 for set 1 (ten animals) and 6 for set 2 (six animals) and represents the number of animals that provided detectible adipokine concentrations out of total animals used in the study. The box represents the 25-75 percentile. The line through the box represents the median, whiskers represent the fence and ▫ represents the mean.

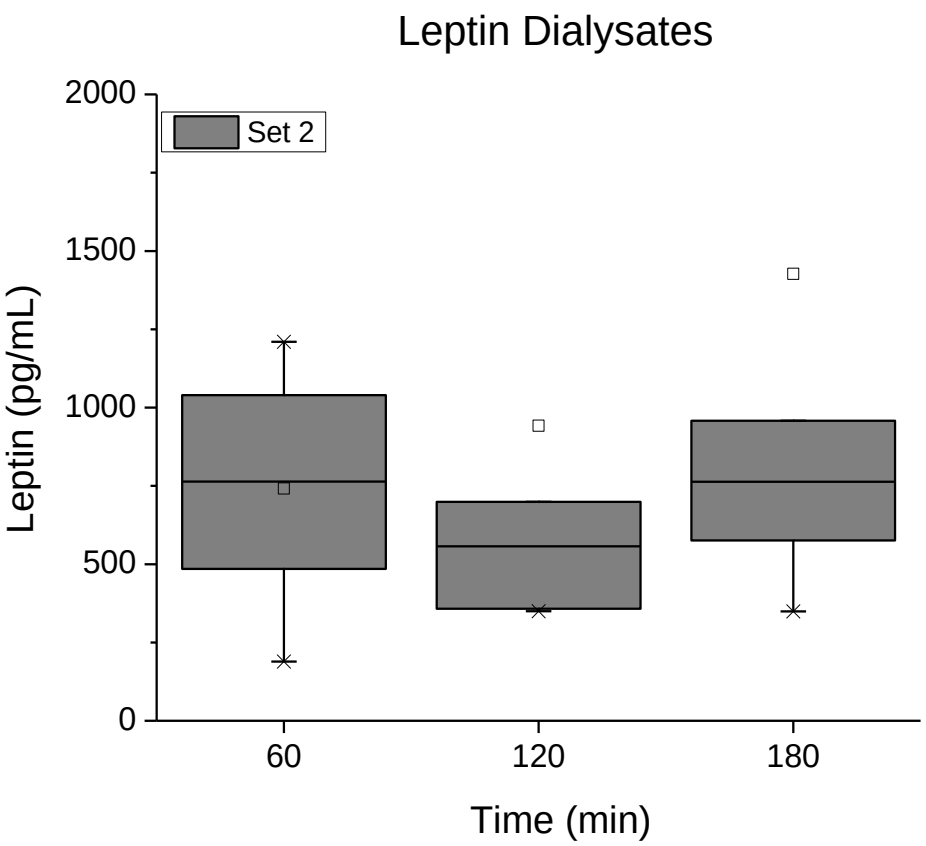

Figure 45. Leptin concentration in dialysates

Leptin dialysate concentrations collected (1 µL min^{-1}) from set 2 animals during the three hour collection period following probe implantation. The "n" value is 6 representing the number of animals that provided detectible adipokine concentrations out of six total animals used in the study. Box represents the 25-75 percentile. The line through the box represents the median, whiskers represent the fence and ▫ represents the mean.

6.3.5 IL-6 and CCL2 Concentrations in Tissue Extracts

The concentrations of CCL2 and IL-6 in mammary tissue extracts are shown in Figure 46. For these studies, tissues around the areas with and without implanted probes were used. No significant differences in tissue CCL2 and IL-6 concentrations were observed. Figure 47 summarizes the adipokine concentrations in tissue extracts when analyzed tissue was limited to an area within 2 mm surrounding the microdialysis implant. For CCL2, concentrations were found to be significantly higher in tissue with than without probe. For IL-6, the concentrations did not differ for tissue with and without implants. It is worth noting the concentrations of CCL2 and IL-6 in control tissue in the second experiment (Figure 47) differed significantly from those in the first set. However, one of the significant advantages of microdialysis sampling procedures is that the animals serve as their own control. Thus, despite the differences in the absolute values in control tissues between the two experiments, their relative values with respect to those for probe-implanted tissue within each experiment did not change.

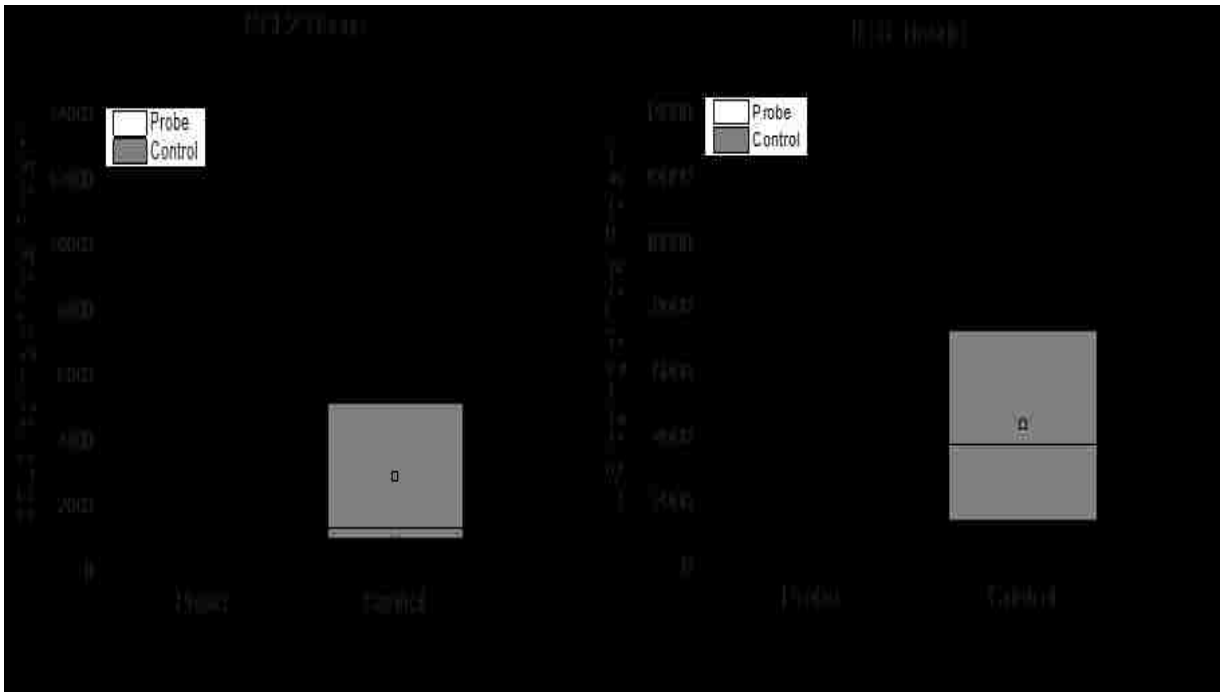

Figure 46. CCL2 and IL-6 concentration in tissue lysates

CCL2 (left) and IL-6 (right) concentrations in the probe-implanted vs. control tissue lysates from animals in set 1. In this set of animals, 1 cm tissue surrounding the probe was harvested. The "n" value is 7 representing the number of animals that provided detectible adipokine concentration out of ten animals in this set. The box represents the 25-75 percentile. The line through the box represents the median, whiskers represent the fence and ▫ represents the mean.

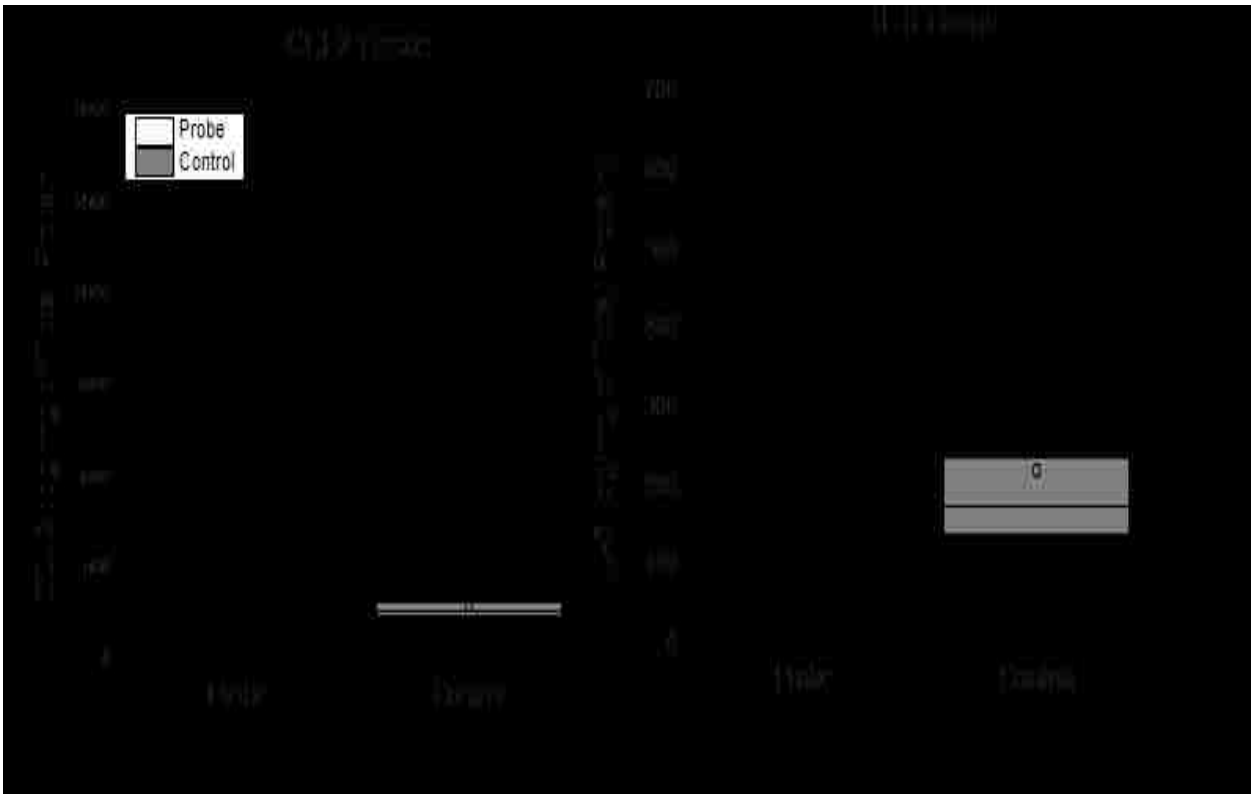

Figure 47. CCL2 and IL-6 concentration in tissue lysates

CCL2 (left) and IL-6 (right) concentrations in probe-implanted vs. control tissue lysates from animals in set 2. In this set of animals, ~2 mm tissue surrounding the probe was harvested. Probe vs. control tissue concentrations are significantly different for CCL2 (†), but not IL-6 using a Kruskal-Wallis ANOVA with a Bonferroni post hoc test ($p < 0.05$). The "n" value is 6 representing the number of animals that provided detectible adipokine concentration out of six animals in this set. The box represents the 25-75 percentile. The line through the box represents the median, whiskers represent the fence and ▫ represents the mean.

6.3.6 Comparison of Tissue vs. Dialysates Concentrations

During microdialysis sampling, solute concentrations obtained in the dialysates represent a fraction of the free and unbound solute concentration in tissues. The *in vitro* recovery values obtained under stirred conditions for the adipokines represent the maximum recovery that might be expected for any solute. This is because tissue properties and other processes (binding to tissue components such as glycosaminoglycans or tissue receptors) can cause an increase in mass transport resistance in a tissue which is otherwise lacking in aqueous solutions. The median IL-6 concentration in dialysates was found to be 1% of the average IL-6 concentration in probe-implanted tissues. Similarly, the median CCL2 concentration in dialysates was 3% that in probe tissue. These values are much lower than the *in vitro* recoveries of 3.3 % and 18.6% for IL-6 and CCL2, respectively. Additional sources of variance between tissue and dialysate concentrations include the presence of various proteins in adipocytes that can bind cytokines or of immune cells recruited to the adipocyte microenvironment due to the implant. Further, differences in the analysis platforms (ELISA for tissue lysates and bead-based assays for dialysate) may contribute to the discrepancies, although the comparable sensitivities of these platforms have been reported previously [175-178].

A challenge to all *in vivo* microdialysis sampling work is the issue of microdialysis probe calibration. Known differences exist between microdialysis calibration *in vitro* vs. *in vivo*. For collection of pharmaceutical solutes, different *in vivo* calibration procedures exist and require solute steady state concentrations typically achieved with drug infusions [179]. For endogenous solutes such as the adipokines that may not exist at steady-state concentrations, *in vivo* calibration methods are not available to determine the true extracellular space concentration. For this reason, we chose to compare total tissue concentrations to the dialysate concentrations.

Analyte transport through any tissue is related to various tissue properties including the metabolism and uptake within the tissue, vascularity, and density of the tissue [180, 181]. Any process that influences solute mass transport through a tissue space will affect the amount of solute that eventually is collected with microdialysis sampling [156, 182]. Additionally chemokines and other cytokines are known to bind to the glycosaminoglycans in the tissue [183]. Solutes that bind to tissue components cannot be collected via the microdialysis sampling approach and thus this binding influences the amount of protein recovered into a microdialysis probe.

Another tissue factor that would have to be considered in longer term studies with microdialysis probes in breast tissue would be differences in tissue density. Rats in different age groups of 21, 28 and 63 days of age have exhibited differences in the tissue density [184]. To minimize this variable, we chose to use a narrow weight range among the animals used for this study.

The placement of microdialysis probe in target tissue requires either incision with removal of enough tissue fascia or use of a guide needle. It is well known that trauma associated with microdialysis probe insertion causes some tissue damage, local blood flow perturbations, and release of inflammatory mediators [185-187]. Trauma stimulates the release of IL-6, IL-8 and CCL2. In previously published data from this lab, CCL2 levels from first day implant in subcutaneous tissue gradually increased from 20 to 135 pg/mL between 40 to 160 min while those from IL-6 increased from 20 to 950 pg/mL [188]. In human subcutaneous tissue studies using microdialysis sampling, the levels of IL-6 and IL-8 were undetectable within the first hour of probe insertion but continuously increased in the next 6 hours [168, 189, 190]. The data presented here showing the temporal concentration increases for CCL2 and IL-6 are consistent with others.

Traditional methods of assessing adipokine expression involve using either qRT-PCR for measurement of mRNA levels or total protein analysis from tissue. While the microdialysis sampling technique is minimally invasive, there are advantages of the microdialysis sampling technique when compared the traditional methods to determine protein expression or concentrations [191]. Microdialysis sampling allows collection of only unbound solutes. This means all the adipokines collected within the dialysis probe were not bound to other tissue components and were released into the extracellular space and not stored within cells. The other advantage of the microdialysis technique is the possibility for reduction of total animals if you can dose the animal while the probe is implanted.

Conclusions

Microdialysis sampling techniques have been successfully applied to the collection of adipokines (CCL2, IL-6 and leptin) from adult rat mammary glands. CCL2 and IL-6 concentrations steadily increased after microdialysis probe implantation. Leptin concentrations did not differ between the sampling points indicating these levels may reflect basal concentrations and not levels induced by microdialysis probe insertion trauma. We suggest that this procedure has significant potential for application in basic studies related to further understanding the signaling biology of the mammary fat pad as targets of inflammatory and obesogenic instigators of breast cancer development and progression. Additionally, the microdialysis sampling technique could be used to collect adipokines during different variable conditions such as animals with different ages, tumors or those given chemotherapeutic agents during the sampling process.

Acknowledgements

This work was supported by NIH grant 1P30RR031154-01 from the National Center for Research Resources (NCRR), a component of the National Institutes of Health (NIH) and the Arkansas Biosciences Institutes (ABI). The manuscript contents are solely the responsibility of the authors and do not necessarily represent the official view of NCRR, NIH, or ABI.

References

59. Kishimoto, T. (1989) The biology of interleukin-6. *Blood* 74, 1-10.

89. Trayhurn, P. (2005) Endocrine and signalling role of adipose tissue: new perspectives on fat. *Acta Physiol Scand* 184, 285-93.

91. Klein, S., Coppack, S. W., MohamedAli, V., Landt, M. (1996) Adipose tissue leptin production and plasma leptin kinetics in humans. Diabetes 45, 984-987.

144. Lorincz, A. M. and Sukumar, S. (2006) Molecular links between obesity and breast cancer. *Endocr Relat Cancer* 13, 279-292.

145. Fruhbeck, G., Nutr, R., Salvador, J. (2004) Role of adipocytokines in metabolism and disease. *Nutr Res* 24, 803-826.

146. Iyengar, P., Combs, T. P., Shah, S. J., Gouon-Evans, V., Pollard, J. W., Albanese, C., Flanagan, L., Tenniswood, M. P., Guha, C., Lisanti, M. P., Pestell, R. G., Scherer, P. E. (2003) Adipocyte-secreted factors synergistically promote mammary tumorigenesis through induction of anti-apoptotic transcriptional programs and proto-oncogene stabilization. *Oncogene* 22, 6408-6423.

147. Grossmann, M. E., Ray, A., Nkhata, K. J., Malakhov, D. A., Rogozina, O. P., Dogan, S., Cleary, M. P. (2010) Obesity and breast cancer: status of leptin and adiponectin in pathological processes. *Cancer Metastasis Rev* 29, 641-653.

148. Hennighausen, L. and Robinson, G. W. (2005) Information networks in the mammary gland. *Nat Rev Mol Cell Biol* 6, 715-25.

149. Yadav, A., Saini, V., Arora, S. (2010) MCP-1: Chemoattractant with a role beyond immunity: A review. *Clin Chim Acta* 411, 1570-1579.

150. Scheller, J., Chalaris, A., Schmidt-Arras, D., Rose-John, S. (2011) The pro- and anti-inflammatory properties of the cytokine interleukin-6. *Biochim Biophys Acta, Mol Cell Res* 1813, 878-888.

151. Nishimoto, N. and Kishimoto, T. (2006) Interleukin 6: from bench to bedside. *Nat Clin Pract Rheumatol* 2, 619-26.

152. Dieudonne, M. N., Machinal-Quelin, F., Serazin-Leroy, V., Leneveu, M. C., Pecquery, R., Giudicelli, Y. (2002) Leptin mediates a proliferative response in human MCF7 breast cancer cells. *Biochem Biophys Res Commun* 293, 622-628.

153. Westerink, B. H. C. and Cremers, T. I. F. H. (2007) Handbook of Microdialysis Sampling: Methods, Applications, and Clinical Aspects. Academic Press, Amsterdam.

154. Ao, X. and Stenken, J. A. (2006) Microdialysis sampling of cytokines. *Methods* 38, 331-41.

155. Bungay, P. M., Newton-Vinson, P., Isele, W., Garris, P. A., Justice, J. B., Jr. (2003) Microdialysis of dopamine interpreted with quantitative model incorporating probe implantation trauma. *J Neurochem* 86, 932-946.

156. Stenken, J. A. (1999) Methods and issues in microdialysis calibration. *Anal Chim Acta* 379, 337-357.

157. Nielsen, N. B., Hojbjerre, L., Sonne, M. P., Alibegovic, A. C., Vaag, A., Dela, F., Stallknecht, B. (2009) Interstitial concentrations of adipokines in subcutaneous abdominal and femoral adipose tissue. *Regul Pept* 155, 39-45.

158. Dostalova, I., Pacak, K., Nedvidkova, J. (2003) Application of in vivo microdialysis to measure leptin concentrations in adipose tissue. *Int J Biol Macromol* 32, 205-208.

159. Murdolo, G., Herder, C., Wang, Z. H., Rose, B., Schmelz, M., Jansson, P. A. (2008) In situ profiling of adipokines in subcutaneous microdialysates from lean and obese individuals. *Am J Physiol Endocrinol Metab* 295, E1095-E1105.

160. Garvin, S. and Dabrosin, C. (2008) In vivo measurement of tumor estradiol and Vascular Endothelial Growth Factor in breast cancer patients. *BMC Cancer* 8.

161. Shaw, D. W. and Britt, J. H. (1995) Concentrations of tumor necrosis factor α and progesterone within the bovine corpus luteum sampled by continuous-flow microdialysis during luteolysis in vivo. *Biol Reprod* 53, 847-54.

162. Clausen, T. S., Kaastrup, P., Stallknecht, B. (2009) Proinflammatory tissue response and recovery of adipokines during 4 days of subcutaneous large-pore microdialysis. *J Pharmacol Toxicol Methods* 60, 281-287.

163. Sjogren, F. and Anderson, C. D. (2010) Are cutaneous microdialysis cytokine findings supported by end point biopsy immunohistochemistry findings? *AAPS J* 12, 741-749.

164. Russo, J., Gusterson, B. A., Rogers, A. E., Russo, I. H., Wellings, S. R., van Zwieten, M. J. (1990) Comparative study of human and rat mammary tumorigenesis. *Lab Invest* 62, 244-78.

165. Shull, J. D. (2007) The rat oncogenome: comparative genetics and genomics of rat models of mammary carcinogenesis. *Breast Dis* 28, 69-86.

166. Szpirer, C. (2010) Cancer research in rat models. *Methods Mol Biol* 597, 445-458.

167. Xu, B. J., Yan, W., Jovanovic, B., Shaw, A. K., An, Q. A., Eng, J., Chytil, A., Link, A. J., Moses, H. L. (2011) Microdialysis combined with proteomics for protein identification in breast tumor microenvironment in vivo. *Cancer Microenviron* 4, 61-71.

168. Clough, G. F., Jackson, C. L., Lee, J. J., Jamal, S. C., Church, M. K. (2007) What can microdialysis tell us about the temporal and spatial generation of cytokines in allergen-induced responses in human skin in vivo? *J Invest Dermatol* 127, 2799-806.

169. Dostalova, L., Kopsky, V., Duskova, J., Papezova, H., Pacak, K., Nedvidkova, J. (2005) Leptin concentrations in the abdominal subcutaneous adipose tissue of patients with anorexia nervosa assessed by in vivo microdialysis. *Regul Pept* 128, 63-68.

170. Duo, J., Fletcher, H., Stenken, J. A. (2006) Natural and synthetic affinity agents as microdialysis sampling mass transport enhancers: Current progress and future perspectives. *Biosens Bioelectron* 22, 449-457.

171. Davies, M. I. and Lunte, C. E. (1995) Microdialysis sampling for hepatic metabolism studies: impact of microdialysis probe design and implantation technique on liver tissue. *Drug Metab Dispos* 23, 1072-9.

172. Schutte, R. J., Oshodi, S. A., Reichert, W. M. (2004) In vitro characterization of microdialysis sampling of macromolecules. *Anal Chem* 76, 6058-6063.

173. Snyder, K. L., Nathan, C. E., Yee, A., Stenken, J. A. (2001) Diffusion and calibration properties of microdialysis sampling membranes in biological media. *Analyst* 126, 1261-8.

174. Fichorova, R. N., Richardson-Harman, N., Alfano, M., Belec, L., Carbonneil, C., Chen, S., Cosentino, L., Curtis, K., Dezzutti, C. S., Donoval, B., Doncel, G. F., Donaghay, M., Grivel, J. C., Guzman, E., Hayes, M., Herold, B., Hillier, S., Lackman-Smith, C., Landay, A., Margolis, L., Mayer, K. H., Pasicznyk, J. M., Pallansch-Cokonis, M., Poli, G., Reichelderfer, P., Roberts, P., Rodriguez, I., Saidi, H., Sassi, R. R., Shattock, R., Cummins, J. E., Jr. (2008) Biological and technical variables affecting immunoassay recovery of cytokines from human serum and simulated vaginal fluid: a multicenter study. *Anal Chem* 80, 4741-51.

175. Khan, S. S., Smith, M. S., Reda, D., Suffredini, A. F., McCoy, J. P., Jr. (2004) Multiplex bead array for detection of soluble cytokines: comparisons of sensitivity and quantitative values among kits from multiple manufacturers. *Cytometry B Clin Cytom* 61B, 35-39.

176. de Jager, W., te Velthuis, H., Prakken, B. J., Kuis, W., Rijkers, G. T. (2003) Simultaneous detection of 15 human cytokines in a single sample of stimulated peripheral blood mononuclear cells. *Clin Diagn Lab Immunol* 10, 133-139.

177. Elshal, M. F. and McCoy, J. P. (2006) Multiplex bead array assays: Performance evaluation and comparison of sensitivity to ELISA. *Methods* 38, 317-323.

178. Chaturvedi, A. K., Kemp, T. J., Pfeiffer, R. M., Biancotto, A., Williams, M., Munuo, S., Purdue, M. P., Hsing, A. W., Pinto, L., McCoy, J. P., Hildesheim, A. (2011) Evaluation of Multiplexed Cytokine and Inflammation Marker Measurements: a Methodologic Study. *Cancer Epidemiol Biomarkers Prev* 20, 1902-1911.

179. de Lange, E. C. M. (2013) Recovery and Calibration Techniques:Toward Quantitative Microdialysis. In Microdialysis in Drug DevelopmentSpringer, New York 13-33.

180. Sykova, E. and Nicholson, C. (2008) Diffusion in brain extracellular space. *Physiol Rev* 88, 1277-1340.

181. Burdett, E., Kasper, F. K., Mikos, A. G., Ludwig, J. A. (2010) Engineering tumors: a tissue engineering perspective in cancer biology. *Tissue Eng Part B Rev* 16, 351-9.

182. Bungay, P. M., Morrison, P. F., Dedrick, R. L. (1990) Steady-state theory for quantitative microdialysis of solutes and water in vivo and in vitro. *Life Sci* 46, 105-19.

183. Shute, J. (2012) Glycosaminoglycan and chemokine/growth factor interactions. *Handb Exp Pharmacol* 207, 307-324.

184. McGinley, J. N. and Thompson, H. J. (2011) Quantitative assessment of mammary gland density in rodents using digital image analysis. *Biol Proced Online* 13, 4.

185. Groth, L., Jorgensen, A., Serup, J. (1998) Cutaneous microdialysis in the rat: Insertion trauma studied by ultrasound imaging. *Acta Derm Venereol* 78, 10-14.

186. Groth, L., Jorgensen, A., Serup, J. (1998) Cutaneous microdialysis in the rat: Insertion trauma and effect of anaesthesia studied by laser Doppler perfusion imaging and histamine release. *Skin Pharmacol Appl Skin Physiol* 11, 125-32.

187. Stenken, J. A., Church, M. K., Gill, C. A., Clough, G. F. (2010) How minimally invasive is microdialysis sampling? A cautionary note for cytokine collection in human skin and other clinical studies. *AAPS J* 12, 73-78.

188. von Grote, E. C., Venkatakrishnan, V., Duo, J., Stenken, J. A. (2011) Long-term subcutaneous microdialysis sampling and qRT-PCR of MCP-1, IL-6 and IL-10 in freely-moving rats. *Mol Biosyst* 7, 150-161.

189. Sjogren, F., Svensson, C., Anderson, C. (2002) Technical prerequisites for in vivo microdialysis determination of interleukin-6 in human dermis. *Br J Dermatol* 146, 375-382.

190. Zweiman, B., Kaplan, A. P., Tong, L. J., Moskovitz, A. R. (1997) Cytokine levels and inflammatory responses in developing late-phase allergic reactions in the skin. *J Allergy Clin Immunol* 100, 104-109.

191. Anderson, C. D. (2006) Cutaneous microdialysis: is it worth the sweat? *J Invest Dermatol* 126, 1207-1209.

Chapter 7: Summary and Future Directions

This dissertation explored the rodent macrophage phenotypic changes in response to modulators both in vitro and in vivo. As mentioned in Chapter 1, there has been an enormous interest in the macrophage activation biology in the context of regenerative medicine and wound healing due to their phenotypic plasticity. It has been hypothesized that immunomodulation of macrophages can be applied to various clinical scenarios, including FBR in an effort to potentially reduce fibrosis around an implant site. However, in order to utilize the full clinical potential of macrophage plasticity, in-depth understanding of the phenotypic plasticity on a case-by-case basis is imperative due to interspecies differences and inherent complexity of the phenomenon.

Many studies have been published demonstrating macrophage activation in response to different modulators in murine macrophages. Also, *in vivo* studies demonstrating translation of the *in vitro* data are lacking. In the context of biomaterials, rats serve as common model organisms. Studies describing macrophage activation biology in rats are sparse. In this research, rats have been used.

Before trying the modulators *in vivo* to direct macrophage polarization in rodent systems, it was important to derive, characterize and establish various phenotypic states of macrophages *in vitro* in response to the modulators. Splenic macrophages were used to study the *in vitro* responses. In murine models both peripheral blood monocytes (PBMC) and bone marrow derived macrophages (BMDM) have been used for studying macrophage polarization/activation. Recently, one study demonstrated the activation potential of macrophages derived from mice spleen [192]. Macrophages derived from various sources can respond differently to the modulators depending on homogeneity, stages of differentiation and naivety which add to the further complexity. Thus,

for in depth understanding of the macrophage activation responses, more studies that compare and contrast immunomodulation of macrophages derived from variety of sources (lung, spleen, blood and bone marrow) are to be performed. These experiments can highlight the differences in responses to the modulators, if there are any, between macrophages derived from various sources. This information would be useful when translating research in vivo as macrophage responses at one implant location might vary from other implant location. Thus, the use of splenic macrophages from rats in this study added to the novelty of the research as spleen also deploys macrophages to the wound site.

Differentially activated macrophages differ from each other in their secretory cytokine/chemokine profile, arginine metabolism and expression of cell surface receptor proteins. As seen in above figure (for example), M1 profile secrete inflammatory cytokine TNF, IL-1, IL-6. The iNOS expression goes up as arginine metabolism is shifted to produce NO for enhance bacterial killing. Surface expression of MHCII CD80 and CD86 is enhanced. While on the M2 spectrum anti-inflammatory cytokine IL-10 is secreted. Arginase expression is enhanced. Surface receptor expression of CD163, CD206 is enhanced compared to the M1 profile. Thus, differentially activated states of macrophages can be distinguished from each other by variety of assays such as ELISA for differences in secreted cytokine profiles, flow cytometry assays for differences in surface receptor expression profiles and gene expression assays for differences in target genes of interest. There is no agreed upon consensus in the scientific community as to which assay should be used. Some studies reply only on flow cytometry assays for the phenotypic analysis and some studies utilize only RT-PCR assays to establish phenotypic profile based on gene expression profiles. Usually, combination of assays are used to establish profile changes at various levels viz secreted proteins, receptor changes and changes in gene expression.

Thus, to establish phenotypic profile at various levels, different assays were used in this study. ELISA were performed to measure secreted proteins in response to the modulators (Chapter 2). Flow cytometry assays were performed to establish phenotypic changes at surface receptor expression level (Chapter 3). RT-PCR assays were performed for further validation of the phenotypic changes at the gene expression level and also, to establish changes in expression profile of iNOS and arginase (Chapter 3).

In Chapter 2, gene expression assays on differentially activated macrophages were performed at two different time points. The data from rat-derived macrophages was similar to what has been observed with murine macrophages. The IL-10 significantly enhanced the CD163 expression which was expected. As expected, CD206 expression was significantly enhanced by dexamethasone and IL-4. The arginase-1 expression was found to be significantly upregulated in all the treatments (LPS, IL-4 and IL-10) except dexamethasone where it was down-modulated. This suggests ambiguity in using arginase-1 as a marker for alternative activation, a problem that recent literature has pointed out. On the contrary, arginase-2 expression was found to be specific for IL-4 activation. The arginase-2 isoform has not been investigated much in macrophage activation studies. The present research has compared both the isoforms side-by-side in differentially activated macrophages and shows that argiase-2 can be used as a specific marker for alternative activation (M(IL-4)) in rat splenic macrophages.

ELISA assays were also performed on the supernatants collected from the differentially activated splenic macrophages. Secreted proteins TNF, IL-6 and IL-10 had higher concentrations in LPS treated macrophages compared to the resting macrophages or IL-4/IL-10 stimulated macrophages. This information is in agreement with information obtained from the gene expression assays. The secreted IL-10 could not be quantified in the cell culture medium in

response to IL-4/Dex. However, RT-PCR shows a mild upregulation in IL-10 transcripts for these treatments. The IL-10 ELISA limit of detection was 15 pg/mL. It is possible that IL-10 upregulation corresponds to the secretion concentration that remained below the assay detection limit. It is also possible that IL-10 mRNA transcript is present that was detected in the gene expression assays but may not have been translated to secreted protein due to other translation control mechanisms.

Also, chitohexose that activated murine macrophages to alternative pathway caused synergistic inflammatory responses when combined with LPS in rat macrophages. Interestingly, chitohexose had no effects on macrophages alone. The combination of LPS with chitohexose resulted in increased secretion of TNF-α, IL-6 and IL-10 in the culture medium. These could be possible interspecies differences which needs further exploration. A gene expression analysis of arginase isoforms, iNOS, CD163, and CD206 from macrophages activated by this combination can be performed in future studies to understand how these markers of activation get affected by this combination or if the observed synergistic response is limited to the secretion of inflammatory cytokines. Also, for future studies this combination could be tested for its potential to activate macrophages towards M1 profile where classical activation is necessary (for example M2 like tumor associated macrophages).

In Chapter 3, flow cytometry assays were developed for the analysis of cell surface receptor expression. In Chapter 2, gene expression assays and ELISA were performed for the characterization of differentially activated macrophages. The cell surface receptor expression also varies in differentially activated macrophages. The motivation to perform flow cytometry assays was to gain information on MHCII, CD80, CD86, CD163 and CD206 receptors of differentially polarized macrophages that could not be established through ELISA. The qRT-PCR assays were

performed on only two of the surface receptor protein (CD163 and CD206) targets. Thus, flow cytometry assays were performed to validate qRT-PCR mRNA transcript data on CD163 and CD206 at protein level as well as to gain insight on above mentioned other surface protein markers.

In splenic macrophages, dexamethasone showed the most dramatic shift towards enhanced CD206 expression. The gene expression data for CD206 in response to dexamethasone also showed significant upregulation for this marker. This is in agreement with the results obtained from the gene expression assays for cells stimulated with dexamethasone. The IL-4 was found to enhance MHCII expression but did not affect CD206 expression. The gene expression data in Chapter 3 shows significant upregulation of CD206 in response to IL-4 treatment. The CD163 surface protein expression was expected to be enhanced in response to IL-10 treatment. However, significant CD163 enhanced expression was not observed in flow cytometry assay though gene expression data in Chapter 3 showed significant upregulation for this marker. The lack of correlation between gene and protein expression data is a known biological problem. A positive gene expression result does not necessarily correlate to positive protein expression. Similarly, positive protein expression may not show positive results for gene expression assay. The transient expression of CD163 and CD206 transcripts without detectable functional protein expression could explain the observed lack of correlation between flow cytometry and gene expression data for CD163 and CD206 proteins. However, lack of positive expression in flow cytometry does not mean no expression. Chromophores not having sufficient concentration to detect combined with a small parent population (~28% CD11b+ macrophages) may have resulted in poor resolution. To further confirm positive protein expression of CD163 and CD206 in response to IL-10 and IL-4, respectively, western blot assays could be performed in future studies.

LPS treatment did not result in any significant enhanced MHCII and CD86 cell surface receptor expression. However, in Chapter 2, ELISA measurement of secreted TNF-α and IL-6 protein, and enhanced iNOS and IL-12a expression confirmed modulation to M1 phenotype in response to LPS. Overall, *in vitro* data from various assays, cytokine ELISA, gene expression and surface receptor analysis through flow cytometry confirmed the successful derivation and characterization of differentially activated macrophages. The data also laid the guiding map for what to expect with respect to markers *in vivo*.

In vivo experiments were then initiated after successful characterization of macrophages in vitro. The IL-4 and IL-10 doses were important considerations in *in vivo* experiments. The IL-4 (50 ng/mL), IL-10 (50 ng/mL), LPS (100 ng/mL) and Dexamethasone (100 µM) doses in *in vitro* cell culture experiments were based on dose response study experiments conducted as well as on previously published literature that confirm immunomodulation of macrophages with these doses. Similar concentrations were used for *in vivo* microdialysis delivery studies. Initially, 50 ng/mL of IL-4 was used for the delivery of IL-4 but no changes between the tissue surrounding the control probe and the treatment probe were observed. Then concentration of IL-4 and IL-10 were increased to account for low in vitro relative recovery values 3.5 % for IL-4 and 1% for IL-10 on the assumption of recovery percentage would be same as delivery. Previously, published study from Ao and Stenken (Methods, 2006) have discussed in vitro relative recovery and delivery of cytokines [152].

The 200 ng/mL concentration of IL-4 and IL-10 were chosen for sponge experiments. Few studies have used IL-4 in vivo in the context of macrophage polarization in wound healing. Different doses have been utilized in different experiments. Table below shows the list of references for doses of IL-4

IL-4 Dose	Purpose	Reference
50 ng/mL *in vitro* 1 µg/mL *in vivo*	*In vitro* rat alveolar cell culture. Subcutaneous, Nerve repair	Mokarram, Nassir, et al. "Effect of modulating macrophage phenotype on peripheral nerve repair." Biomaterials (2012). [130]
0.1, 1 and 100 ng/mL *in vitro* 1 and 100 ng/mL *in vivo*	*In vivo* administration in ligament healing model in wistar rats	Chamberlain, Connie S., et al. "The influence of interleukin-4 on ligament healing." Wound Repair and Regeneration 19.3 (2011): 426-435. [128]
250 ng/mL	4 day administration in experimental wound healing in mice	Salmon-Ehr, Véronique, et al. "Implication of interleukin-4 in wound healing." Laboratory investigation 80.8 (2000): 1337-1343. [129]
0.1, 1 and 10 mg in wounds	Sprague-Dawley rats. Subcutaneous healing in diabetic rats	Schwarz, Martin A., et al. "Method for enhancing wound healing/repair with IL-4. U.S. Patent No. 5,723,119. 3 Mar. 1998.

In Chapter 4, *in vivo* experiments to direct macrophages towards an alternative pathway were initiated with IL-4 and IL-10 delivery using microdialysis probes. These experiments were

completely novel. The microdialysis model was not trivial, and proved to be challenging especially due to random probe malfunctioning, probe failures and sampled analyte being below the limit of detection of the cytokine assays. From microdialysis infusion studies where high concentration of IL-4 and IL-10 were used, it appears that some changes in CCL2 and IL-6 gene expression profiles occurred. However, it is too early to derive any conclusion from those experiments as studies need to be repeated with more animals to have statistical power. Also *in vitro* delivery of active IL-4 or IL-10 has to be established and tested as well. It could be possible that IL-4/IL-10 did not diffuse out of the probe at all, and thus no changes have been observed. Thus, establishment of successful delivery of analyte has to be addressed first and foremost in future experiments.

In Chapter 5, sponge experiments were undertaken as an alternative methodology to answer whether or not IL-4 and IL-10 would cause any effects *in vivo* in rat. In microdialysis delivery experiments, sampled cytokine were below detection limits. Any conclusive data could not be derived from cytokine analysis. Histological analyses of tissue surrounding the control probe and treated probe appeared similar. As discussed in Chapter 1, collection of wound fluid and cells from sponges makes them highly desirable in wound healing studies. However, animals have to be terminated to explant the sponges to study a particular time point thus many animals have to be sacrificed for studies involving different time points. Whereas, with long term microdialysis sampling fewer animals can be used. This is one of the contrasting differences between the two methodologies. The cytokines extracted from the sponge wound fluid can be considered as representative of the near true tissue concentrations. However, cytokines sampled from the microdialysis probe are only a certain fraction of what is present in the extracellular fluid space (<1%). The *in vitro* relative recovery for a given analyte can be used as an estimate for the in vivo recovery of that analyte. The *in vitro* relative recovery of cytokines (depending on the size and

structure) can vary from ~1% (for IL-10) to ~15% (CCL2). Also, there are differences in the impact surface area of the two implants. The microdialysis probe surface area is 15 mm^2 and, on the other hand the surface area of sponge is 1131 mm^2. Thus, the sponge implants had a significantly larger surface area resulting in larger tissue impact than the microdialysis probes. Another contrasting point between the two implants is regarding the delivery of IL-4/IL-10. With microdialysis, the delivered cytokine concentration is only a certain fraction of what is present inside the dialysis probe and can be estimated based on the *in vitro* relative recovery values. The exact concentration of the cytokines diffused out of the probe is hard to estimate. Whereas, the sponges could be impregnated or injected with the known concentration and volume of the target cytokine.

Interesting results were observed through the sponge experiments in this research. At day 7 time point, IL-4 treatment resulted in significantly lower concentrations of IL-1β compared to control sponge wound exudate. On the other hand, IL-10 treatment resulted in significant down regulation of inflammatory genes. Also, CCL2 levels in wound exudate were significantly lower in IL-10 treated sponge. At the day 3 time point, no significant differences in IL-1β, CCL2 and IL-6 protein concentrations were found between the control and IL-10 treated sponges. However, in gene expression assays, CCL2 was found to be upregulated in cells extracted from IL-10 treated sponges. This data suggests that time point is an important consideration as to when to administer the cytokine. It is important to note that gene expression data from macrophages extracted from the sponges also suggests a mixed phenotype that does not fit completely into M1 or M2 paradigm and is not influenced by the infusion of IL-4 and IL-10 at chosen concentration but down-modulates the inflammatory cytokines IL-1β, TNF-α and CCL2. Overall, from the gene expression and protein assays, minor extent of immunomodulation could be established. The major conclusion

from the lack of observed dramatic shift in macrophage phenotype suggests the need for the prolonged presence of modulator cytokine in the biological matrix. This brings to another question of how dramatic the shift in should be in phenotype to cause a desirable anti-fibrotic outcome. These questions cannot be answered without performing further exploratory research. However, this research presents the first step towards the *in vitro* to *in vivo* basic translational research with respect to macrophage activation.

From chapter 6, successful collection and quantification of important breast cancer biomarkers using microdialysis sampling is established in the mammary fat pad of female rats. The study has important future implications. The technique can be employed to sample breast cancer cytokine markers in tumor microenvironment in model organisms. An altered type-2 like macrophage phenotype is present in breast tumors. The interaction and cytokine signaling between M2 like altered macrophages and adipose tissue contribute significantly to the progression of breast tumors. This technique can also be employed to deliver potential drugs right at the action area (mammary tissue) followed by cytokine sampling to monitor the changes in response to the drug candidate.

Combined together, this research presents interesting results and provides an opportunity for further research and exploration in the area of macrophage activation in response to various modulators. Many possibilities can be tested and characterized. As mentioned before, optimization of microdialysis experiments are important which will further allow its use in localized delivery of cytokines with confidence. Immediate next step would be to confirm the *in vitro* delivery of bioactive protein via microdialysis probe using a culture system. A simple experiment would be to induce the NR8383 macrophages with LPS at 100 ng/mL concentration as already performed in this research. Then inserting the microdialysis probe and performing the delivery of IL-4/IL-10

for 4 hours (as a starting point). Then measuring and comparing the secreted TNF-α concentrations between IL-4/IL-10 infused LPS treated macrophage wells and non-infused LPS treated macrophage wells. The concentration of IL-4/IL-10 and length of infusion would need optimization based on the results of preliminary experiments. Upon unambiguously establishing the delivery of IL-4/IL-10 with observable biological effects *in vitro*, *in vivo* delivery experiments can be initiated again.

For future studies, if robust probes can be procured, then it would be interesting to employ the delivery of IL-4 or IL-10 (with simultaneous sampling) for up to the day 14 and monitor the long term delivery effects of these cytokines on fibrosis, as fibrosis starts and begins to peak around this time point. Results of long-term experiments can provide a detailed time profiling of cytokines in response to IL-4 and IL-10 delivery without sacrificing many animals. Tissue around the probe can be decellularized and analyzed by flow cytometry for phenotypic changes in macrophages in response to the cytokines. This has not been done yet in microdialysis experiments but could be employed in the future experiments.

The immediate next step with the sponge experiments would be to perform a dose response study. As mentioned before, data from the sponge experiments show a lack of dramatic shift in the macrophage phenotype at 200 ng/mL (with booster dose on day 3) of IL-4/IL-10, suggesting the need for a higher dose or everyday administration of the booster dose. The following experimental plan can be carried out as next step to test two possibilities;

1) Lower dose of 200 ng/mL administration on day 0 followed by booster doses of same concentration administered every day. Analysis at day 7 time point.

Group 1, n=6	2 IL-4 treated sponges and 2 untreated sponge control subcutaneously implanted along the midline on each side in each rat	Dose of IL-4 : 200 ng/mL on day 0 (day of implantation) On day 3, 4, 5 &6: booster dose of starting concentrations would be injected in each sponge
Group 2, n=6	2 IL-10 treated sponges and 2 untreated sponge control subcutaneously implanted along the midline on each side in each rat	Dose of IL-10: 200 ng/mL day 0 (day of implantation) On day 3, 4, 5 &6: booster dose of starting concentration would be injected in each sponge

2) Higher dose of 1000 ng/mL administration on day 0 followed by booster dose on day 3.

Group 1, n=6	2 IL-4 treated sponges and 2 untreated sponge control subcutaneously implanted along the midline on each side in each rat	Dose of IL-4 : 200 ng/mL on day 0 (day of implantation) On day 3: booster dose of respective 1000 ng/mL would be injected in each sponge
Group 2, n=6	2 IL-10 treated sponges and 2 untreated sponge control subcutaneously implanted along the midline on each side in each rat	Dose of IL-10: 1000 ng/mL day 0 (day of implantation) On day 3: booster dose of 1000 ng/mL would be injected in each sponge

End point analysis by cytokine measurement, sponge histology and macrophage phenotype determination from these experiments can provide following insights;

1) An estimation of whether to utilize even higher concentrations of IL-4/IL-10 to cause more dramatic shift in macrophage phenotype.

2) Whether the sustained presence of low doses or administration of higher dose followed by one booster dose is more desirable for resolution of wound healing while sustaining the shift in the macrophage phenotype

The sponge experiments can be taken up further to study day 14 and day 21 time points as well in future studies. If the complete shift in the macrophage phenotype is achieved *in vivo*, how this would actually affect the fibrosis needs to be determined by long term studies.

Based on current understanding, it is difficult to answer how the research would translate in clinic as of now. It is too early to answer the hypothetical question as activation and immunomodulation of macrophage is a new area in the fields of regenerative medicine and requires further exploration in the context of FBR. To briefly summarize, the observation that scar-less healing of fetal wounds was attributed to IL-10, led to it being a potential candidate in regenerative healing. Its role as a therapeutic agent is under investigation for various conditions including, but not limited to, psoriasis, arthritis, Crohn's disease and pulmonary fibrosis. Various *in vitro* studies have shown IL-10 mediated anti-inflammatory effects of macrophages and generation of CD163+ phenotypes that have been implicated in tissue remodeling. The hypothesis that M(IL-10) activation will lead to scar-less healing is based on what has been observed in in vitro studies. However, *in vivo* studies are scarce that can provide insights to in vitro to in vivo translation. Some of the studies where exogenous application of IL-10 in the context of pulmonary fibrosis was tested, have given contradictory results. Kradin et al., compared the outcomes of bleomycin induced lung fibrosis in wild type and IL-10 deficient (IL-10-/-) mice. Their finding suggested protective role of IL-10 against inflammation but did not impart protection against

fibrosis [140]. Nakagome et al., delivered IL-10 gene to mice to alleviate bleomycin induced lung fibrosis [141]. The contrasting results from both the study suggest in wild type mice IL-10 did not affect fibrosis but exogenous gene delivery attempted at over expression of IL-10 did impart protective role against pulmonary fibrosis. This suggests the dosage of IL-10 required would be a critical factor and it is going to depend on the severity of the situation.

In the context of biomaterials, not many published studies are available that focus on its exogenous administration *in vivo* to alleviate FBR and fibrotic encapsulation. In a recent study by Boehler et al., lentiviral mediated gene delivery of IL-10 was proposed at the implant site to sustain an alternative phenotype of macrophages that would mark down the inflammation. The study was performed *in vitro* using murine macrophages. As mentioned, various *in vitro* studies have shown IL-10 mediated anti-inflammatory effects of macrophages and generation of CD163+ phenotypes that have been implicated in tissue remodeling. However, *in vivo* studies are scarce that can provide insights to *in vitro* to *in vivo* translation.

In the present study IL-10 at 200 ng/mL concentration marked down the inflammatory cytokines but had no significant effect on CD163 gene expression.

Points to consider are;

1. More basic research needs to be performed with various dosage of IL-10 and timing of administration. The question is whether small dose of IL-10 needs to be administered every day or a higher dose needs to be administrated in a week needs to be tested.

2. How this dose would affects the CD163 expression in macrophage phenotypes needs to be determined.

3. How the shift in CD163 positive macrophages would affect the FBR outcome needs to be determined.

4. How dramatic shift in macrophage phenotype is needed? Does recurrent doses would be beneficial or permanent shift in the macrophage phenotype at a certain stage of FBR would be important to alleviate the fibrosis?

However, to answer the hypothetical question with present limited knowledge, a gene delivery of IL-10 can be considered as an option once it is determined that permanent shift in the macrophage phenotype in the FBR stages would be required to alleviate the fibrosis. Drug releasing hydrogels and tissue scaffolds are under investigation for chronic wounds and tissue injuries. These scaffolds can be used provided they do not interfere with the continuous glucose sensor functioning.

References

192. Mulder, R., Banete, A., Basta, S. (2014) Spleen-derived macrophages are readily polarized into classically activated (M1) or alternatively activated (M2) states. Immunobiology 219, 737-45.